Modeling Hard & Soft Materials through Density Functional Theory at Different Length Scales

Swapan K. Ghosh

skghosh@barc.gov.in

Bhabha Atomic Research Centre, Mumbai, India

What do we do ?

Interdisciplinary Basic Research at the Interface between Chemistry, Physics, Materials Science, Chemical Engineering & Biology

Materials Related: Nanomaterials

Energy Related: Hydrogen energy

Waste-Management related: Ligand Design

Dynamics in Condensed Phase

Soft Matter under Confinement

Experiment-Driven Theoretical Studies

Biology-Inspired Theoretical Studies

Curiousity-Driven Investigations

Theory & Computation

- Development of new Theoretical Formalisms & Modeling/ Simulation Strategies

- Nonequilibrium thermodynamics at short length & time scales
- Coarse-Graining procedure for simulation

What we do: Theoretical Chemistry Research

Theory, Modeling & Simulation of Systems & Processes of Interest

Structure of Materials at Different Length Scales	↔	Dynamics of Phenomena at Different Time Scales

Theoretical Tools

Structure

Dynamics

Structure	Dynamics
Ab-initio Molecular Orbital Theory	**Density Functional Theory (TD)**
Density Functional Theory	**Statistical Mechanics**
Integral Equation Theory	**Mode Coupling Theory**
Computer Simulation	**Computer Simulation**
(MC & MD & CPMD)	**(MD & CA & CPMD)**

PLAN

- Introduction
- Materials at Different Length Scales
- Concept of Density
- Density to Density Functional Theory (DFT)
- DFT of Hard Matter
  - Carbon Nanomaterials & Hydrogen Storage
  - Cluster-assembled Materials
  - Coarse-grained approach via atomic multipoles (charges and dipoles)
- DFT of Soft Matter
  - Structure & Dynamics at Interfaces
  - Flow through Nano Pores
- Dynamical Phenomena

Theory & Modeling

Systems

Phenomena

- Molecules
- Materials

- Chemical Reactions
- Physical Processes
- Biological Phenomena

Different Nuclei bonded together by Electron Glue

- Transition from one Spatial Configuration of Atoms to another.
- Spontaneous: Fluctuation Driven
- External Stimulus Driven: Response

Modeling: Complexity
Large Number of Variables:
          Many-Body Problem

- Hierarchical nature of scales inherent in all materials
  For understanding a property on a given length and time scales, it is crucial to understand / simulate the properties / mechanisms at all shorter length and time scales

- Multiscale ?

- Why Density ?

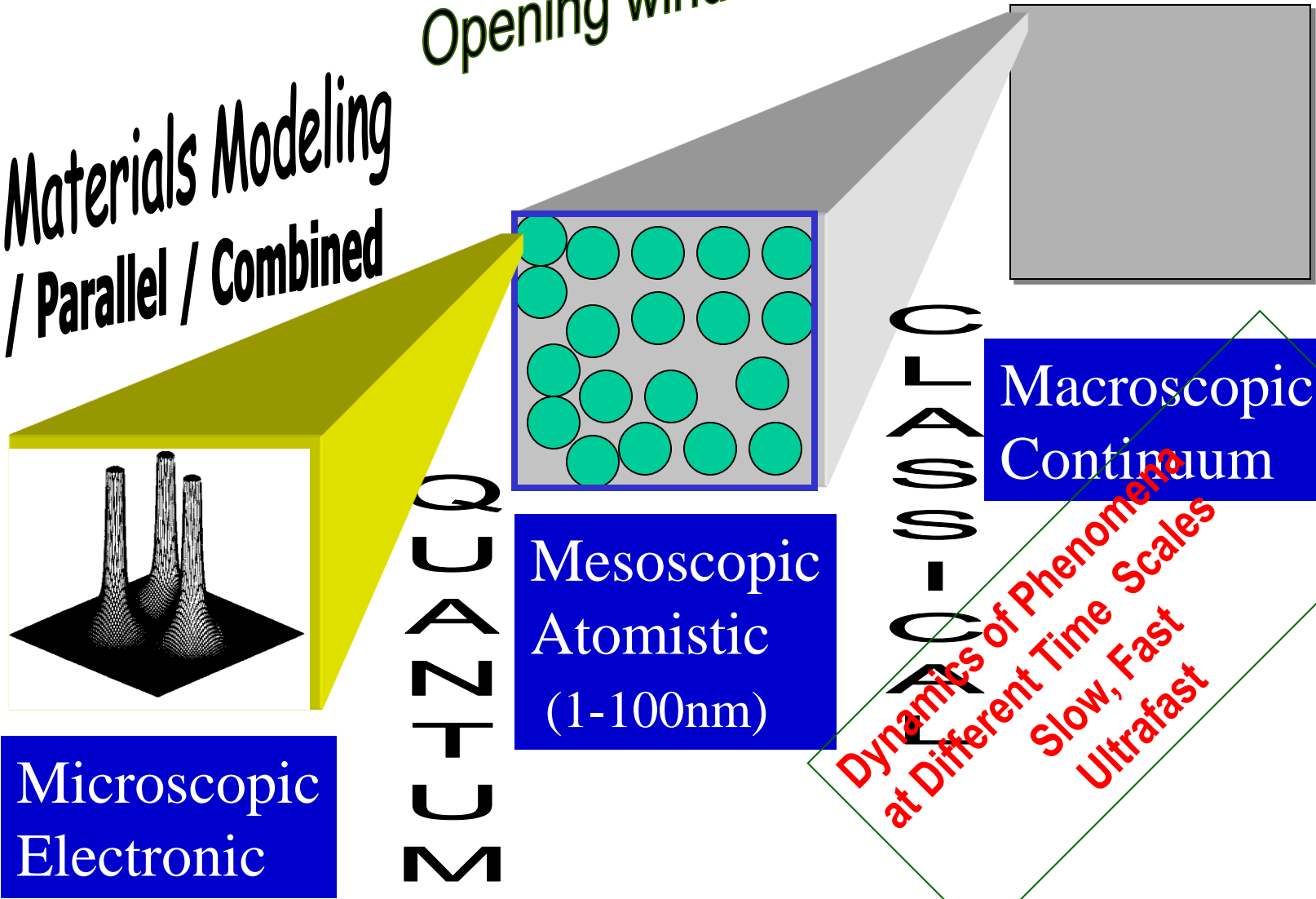- Density is a unique variable at all length scales and helps in unified approaches & hence comes as a rescue

Materials Modeling
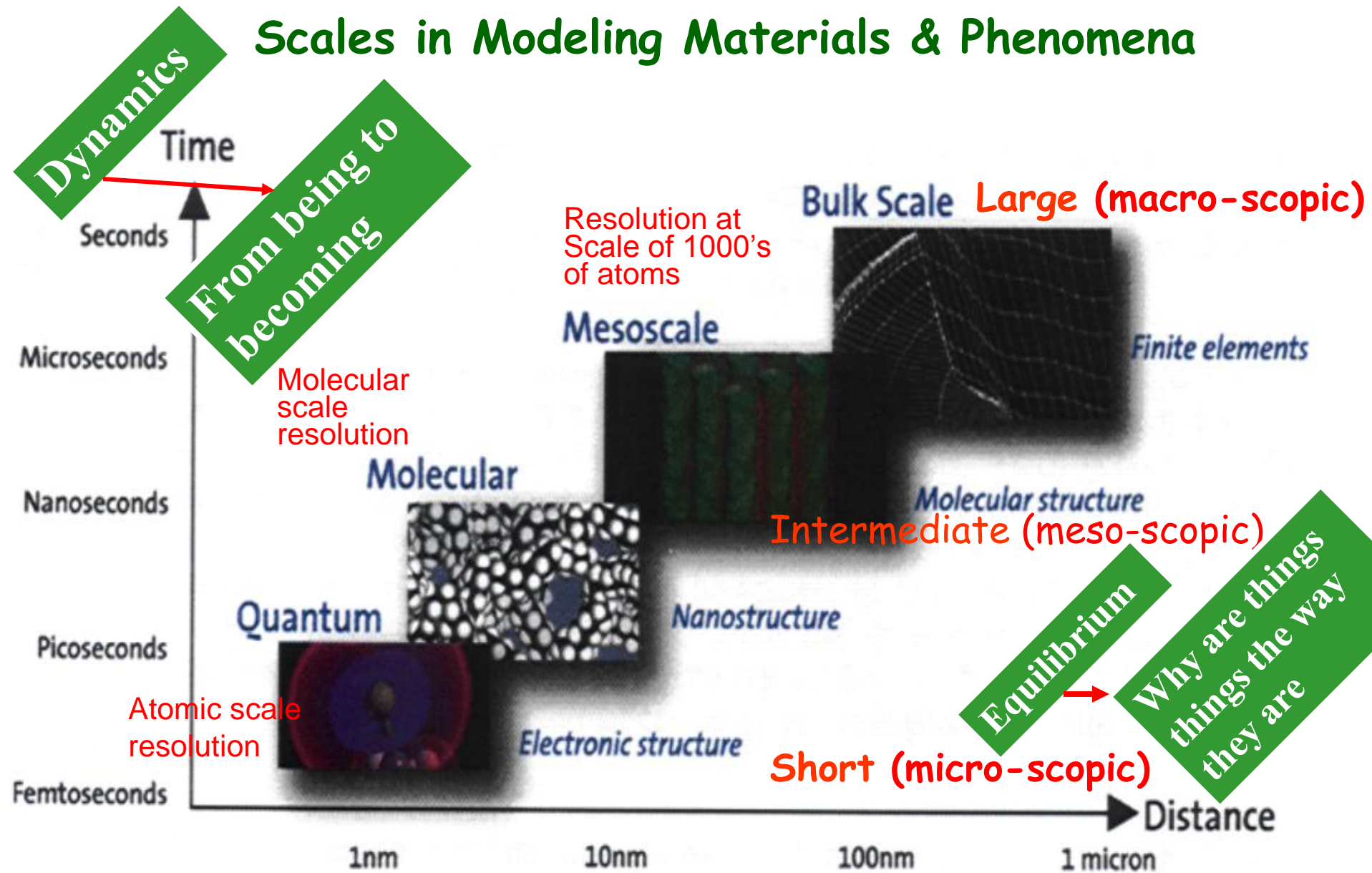
Design of Materials with Tunable Properties

Building bridges

Opening windows

Multiscale Materials Modeling
Sequential / Parallel / Combined

QUANTUM

CLASSICAL

Macroscopic
Continuum

Mesoscopic
Atomistic
(1-100nm)

Microscopic
Electronic

Dynamics of Phenomena
at Different Time Scales
Slow, Fast
Ultrafast

Scales in Modeling Materials & Phenomena

Dynamics

From being to becoming

Resolution at Scale of 1000's of atoms

Molecular scale resolution

Atomic scale resolution

Equilibrium

Why are things things the way they are

Large (macro-scopic)

Intermediate (meso-scopic)

Short (micro-scopic)

Time

Seconds

Microseconds

Nanoseconds

Picoseconds

Femtoseconds

Bulk Scale

Finite elements

Mesoscale

Molecular

Molecular structure

Quantum

Nanostructure

Electronic structure

Distance

1nm   10nm   100nm   1 micron

Concept of Density at Different Length Scales:

Density Concept in Materials Modelling at Different Length Scales

- Introduction & overview:
  - Electronic, atomistic & continuum descriptions
  - **Unifying theme: Density at different length scales**

- **Many-body problem: Need for a density description**
  - **Formal DFT: Density as the basic variable:**
  - **Practical scheme: Quantum vs Classical DFT**

- Application of quantum (electronic) DFT to materials
  - Chemical concepts: application to molecules & alloys
  - Cluster-assembled materials
  - Carbon Nano-systems: Curvature effect, H_2 storage

Application of classical (atomistic) DFT to materials
  - Soft condensed matter: Structure & ordering

- Application of Density Concept to dynamical phenomena
  - Diffusion & Relaxation in complex materials

- Summary & conclusion

Distribution of Particles in Space and Time:

The Concept of Density

Covers all length scales

Provides a unified nature of Methodology
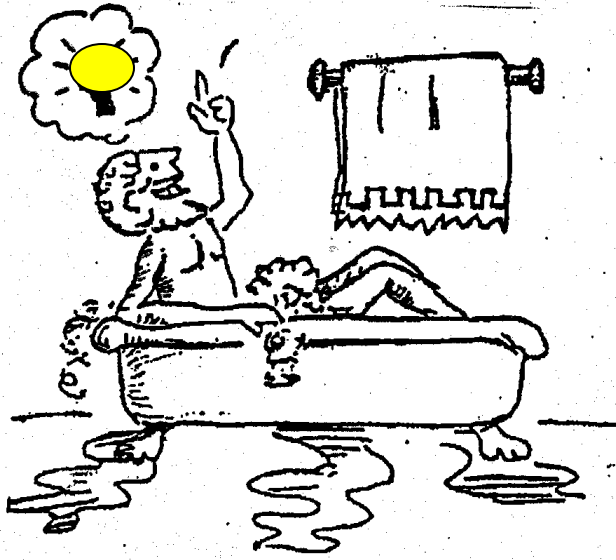
$\rho_0 d^3 = 0.6$

Present Work

Simulation

g(r)

r/d

O

H

H
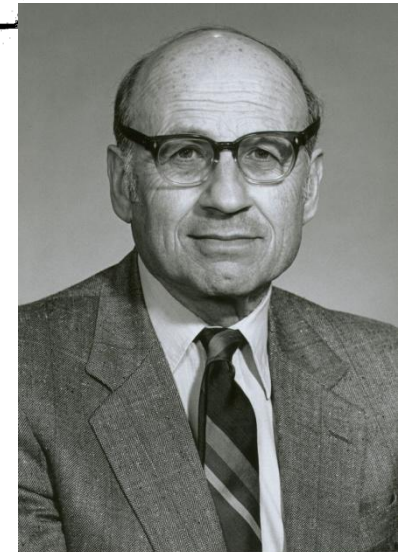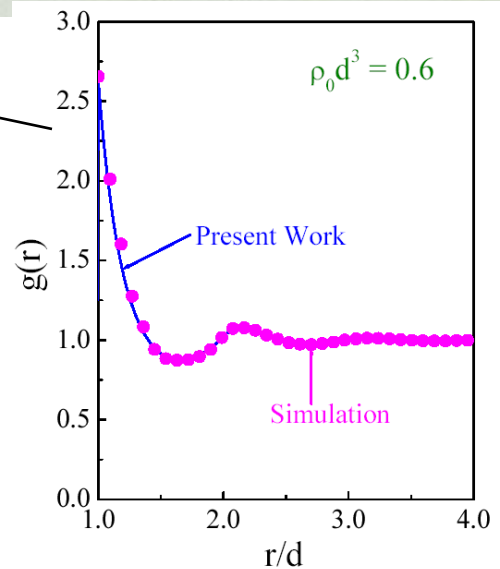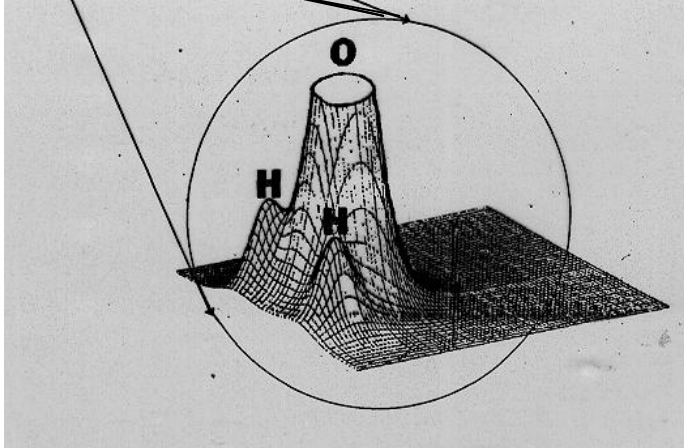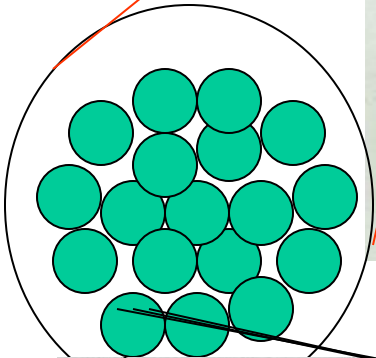
Length scale	Unit	Basic variable
Short	electron	electron density
Intermediate	atom	atom number density
Large	volume element	property density

:Problem:

How to calculate the density distribution for particles subjected to an external field/potential

Density: $\rho(r_1) = N \int .. \int dr_2 .. dr_N \, P(r_1, r_2, ..., r_N)$

DENSITY FUNC T IONAL THEORY (DFT)

DFT in Position Space $\rho(r)$, Momentum Space $\rho(p)$

Density Functional Theory in Property Space:
- Basic variable: P (E, t)
  - Probability of the system to have energy E at time t

:DFT at different length scales is not new:

- Well known as hydrodynamics for **macroscopic** length scale

- Hydrodynamics for **microscopic** length scale developed by Madelung (1928) by substituting $\psi(r,t)=R(r,t)\ exp[iS(r,t)/h]$
  - Quantum Hydrodynamics
  - Electron density $\rho(r,t) = R^2(r,t)$
  - Current density $j(r,t) = -\rho(r,t)\ \nabla S(r,t)$
    $(\partial\rho/\partial t)= - \nabla.j\ ;$
    $(\partial j/\partial t)= -\rho(r,t)\rho\nabla[\phi_{cl}(r,t) + V_{qu}(r,t;\ \rho)]$
  - Bloch (1930): Application to Optical Absorption

  Time-dependent

- Hydrostatics for **microscopic** length scale
  - Thomas Fermi theory for atoms (quantum)

- Hydrostatics for **mesoscopic** length scale
  - Debye-Huckel theory of electrolytes

  Time-independent

Quantum and classical DFT in the early days
Thomas Fermi & Debye Huckel theories

Quantum DFT (microscopic)
Thomas Fermi theory (1926-28)

- Electron density in atoms.
- Distribution of electrons around the nucleus
- Density $\rho(r)$ and potential $\phi(r)$
- TF Equation:
$$C \rho^{2/3} + \phi(r) = \mu = 0$$
- Poisson equation:
$$\nabla^2 \phi(r) = -4\pi\rho(r)$$
- Universal relation for atoms
$$E = \text{const. } Z^{7/3}$$
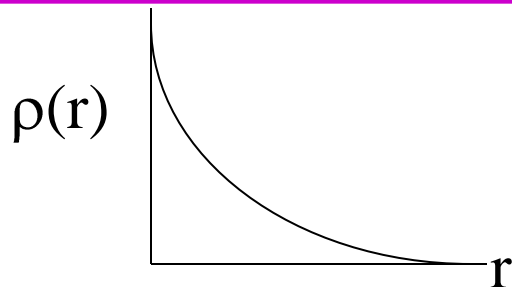
Classical DFT (mesoscopic)
Debye-Huckel theory (1923)

- Electrolyte solutions
- Distribution of ions around a charged object/ion.
- Density $\rho(r)$ and potential $\phi(r)$
- Boltzmann distribution:
$$\rho_\alpha(r) = \rho_\alpha^0 \exp(-q_\alpha\phi(r)/kT)$$
- Poisson equation:
$$\nabla^2 \phi(r) = -4\pi\Sigma_\alpha \, q_\alpha\rho_\alpha(r)$$
- Screened Coulomb potential:
$$\phi(r) = A \exp(-\kappa r)/r$$

$\rho(r)$ vs r

$\rho_\alpha(r)$ vs r
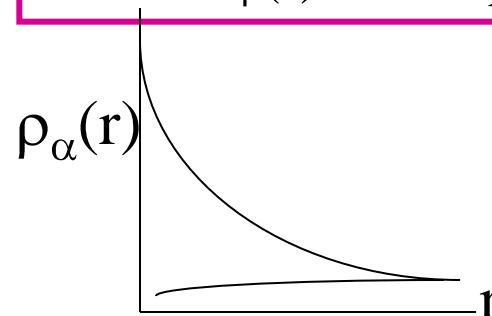
Birth of Formal Density Functional Theory

Problem: Energy or Free Energy cannot be as such expressed in terms of density alone

Quantum Systems: Energy

$$E = \langle \psi | H | \psi \rangle = \langle \psi | \Sigma_i v(r_i) + KE + \Sigma_i \Sigma_j 1/r_{ij} | \psi \rangle$$
$$= \int dr\, v(r)\rho(r) + T[\gamma(r;r')] + (1/2)\iint dr_1 dr_2 \Gamma_2(r_1, r_2)/r_{12}$$

Classical Systems: Free Energy

$$F = \int dr\, v(r)\rho(r) + F_{id}[\rho(r)] + (1/2)\iint dr_1 dr_2 \Gamma_2(r_1,r_2)u(r_1,r_2)$$

Solution: Hohenberg-Kohn-Mermin theorem (1964/1965)

(**1**) For a system of N-particles, characterised by an external potential $v(\mathbf{r})$, its density $\rho(\mathbf{r})$ determines $v(\mathbf{r})$ uniquely.

(**2**) The energy (Free Energy) is, in principle, uniquely determined by the single particle density $\rho(r)$.
It also assumes a minimum value at the true density.

Proof is only formal. Approximation needed in practice.

• Problems in Electronic DFT ?

> • Kinetic Energy Functional:
>> • Orbital free DFT
>
> • Exchange-correlation Energy Functional:
>> • Electrons in magnetic field in 2-D: Graphene
>
> • Simplification through coarse graining:
>> • Modeling through atomic Charges & dipoles
>
> • Cluster-assembled materials:
>> • Jellium model clusters

• Problems in Mesoscopic DFT ?

> • Soft matter under confinement
> • Passage through nanopores

• Problems in Property based DFT ?

> • Unified 1-D approach to multidimensional processes
> • Electron transfer reactions & solvation
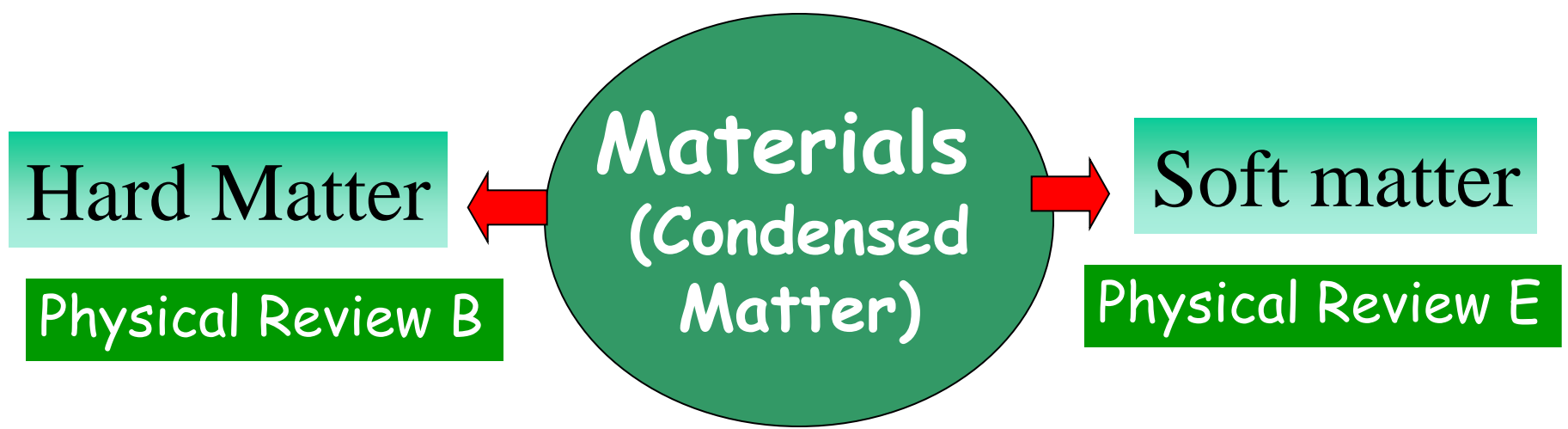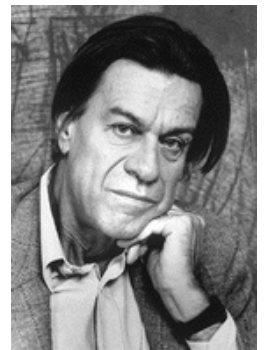
Form of MATTER that MATTERS

- *Traditional Bulk Solids : 3-D*
  - New class of materials of nanometer dimensions
    - $\Rightarrow$ Nanomaterials: *"Small is beautiful"*
      - Confinement: 2-D : Interfaces: Thin Films
      - 1-D : Quantum Wires
      - 0-D : Quantum Dots
  - Cluster-assembled materials: Quantum Dot Solids
    - Clusters (artificial atoms) as building blocks
- *Traditional Bulk Liquids : 3-D*
  - Confinement: Liquids at interfaces: 2-D
  - Soft Matter: Liquids, polymers, colloids, biological fluids
  - Granular Matter: Sands etc: Liquid like flow patterns
- *Molecules: Chemistry & biology*

Molecules & Materials through Theorist's Window:
Atoms (Nuclei) bonded together by Electron Glue

Conventional approaches

Microscopic

ATOMS, MOLECULES, CLUSTERS, SOLIDS

- Quantum mechanical approach

LIQUIDS & SOLIDS

Mesoscopic

- Statistical Mechanical approach
- Computer Simulation
  - Atomistic Description:
    - Classical (interaction assumed)
    - Ab-initio (on the fly quantum calculation)

Macroscopic

- Continuum Approach:
  - Hydrodynamics
  - Continuum mechanics

"Density based Multiscale Modeling: Theory & Application to Properties of Hard & Soft Materials"

Aim: Theory & Modeling within each length scale & also building bridges between the different length scales through the relevant density variables in two major ways:

(i) In a sequential approach, where different properties are calculated within the shorter length scale, which are then used either in simulation or a theoretical modelling in the next higher length scale

(ii) In a combined or simultaneous approach, where the two adjacent length scales are treated in a coupled manner.

BUILDING BRIDGES & OPENING WINDOWS

Multi-Scale Materials Modeling

Microscopic
• Electronic
• Quantum

Mesoscopic
• Atomistic
• Classical

Macroscopic
• Continuum
• Classical

Interatomic Potentials

Property Parameters

Atomic parameters

Atomistic Simulation

Modeling binding:
the atom-atom glue

Density based theory

Mixed length scales simultaneously treated
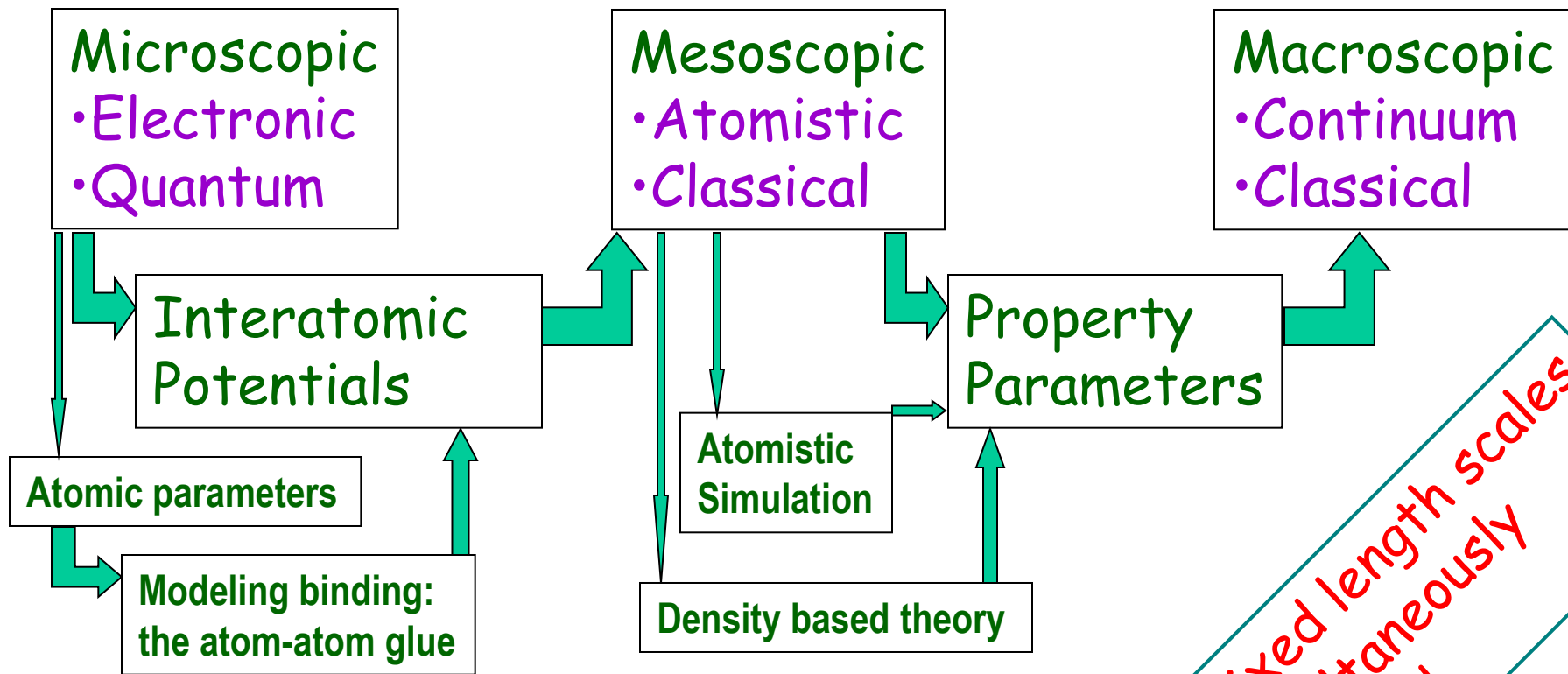
Sequential approach: **Divide & Conquer**

Combined approach : **Bridging the Length Scales**
: **Car-Parrinello & Analogous approaches**

SEQUENTIAL APPROACH

Electronic Length Scale:
- Interelectronic potential is known
- Pseudopotentials used for simplification of ion-electron potential

Atomistic Length Scale

Interatomic potential unkown (obtainable from Electronic Length Scale)

Ab initio calculation at various atomic positions

Problem: Too many data: Parametrization

Modeling the atom-atom glue

Hard Sphere, Lennard Jones

Point charge / dipole model, (Polarizable charge/dipole)

Embedded atom model

Reactive force field

Electronegativity equalization method

To next length scale ....

COMBINED APPROACH

Electronic & atomistic length scales

Interatomic potential in situ

Car Parrinello approach

Others ??? To next length scale......

1985 Trieste
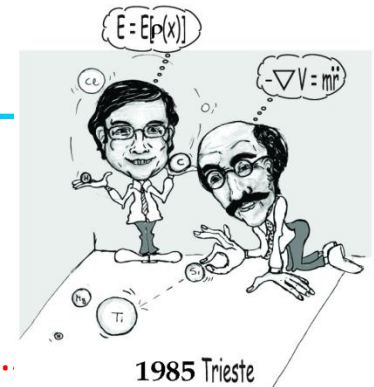
Multiscale Materials Modeling:

· Mixed length scale treatment of materials:

Approaches that unify all length scales

Distribution of Particles in Space and Time:
The Concept of Density
Covers all length scales
Unified nature of Methodology

Lattice Model
· Widely used in Magnetism & Physics in general
· Obvious in atomistic / mesoscopic domain
Macroscopic: Lattice Boltzmann approach / Finite element
Microscopic: Lattice model of the electron cloud

Modeling Hard & Soft Materials through Density Functional Theory at Different Length Scales

- Introduction & overview:
  - Electronic, atomistic & continuum descriptions
  - Unifying theme: Density at different length scales

- Many-body problem: Need for a density description
  - Formal DFT: Density as the basic variable:
  - Practical scheme: Quantum vs Classical DFT

- Application of quantum (electronic) DFT to materials
  - Chemical concepts: application to molecules & alloys
  - Cluster-assembled materials
  - Carbon Nano-systems: Curvature effect, H_2 storage

Application of classical (atomistic) DFT to materials
  - Soft condensed matter: Structure & ordering

- Application of Density Concept to dynamical phenomena
  - Diffusion & Relaxation in complex materials

- Summary & conclusion

Modern DFT: Practical Implementation

Quantum DFT

Classical DFT

Non-interacting particles

One-particle Schrodinger eqn.
$\{-(1/2)\nabla^2 + v(r)\} \psi_i = \varepsilon_i \psi_i$

Boltzmann distribution
$\rho_\alpha(r) = \rho_\alpha^0 \exp(-v_\alpha(r)/kT)$

Real interacting system

Concept of noninteracting particles moving in an effective potential

Interacting particles

$V_{ext}(r)$
Actual potential

Non-interacting particles

$V_{eff}(r)$
Effective potential

Modern DFT: Practical Implementation

Quantum DFT   *Non-interacting particles*   **Classical DFT**

One-particle Schrodinger eqn.

$$\{-(1/2)\nabla^2 + v(r)\}\ \psi_i = \varepsilon_i \psi_i$$

Boltzmann distribution

$$\rho_\alpha(r) = \rho_\alpha^0 \exp(-v_\alpha(r)/kT)$$

Real interacting system

Concept of noninteracting particles moving in an effective potential

Kohn-Sham equation: Effective one-particle Schrodinger eqn.

$$\{-(1/2)\nabla^2 + v_{eff}(r)\}\ \psi_i = \varepsilon_i \psi_i$$

$$\rho(r) = \sum n_i |\psi_i|^2$$

Energy $E = \int dr\ v(r)\rho(r)$

$+ T_s[\rho(r)] + E_{COUL}[\rho] + E_{xc}[\rho]$

$v_{eff}(r; \rho) = v(r) + (\delta E_{COUL}[\rho]/\delta\rho)$

$+ (\delta E_{xc}[\rho]/\delta\rho)$

Kinetic energy functional (exact)

Exchange correlation energy functional (need approximation)

Density equation: Effective Boltzmann like distribution

$$\rho_\alpha(r) = \rho_\alpha^0 \exp(-v_{eff,\alpha}(r)/kT)$$

Free Energy $F = \int dr\ v(r)\rho(r)$

$+ F_{id}[\rho(r)] + F_{ex}[\rho(r)]$

$v_{eff}(r; \rho) = v(r) + kT\ C^{(1)}(r;\rho)$

where $kT\ C^{(1)}(r;\rho) = (\delta F_{ex}[\rho]/\delta\rho)$

Ideal gas free energy functional:

Classical entropy terms (exact)

Excess free energy functional (need approximation)

QUANTUM MECHANICS of
MOLECULES, CLUSTERS, SOLIDS
An Electron Density Description

$$\{-(1/2)\nabla^2 + v_{eff}(r)\} \psi_i = \varepsilon_i \psi_I ; \quad \rho(r) = \Sigma\, n_i |\psi_i|^2$$

$$v_{eff}(r; \rho) = v(r) + (\delta E_{COUL}[\rho]/\delta\rho) + (\delta E_{xc}[\rho]/\delta\rho)$$

Hard Matter

Interparticle correlations

Statistical mechanics of LIQUIDS:
A Mesoscopic Density Description

$$\rho_\alpha(r) = \rho_\alpha^0 \exp(-v_{eff,\alpha}(r)/kT)$$

$$v_{eff}(r; \rho) = v(r) + kT\, C^{(1)}(r;\rho); \quad kTC^{(1)}(r;\rho) = (\delta F_{ext}[\rho]/\delta\rho)$$

Soft Matter

Interparticle correlations

Hell on Wheels for Commuters: Highly Concentrated Dispersed System

Short range correlation

Hell on Wheels for Commuters: Highly Concentrated Dispersed System

Short range correlation

"Dilute Dispersed System".

Long range correlation

On the right hand side, free seats are available and *solute particles can sit in the free seats. Most solute particles, however, sit voluntarily on the left hand side. This indicates some kind of correlations (attractive here) between the solute particles.*

DFT for Quantum Systems:
(Electron density as basic variable)

Electronic structure calculation using DFT
- **Carbon based Nano-Materials**
  - Application to Hydrogen storage materials
- **Cluster-assembled materials**
  - Clusters (artificial atoms) as building blocks

Simple Concepts in DFT: Quantum Systems
- A **LIGHT** step to a **SOUND** interpretation
  - Coarse-graining of electron density
    Atomic charges & dipoles:
      Lattice model for molecules
        & Cluster assemblies

Carbon based nanomaterials

Carbon nanostructured materials: Fullerenes, nanoscrolls, nanofibers, graphene, multiwall nanotubes, carbon platelets, etc.

Although the basic building unit in all these materials is carbon atom, why are their properties so different from each other?

Graphite

Graphene

A. Saber, 2003.

Nanotubes
Iijima 1991
Smalley 1993

Layered poorly conducting semimetal used in pencils, fuses and nuclear fusion moderators
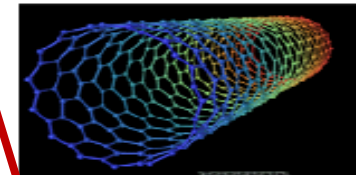
Curvature is one of the key factors

Physical Properties of Carbon Nanotubes
Satoh, Dresselhau, Dresselhaus, Imperial College Press 1998

- Chemical reactivity of various types of carbon nanomaterials
  - Curvature of the materials
  - Charge at the Surface
    - Role in enhancement of Hydrogen adsorption

Nanoscale Curvature-Induced Hydrogen Adsorption in Alkali Metal Doped Carbon Nanomaterials

K. R. S. Chandrakumar, K. Srinivasu, and Swapan K. Ghosh*

Theoretical Chemistry Section, Chemistry Group, Bhabha Atomic Research Centre, Mumbai—400 085, India

Received: March 5, 2008; Revised Manuscript Received: July 22, 2008
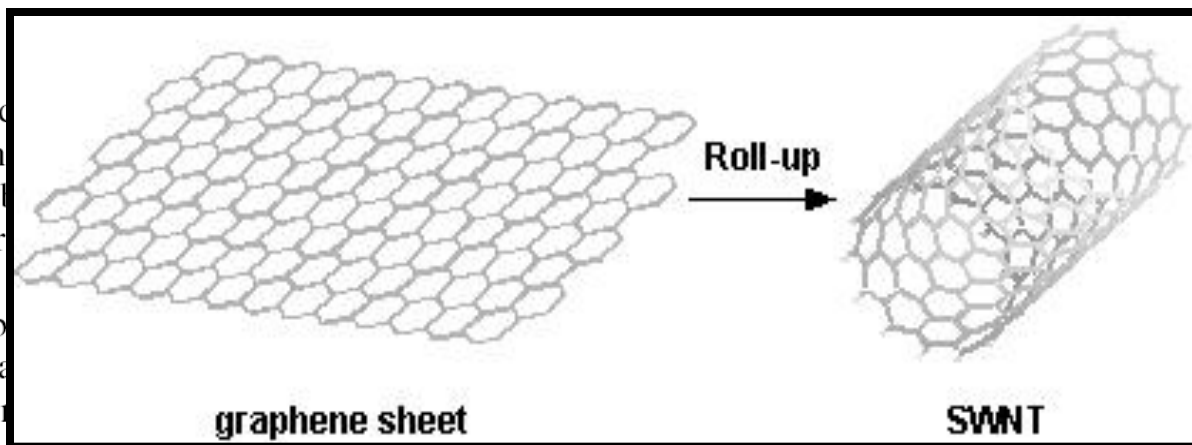
We have ... rbon nanomaterials can be en... nanosurface. This effect is o... ncept of curvature, derived fr... tor to measure the reactivity ... ter or radius alone may not b... s its magnitude can give valua... e demonstrate the application... ydrogen adsorption.

graphene sheet   Roll-up   SWNT
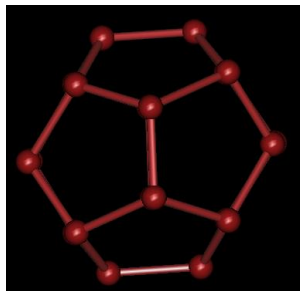
Fullerenes ----------

C
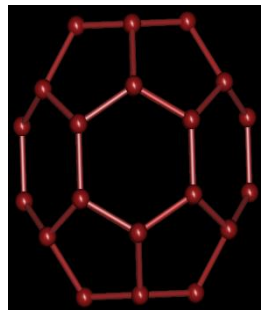
C

C28

C

C

C

Nanotubes-----

H₂

X⁺(X=Li,Na)

Li⁺(H₂)₄

Na⁺(H₂)₆
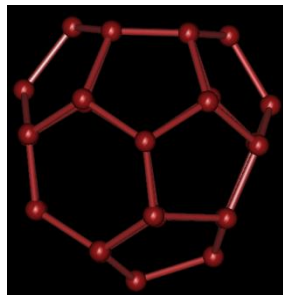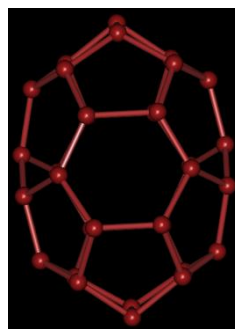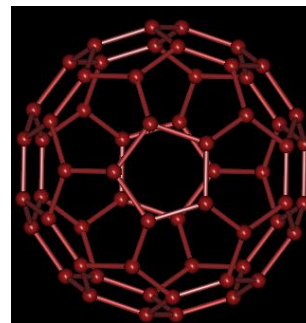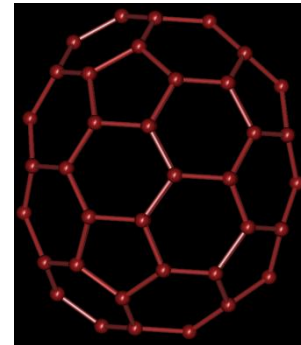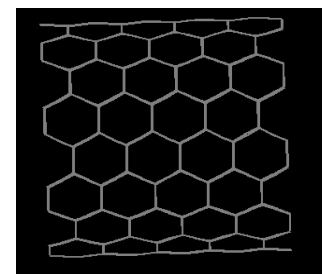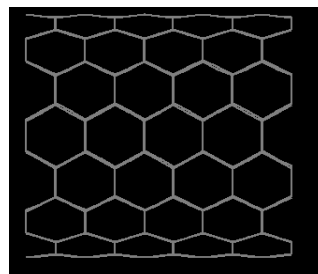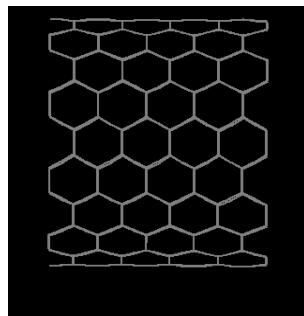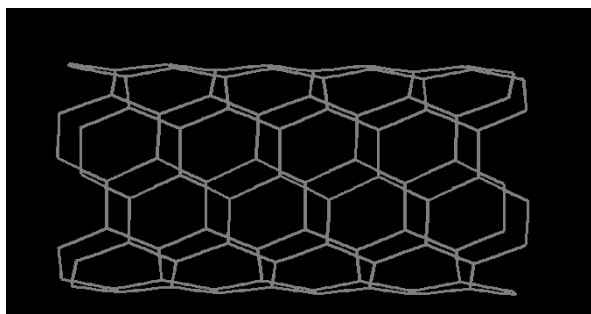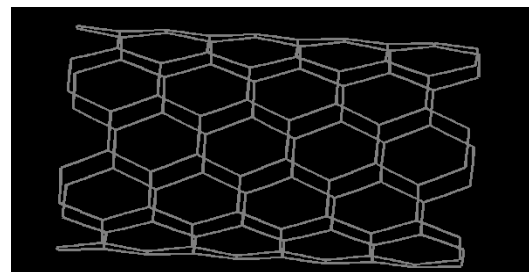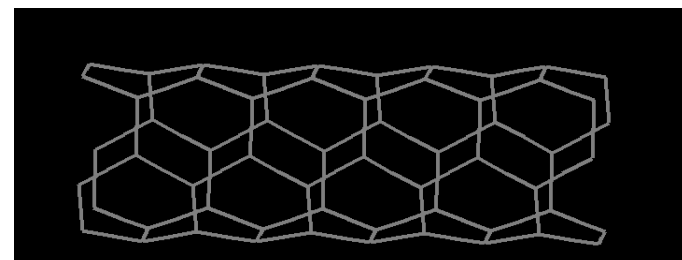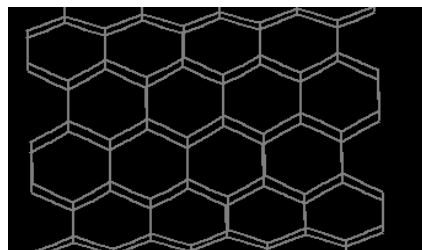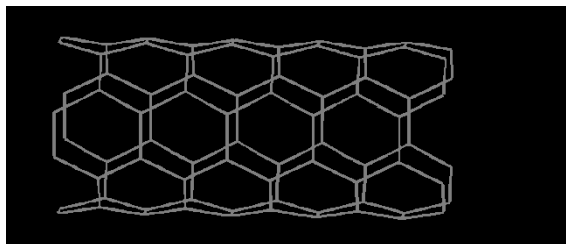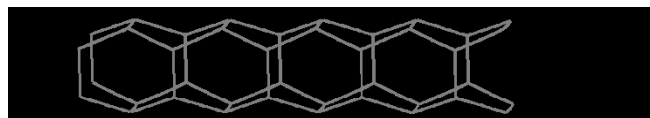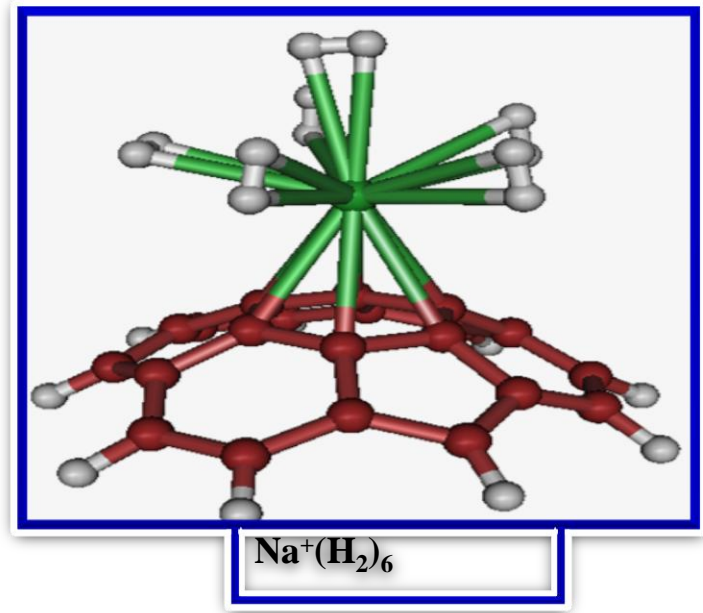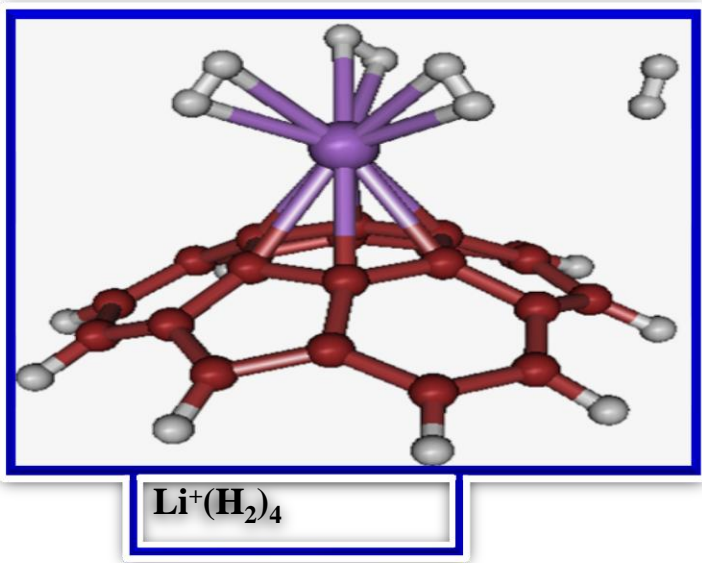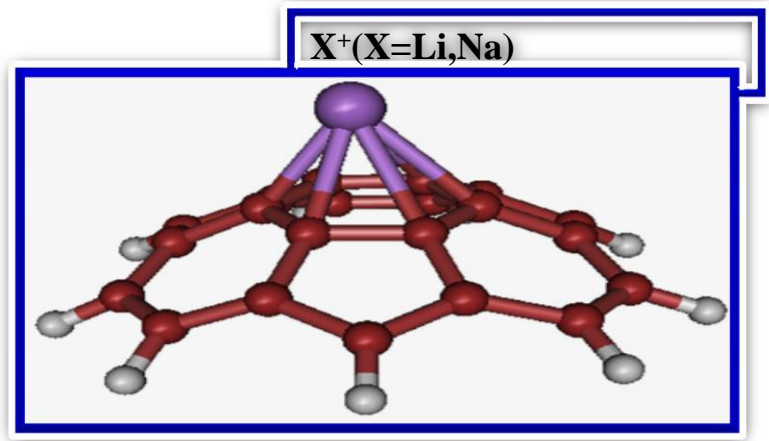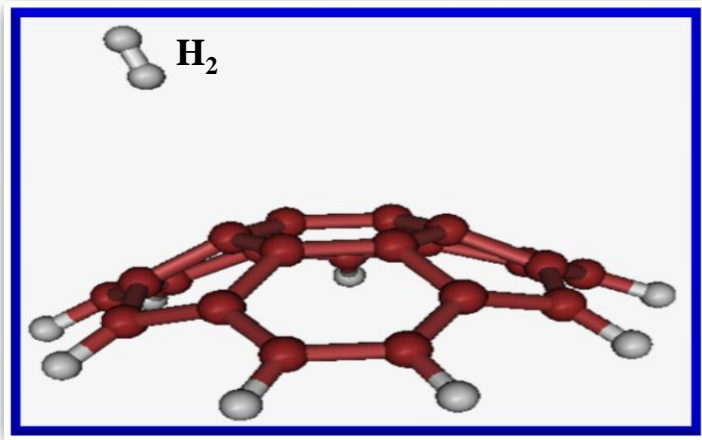
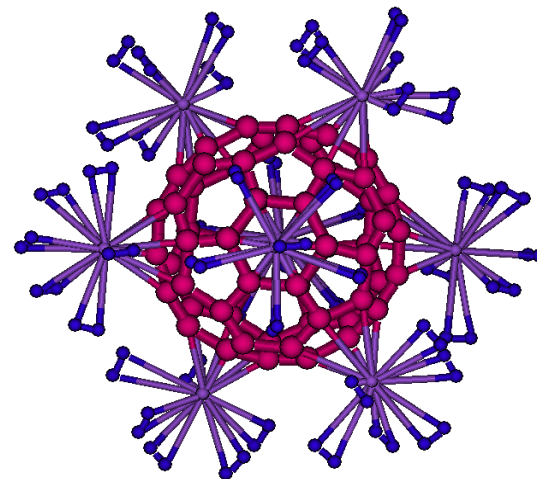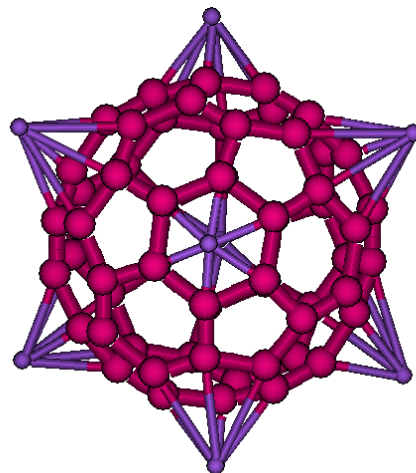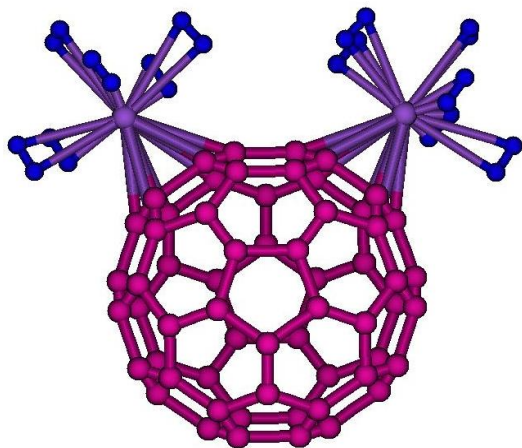# Alkali-Metal-Induced Enhancement of Hydrogen Adsorption in C_{60} Fullerene: An *ab Initio* Study

K. R. S. Chandrakumar* and Swapan K. Ghosh

Theoretical Chemistry Section, Chemistry Group, Bhabha Atomic Research Centre, Mumbai 400 085, India

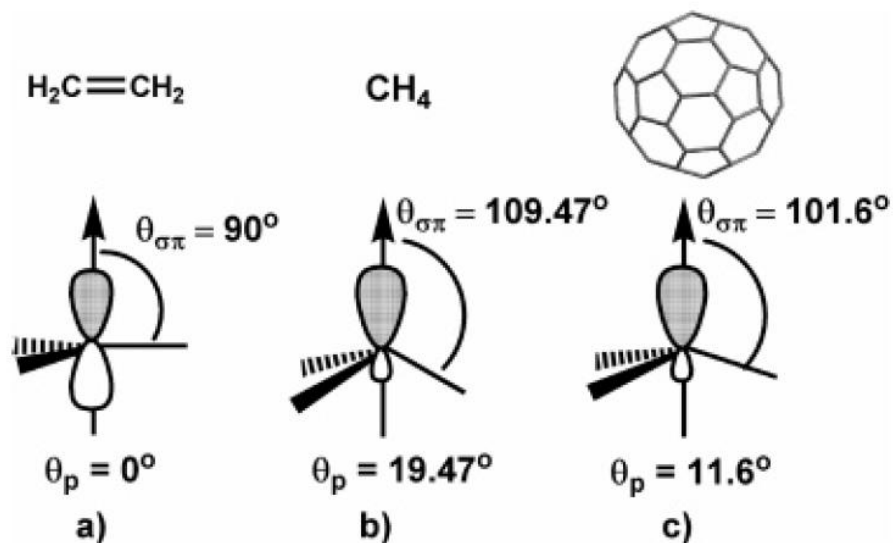| Systems	C-X Bond length	MetalC_{60} Binding energy	Charge on the metal atoms	Bond length M-H_2	Binding energy of H_2	Charge on the metal atoms
LiC_{60}	2.268	-35.02	0.42 (0.74)	2.200	-5.33 (2)	0.14 (0.53)
NaC_{60}	2.478	-32.61	0.55 (0.89)	2.581	-10.33 (6)	0.11 (0.59)
KC_{60}	2.971	-32.75	0.62 (0.68)	3.080	-7.24 (6)	0.62 (0.68)
Na$_2$C$_{60}$	2.430	-65.61	0.50 (0.86)	2.562	-19.25 (12)	0.26 (0.57)
Na$_8$C$_{60}$	2.460	-220.93	0.35 (0.71)	2.591	-97.85 (48)	0.11 (0.59)

Curvature induced molecular interaction: Possible Origin

Curvature might be an important factor behind the reactivity of fullerenes or nanotubes in comparison to graphene or graphite

- The configuration at each carbon atom in fullerenes is not planar, but slightly pyramidal in nature: consistent with some sp3 character present in the essentially sp2 carbons.

- Presence of 5-membered rings provide the curvature necessary for forming a closed cage structure.

- The *sp*2-hybrized carbon atom in C_{60} is slightly pyramidal; the angle between its pπ-orbital and the σ-bonds is larger than 90° leading to formation of curved π-conjugation within the carbon surfaces of fullerenes .

$H_2C = CH_2$ CH_4

$\theta_{\sigma\pi} = 90°$ $\theta_{\sigma\pi} = 109.47°$ $\theta_{\sigma\pi} = 101.6°$

$\theta_p = 0°$ $\theta_p = 19.47°$ $\theta_p = 11.6°$

a)   b)   c)

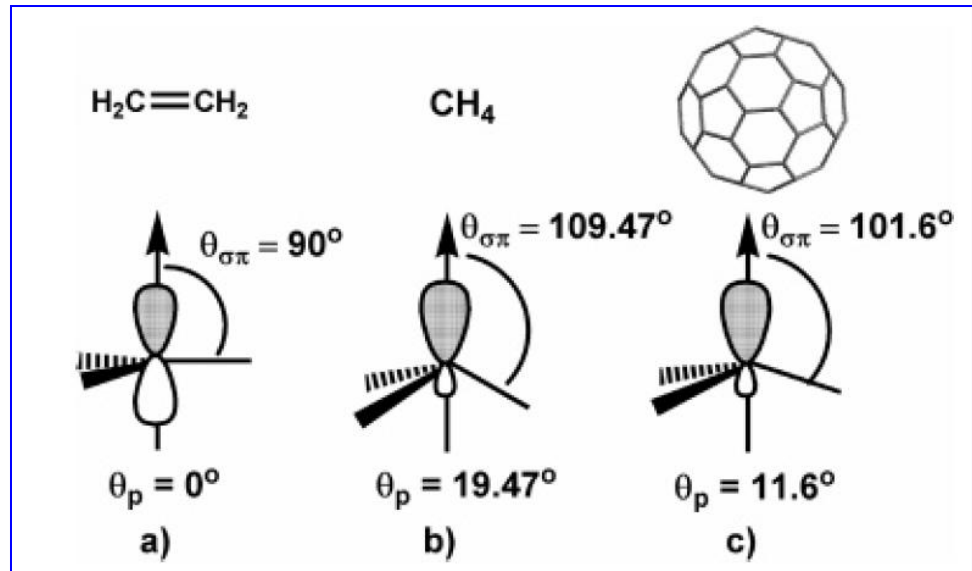Curved hexagonal or hybrid hexagon - pentagon carbon-carbon networks.

Curvature induced molecular interaction: Possible Origin

Curvature might be an important factor behind the reactivity of fullerenes or nanotubes in comparison to graphene or graphite

- The configuration at each carbon atom in fullerenes is not planar, but slightly pyramidal in nature: consistent with some sp3 character present in the essentially sp2 carbons.

- Presence of 5-membered rings provide the curvature necessary for forming a closed cage structure.

- The *sp*2-hybrized carbon atom in C_{60} is slightly pyramidal; the angle between its $p\pi$-orbital and the σ-bonds is larger than $90°$ leading to formation of curved π-conjugation within the carbon surfaces of fullerenes .

Curved hexagonal or hybrid hexagon - pentagon carbon-carbon networks.

- The structural diversity in carbon based nanomaterials is predominantly due to the modifications in the electronic structure essentially driven by the degree & nature of hybridization of the valence orbitals of carbon atoms depending on structural topology & dimensionality.
- The curvature of the carbon surface plays an important role in determining the physical and chemical properties of these materials in a significant way. The effect of curvature can be as large as the effects due to the defects or vacancies created at the surface.
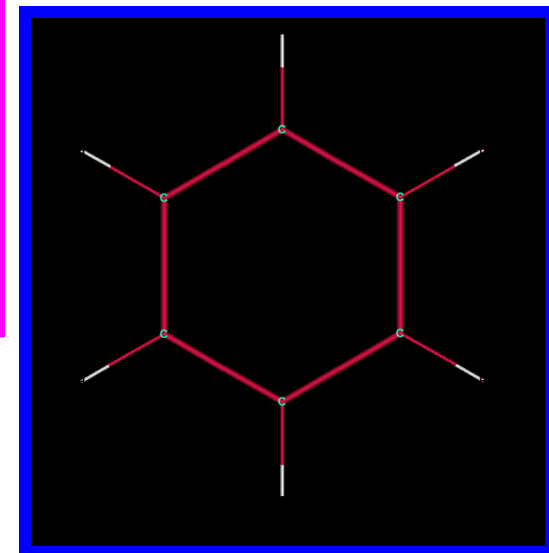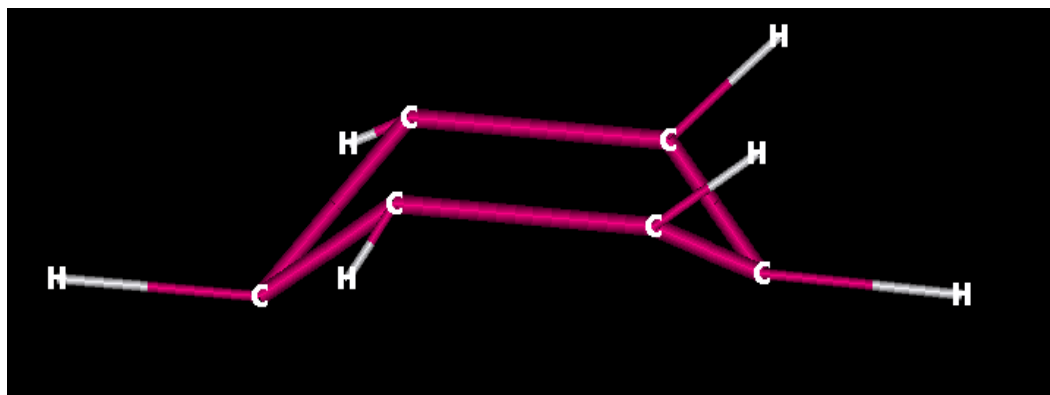
Structure of planar and curved benzene

- Consider Benzene molecule as prototype system
- Create the effect of curvature artificially
- The dihedral angle is varied (0^0 to 35^0)
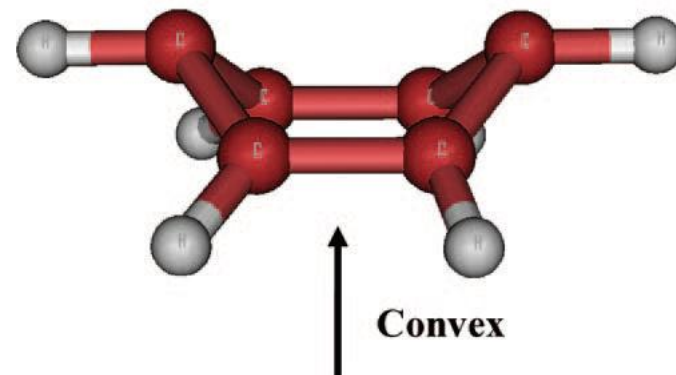- The structurally deformed benzene molecule is allowed to interact with H_2 molecule & Na atom

Intra-deformed Benzene-Concave
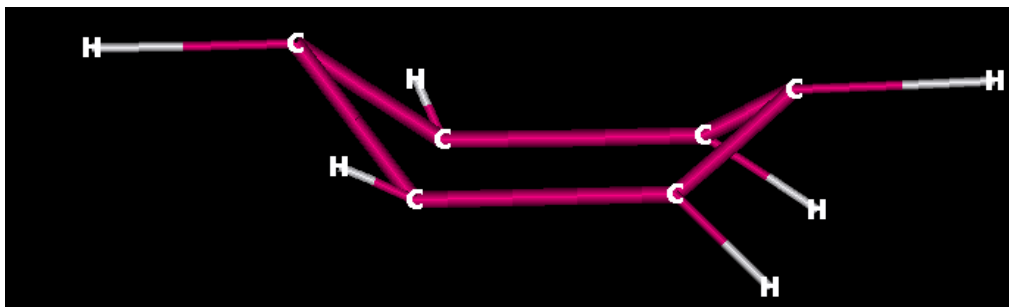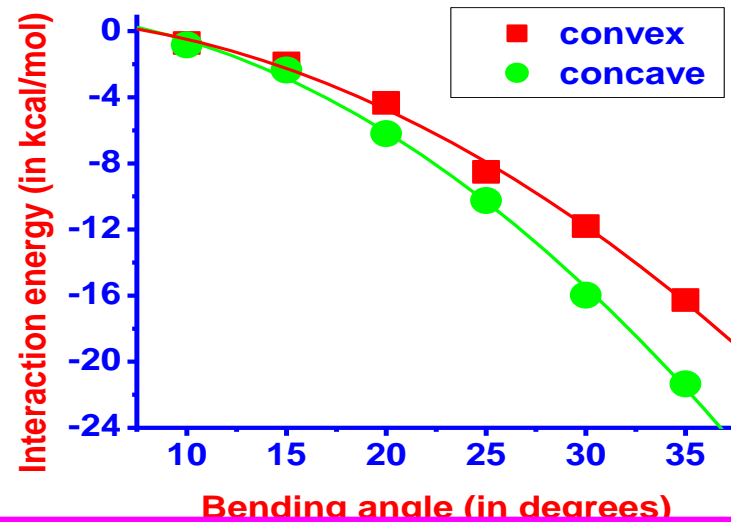

Intra-deformed Benzene-Convex
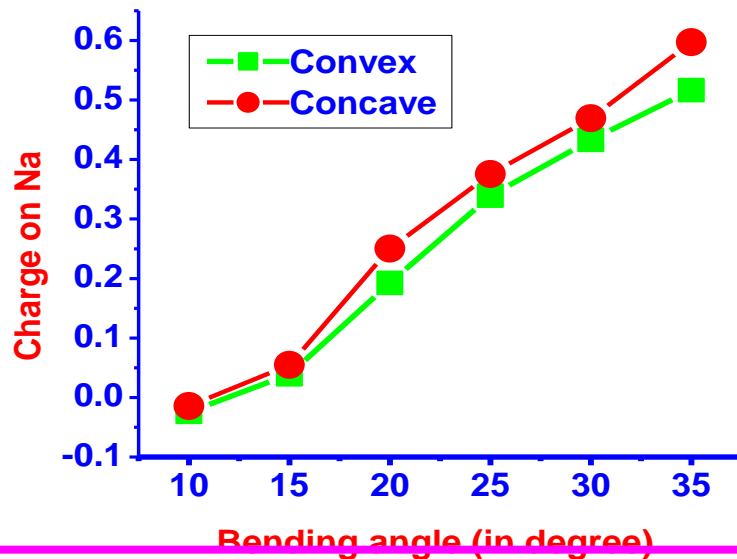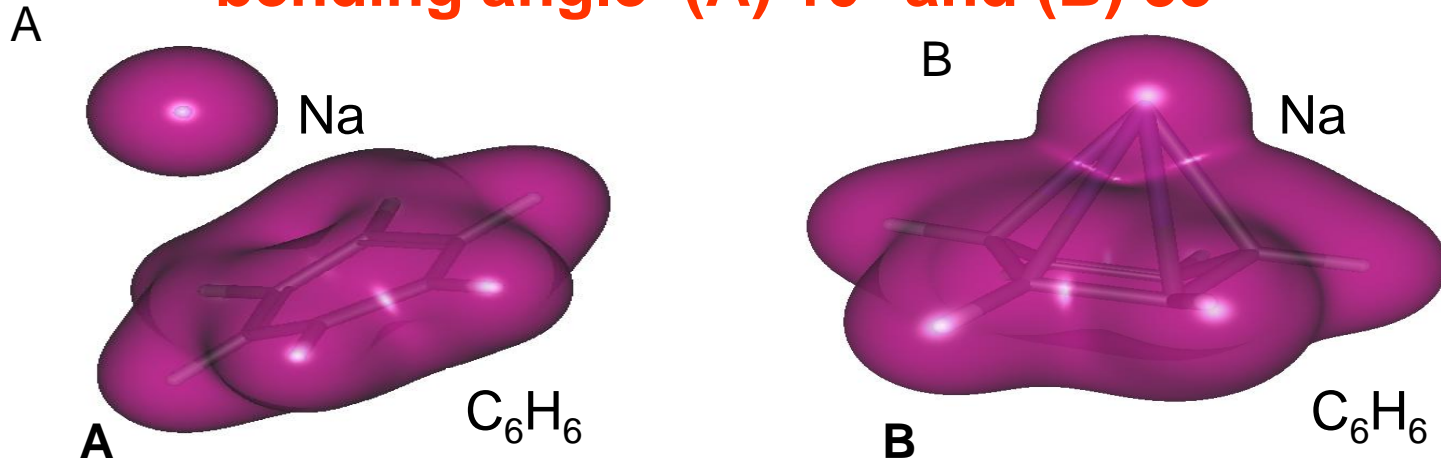

Concave

Convex

Curvature induced molecular interaction

Electron charge density distribution in Na-C_6H_6 with the bending angle (A) 10° and (B) 35°


What is the optimum curvature to have the desired property of a nanomaterial ?

What do we address ?

1. Isolated single alkali metal cation:
   - Interaction with molecular Hydrogen:
     - Energetics ?
     - Number of Hydrogen Molecules that can be bound to a single ion ?
     - **Nature & strength of the cation-hydrogen interaction**

2. Can the alkali metal systems be suitable as components of materials for hydrogen storage ?

3. Whether these cations can still retain their affinity towards the hydrogen even in the presence of solid frameworks (host materials) supporting the ions ?

4. How do we prepare such materials ?

5. Whether there is a preference of alkali metal cations in comparison to transition metal ions ?
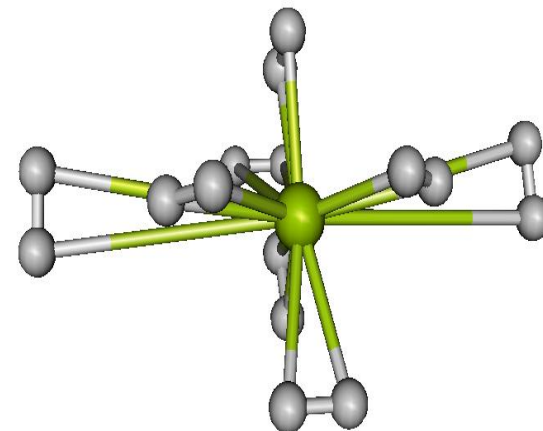
Adsorption of hydrogen molecules at single metal ion center
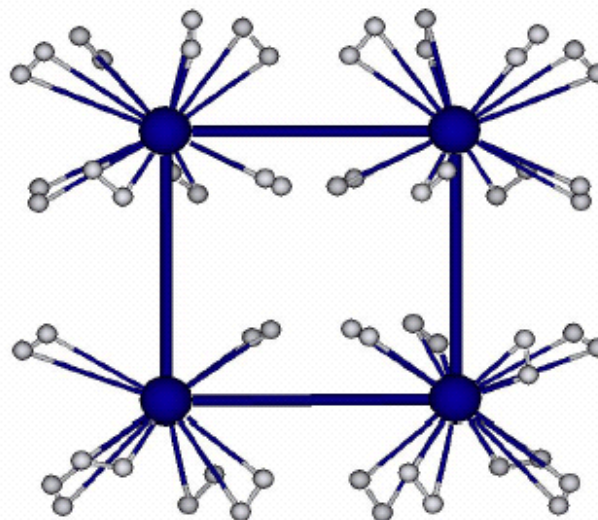
MH_{16}
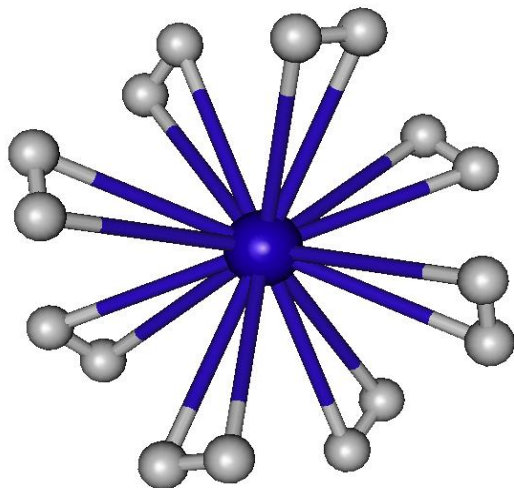
LiH_{12}
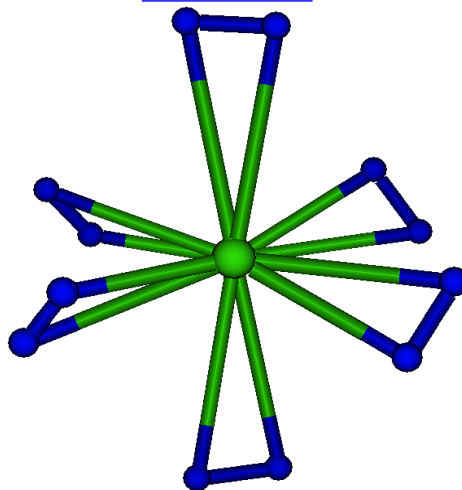
BeH_{12}

Model for adsorption of hydrogen molecules at multiple metal ion centers at fixed distance

Optimized dimer structure of $Na(H_2)_8$ With the cation-cation distance of 4Å
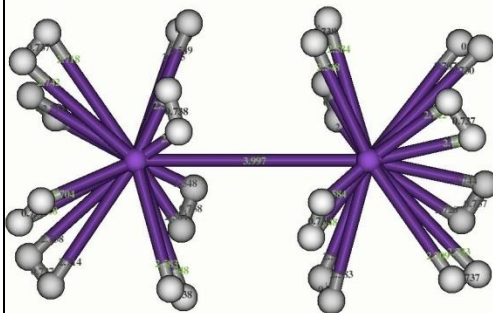
Optimized tetramer structure of $Na(H_2)_8$ with the cation-cation distance of 5Å.

Concept of negative ion-molecular hydrogen interactions

F⁻(H₂)₈   Cl⁻(H₂)₈   Br⁻(H₂)₈

$F^-(H_2)_8$ $Cl^-(H_2)_8$ $Br^-(H_2)_8$
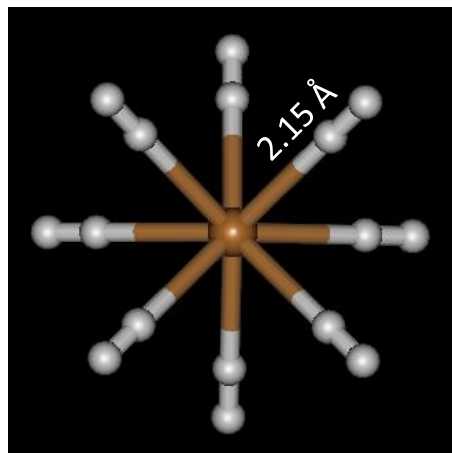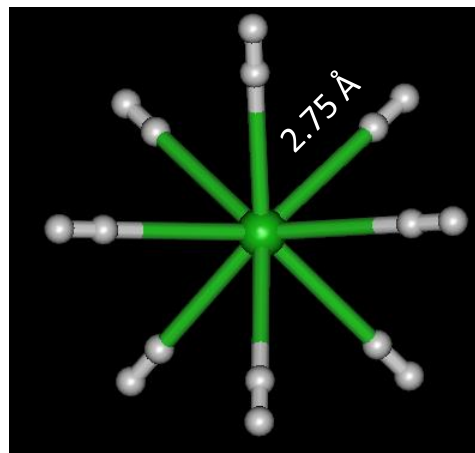
$E_{int} = -4.22$ kcal/mol $E_{int} = -2.47$ kcal/mol $E_{int} = -2.43$ kcal/mol
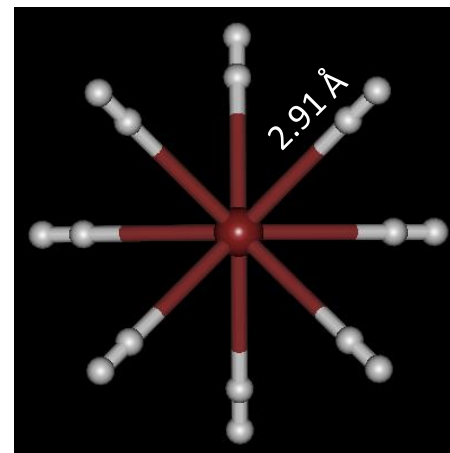
◆ Halide ions and molecular hydrogen interactions are stronger than that of cation interactions …
◆ Halide ion complex of metal ions or Prussian blue

Alkali metal cluster aggregation on Fullerenes
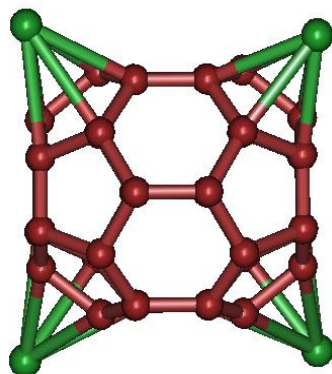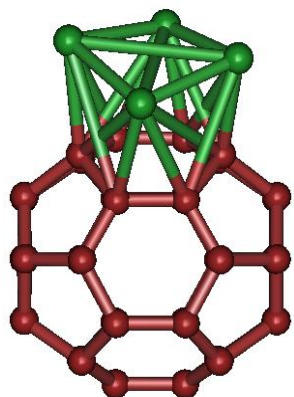
ΔE = -9.42 kcal/mol
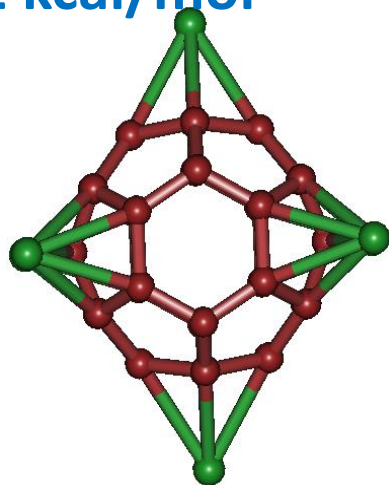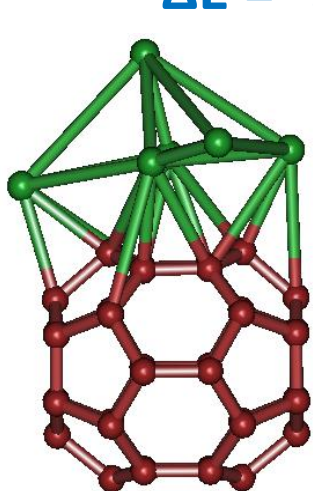
ΔE = -34.52 kcal/mol

- **Transition metal atoms tend to aggregate on fullerenes which will have adverse effects on the hydrogen adsorption.**
- **However, alkali metal atoms do not form aggregates & remain as atoms with fullerenes**

- **Fullerene-alkali atoms adduct is preferred in comparison to the alkali metal atom clusters**

(1) **The cohesive energy of transition metal atoms is more than that of alkali atoms.**
(2) **Alkali metal atom-atom interaction is much weaker than the fullerene-alkali metal atom interactions**

- **Alkali metal atom doped fullerene complexes can act as an effective hydrogen storage materials.**

Molecules to Functional Materials

$E_{int}(Na)=-40.0$ kcal/mol per Na

$E_{int}(H_2)=-1.90$ kcal/mol per H_2
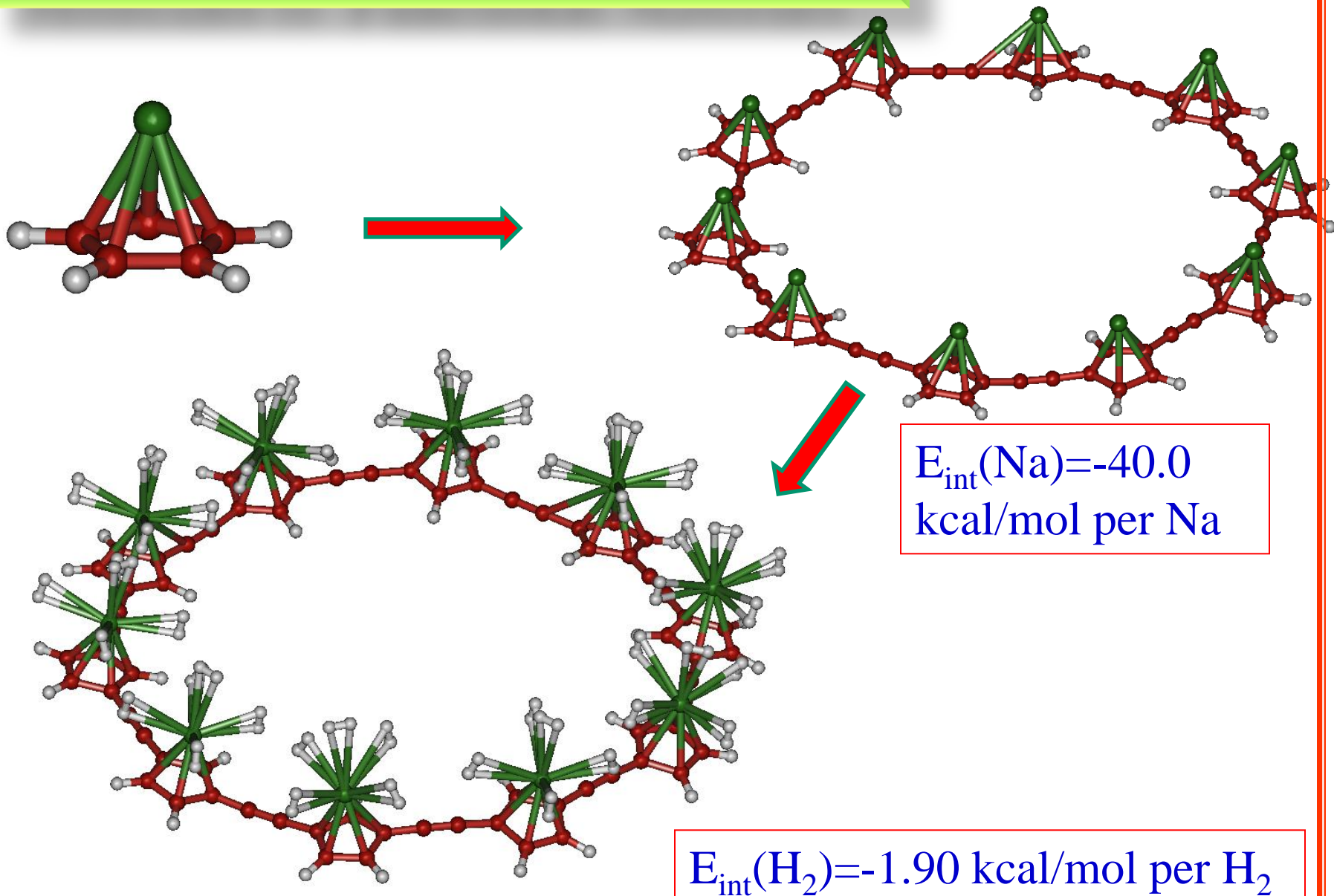
METAL DECORATED CARBON NANOMATERIALS AS FUNCTIONAL MATERIALS FOR HYDROGEN STORAGE

1. Conventional Hydrogen Storage Materials do not yet satisfy all the criteria for efficiency & cost effectiveness

2. Major challenge : Search for a cost effective material with high hydrogen adsorption capacity with reversible hydrogen adsorption/ desorption characteristics at ambient conditions

Two major forms of Hydrogen Storage

Atomic Hydrogen
Chemisorption

Molecular Hydrogen
Physisorption/
Chemisorption

Present work: Theory and modeling of the interaction of Molecular Hydrogen with Novel Molecules and Materials to gain basic understanding & insight into the problems for the design of efficient Hydrogen Storage Materials

Our approach : Molecules to Materials

1. Insight into various aspects of the design or development of novel materials for hydrogen storage requires an understanding of the fundamentals of hydrogen adsorption at the molecular level.

2. Some prerequisite Conditions:
   a) Light weight materials
   b) Number of adsorbed hydrogen molecules should be as high as possible
   c) The interaction strength should be moderate (4-12 kcal/mol)

Our approach : Molecules to Materials

1. Insight into various aspects of the design or development of novel materials for hydrogen storage requires an understanding of the fundamentals of hydrogen adsorption at the molecular level.

2. Some prerequisite Conditions:
   a) Light weight materials
   b) Number of adsorbed hydrogen molecules should be as high as possible
   c) The interaction strength should be moderate (4-12 kcal/mol)

3. Our system : s-block metals & their ions:
   Li, Na, K, Be, Mg and Ca

4. The chemistry of interaction between metal cations and molecular hydrogen is important for the applications in hydrogen storage materials and to understand many catalytic processes.

DFT for Quantum Systems:
(Electron density as basic variable)

Electronic structure calculation using DFT
- **Carbon based Nano-Materials**
  - Application to Hydrogen storage materials
- **Cluster-assembled materials**
  - Clusters (artificial atoms) as building blocks)

Simple Concepts in DFT: Quantum Systems
- A **LIGHT** step to a **SOUND** interpretation
  - Coarse-graining of electron density
    Atomic charges & dipoles:
      Lattice model for molecules
        & Cluster assemblies

- Atomic Parameters for modelling Molecules
- An Atomic Lattice Model for Molecules
- Molecular electron density $\rho(r)$ as a superposition of densities at atomic sites

Electronegativity equalisation: A principle for binding

Limitations: *no rigorous quantum mechanical definition*
no theoretical basis for equalisation
no description of covalent binding

$$E[\rho] = \int dr\, v(r)\, \rho(r) + F[\rho]; \qquad \mu = \delta E/\delta\rho(r) = v(r) + \delta F[\rho]/\delta\rho(r)$$

Covalent binding: *Quantum mechanical effect*
no interatomic charge transfer
electron delocalisation
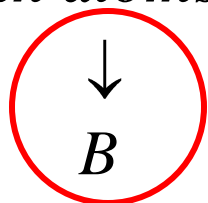*interatomic spin transfer*

Electronegativity and chemical binding

(1) Electron delocalisation:

   charge transfer to the bond region

(2) Spin transfer: Role of unpaired electrons

   in atoms for covalent bond formation
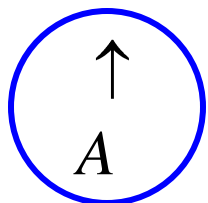
charge density: $\rho(r) = \rho_\uparrow(r) + \rho_\downarrow(r)$

spin density: $s(r) = \rho_\uparrow(r) - \rho_\downarrow(r)$

Spin-dependent generalised electronegativity:

$$\mu_\uparrow = \delta E/\delta\rho_\uparrow \qquad \mu_\downarrow = \delta E/\delta\rho_\downarrow$$
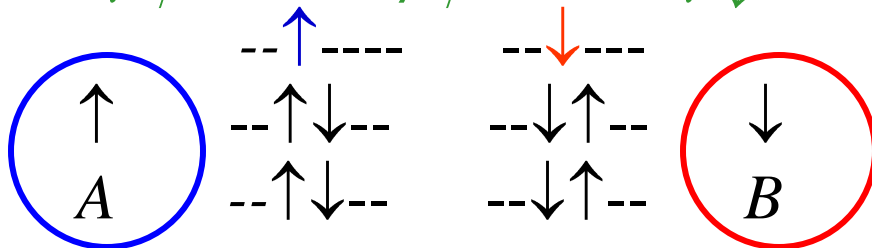
Equalisation of $\mu_\uparrow$ and $\mu_\downarrow$ in the two atoms determine $\Delta N_\uparrow$ and $\Delta N_\downarrow$ and hence charge and spin transfer. providing measures of ionicity & Covalency.

Spin transfer alone accounts for homonuclear binding.

T. K. Ghanty and S. K. Ghosh, *J. Amer. Chem. Soc. (1994).*

Miedema theory & heat of formation of alloys

Heat of formation of AB alloy

$$\Delta H_{AB} = -P(\chi_A - \chi_B)^2 + Q\,[\,(\rho_{ws}{}^{A})^{1/3} - (\rho_{ws}{}^{B})^{1/3}\,]^2$$
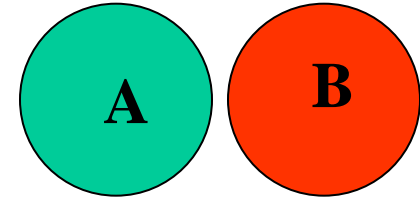
$\chi \rightarrow$ *electronegativity* ; $\rho_{ws} \rightarrow$ *density at the boundary*

Volume change on alloy formation (chemical origin)

$$\Delta V \approx P(\chi_A - \chi_B) + [\,(\rho_{ws}{}^{A})^{-1} - (\rho_{ws}{}^{B})^{-1}\,]$$
$$[\,(\rho_{ws}{}^{A})^{-1/3} - (\rho_{ws}{}^{B})^{-1/3}\,]^{-1}$$

Solid solubilities

Linear relation between metal compressibility and electron density at the boundary
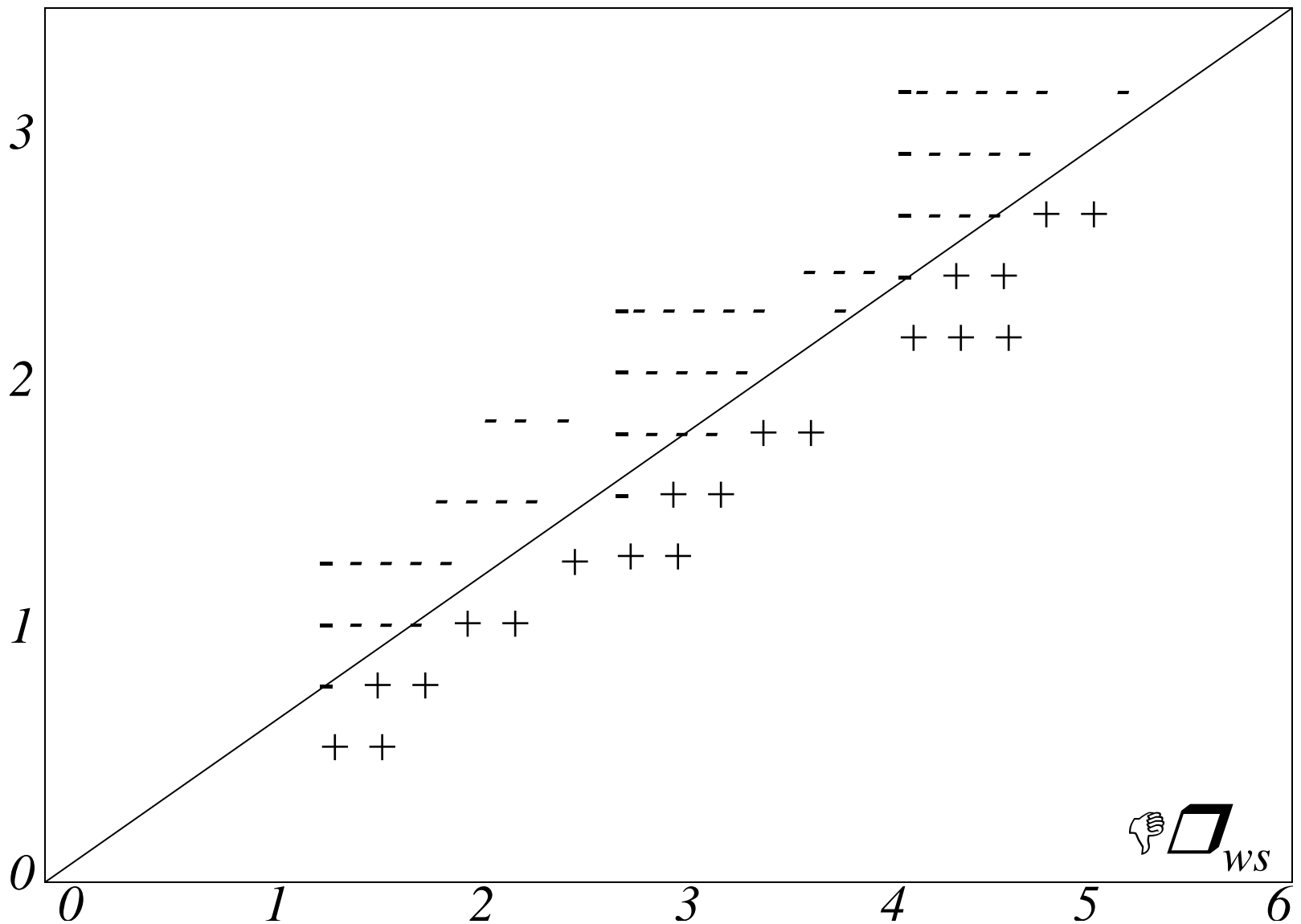
Sign of heat of formation for alloys of two transition metals plotted as a function of the difference of electronegativity, ☞χ and the discontinuity of electron density, ☞$\square_{ws}$

An Atomic Lattice Model for Molecules

Coarse graining of electron density in terms of partial atomic charges & atomic dipoles

- *Modelling chemical binding and response properties in terms of atomic charges & dipoles, the zeroeth and first moments of the electron density rather than the full function*

- *Binding energy through a functional perturbation in terms of the electron density change*

A density functional theory-based chemical potential equalisation approach to molecular polarizability

AMITA WADEHRA[1] and SWAPAN K GHOSH*

Theoretical Chemistry Section, Chemistry Group, Bhabha Atomic Research Centre, Mumbai 400 085, India

[1]Present address: Department of Physics, Ohio State University, Columbus, OH 43210, USA

e-mail: skghosh@magnum.barc.ernet.in

Response of molecular assemblies to an external electric field

$$E_v[\rho(\mathbf{r})] = \int d\mathbf{r} \rho(\mathbf{r}) v(\mathbf{r}) + F[\rho(\mathbf{r})]$$

$$\mu = \frac{\delta E_v[\rho(\mathbf{r})]}{\delta \rho(\mathbf{r})} = v(\mathbf{r}) + \frac{\delta F[\rho(\mathbf{r})]}{\delta \rho(\mathbf{r})} \qquad \eta(\mathbf{r}, \mathbf{r}') = \left(\frac{\delta^2 F[\rho(\mathbf{r})]}{\delta \rho(\mathbf{r}) \delta \rho(\mathbf{r}')} \right)$$

Binding energy through a functional perturbation in terms of the electron density change

$$\Delta E = E[\rho(\mathbf{r}) + \delta\rho(\mathbf{r}), v(\mathbf{r}) + \delta v(\mathbf{r})] - E[\rho(\mathbf{r}), v(\mathbf{r})]$$

$$= \int d\mathbf{r} \left(\frac{\delta E[\rho(\mathbf{r})]}{\delta \rho(\mathbf{r})} \right)_{v(\mathbf{r})} \delta\rho(\mathbf{r}) + \int d\mathbf{r} \left(\frac{\delta E[\rho(\mathbf{r})]}{\delta v(r)} \right)_{\rho(\mathbf{r})} \delta v(\mathbf{r})$$

$$+ \frac{1}{2} \iint d\mathbf{r} d\mathbf{r}' \left(\frac{\delta^2 E[\rho(\mathbf{r})]}{\delta \rho(\mathbf{r}) \delta \rho(\mathbf{r}')} \right)_{v(\mathbf{r})} \delta\rho(\mathbf{r}) \delta\rho(\mathbf{r}')$$

$$+ \frac{1}{2} \iint d\mathbf{r} d\mathbf{r}' \left(\frac{\delta^2 E[\rho(\mathbf{r})]}{\delta v(\mathbf{r}) \delta v(\mathbf{r}')} \right)_{\rho(\mathbf{r})} \delta v(\mathbf{r}) \delta v(\mathbf{r}')$$

$$+ \iint d\mathbf{r} d\mathbf{r}' \left(\frac{\delta^2 E[\rho(\mathbf{r})]}{\delta \rho(\mathbf{r}) \delta v(\mathbf{r}')} \right) \delta\rho(\mathbf{r}) \delta v(\mathbf{r}').$$

Model the molecular density in terms of atomic ones

$$\delta\rho(\mathbf{r}) = \sum_\alpha \delta\rho_\alpha(\mathbf{r}) = \sum_\alpha \delta\rho_\alpha(\mathbf{r}_\alpha),$$

where $\mathbf{r}_\alpha = \mathbf{r} - \mathbf{R}_\alpha$ denotes the atom-centered coordinate with the origin located at the α-th atom.

$$\mu_\alpha = \mu_\alpha^0 + \delta v(\mathbf{r}_\alpha) + \int d\mathbf{r}' \eta(\mathbf{r}_\alpha, \mathbf{r}') \delta\rho(\mathbf{r}')$$

$$= \mu_\alpha^0 + \delta v(\mathbf{r}_\alpha) + \sum_\beta \int d\mathbf{r}'_\beta \eta(\mathbf{r}_\alpha, \mathbf{r}'_\beta) \delta\rho_\beta(\mathbf{r}'_\beta)$$

$$\delta v(\mathbf{r}_\alpha) = \delta v(\alpha) + \mathbf{r}_\alpha \cdot \nabla_\alpha \delta v(\alpha) + \tfrac{1}{2}\mathbf{r}_\alpha^2 \nabla_\alpha^2 \delta v(\alpha) + \dots$$

$$\eta(\mathbf{r}_\alpha, \mathbf{r}'_\beta) = \eta(\alpha, \beta) + \mathbf{r}_\alpha \cdot \nabla_\alpha \eta(\alpha, \beta) + \mathbf{r}'_\beta \cdot \nabla_\beta \eta(\alpha, \beta)$$

$$+ \tfrac{1}{2}\mathbf{r}_\alpha^2 \nabla_\alpha^2 \eta(\alpha, \beta) + \tfrac{1}{2}\mathbf{r}'^2_\beta \nabla_\beta^2 \eta(\alpha, \beta)$$

$$+ \mathbf{r}_\alpha \mathbf{r}'_\beta \nabla_\alpha \nabla_\beta \eta(\alpha, \beta) + \dots,$$

Model the molecular density in terms of atomic ones

$$\delta\rho(\mathbf{r}) = \sum_\alpha \delta\rho_\alpha(\mathbf{r}) = \sum_\alpha \delta\rho_\alpha(\mathbf{r}_\alpha),$$

where $\mathbf{r}_\alpha = \mathbf{r} - \mathbf{R}_\alpha$ denotes the atom-centered coordinate with the origin located at the α-th atom.

$$\mu_\alpha = \mu_\alpha^0 + \delta v(\mathbf{r}_\alpha) + \int d\mathbf{r}' \eta(\mathbf{r}_\alpha, \mathbf{r}')\delta\rho(\mathbf{r}')$$

Express the chemical potential in terms of density moments

$$q_\beta = -\Delta N_\beta^{el} = -\int d\mathbf{r}'_\beta \delta\rho_\beta(\mathbf{r}'_\beta)$$

$$\mathbf{p}_\beta = \int d_\beta' \mathbf{r}' \, \delta\rho_\beta(\mathbf{r})$$

to obtain

$$\mu_\alpha = \mu_\alpha^0 + \delta v(\alpha) - \sum_\beta \eta(\alpha, \beta)q_\beta + \sum_\beta \nabla_\beta \eta(\alpha, \beta)\mathbf{p}_\beta$$

$$0 = \mathbf{E}_\alpha + \sum_\beta \nabla_\alpha \eta(\alpha, \beta)q_\beta - \sum_\beta \nabla_\alpha \nabla_\beta \eta(\alpha, \beta)\mathbf{p}_\beta$$

$$\mu_\alpha = \mu_\alpha^0 - \eta_\alpha^0 q_\alpha + \left(\phi_\alpha^0 - \sum_{\beta=1}^{N}{}' \eta_{\alpha\beta}^{0,0} q_\beta + \sum_{\beta=1}^{N}{}' \vec{\eta}_{\alpha\beta}^{0,1} \cdot \mathbf{p}_\beta \right),$$

$$\alpha = 1, 2, ..., N$$

$$\delta\mathbf{p}_\alpha = \overleftrightarrow{\alpha}_\alpha \cdot \left(\mathbf{E}^0 - \sum_{\beta=1}^{N}{}' \overleftrightarrow{\eta}_{\alpha\beta}^{1,1} \delta q_\beta - \sum_{\beta=1}^{N}{}' \overleftrightarrow{\eta}_{\alpha\beta}^{1,1} \delta\mathbf{p}_\beta \right),$$

$$\alpha = 1, 2, ..., N,$$

Linear equations for the atomic charges & dipoles

$$\sum_{\beta=1}^{N} b_{\alpha\beta}^{0,0} \delta q_\beta + \sum_{\beta=1}^{N} \vec{c}_{\alpha\beta}^{0,1} \cdot \delta\mathbf{p}_\beta = d_\alpha, \quad \alpha = 1, 2, ..., N,$$

$$\sum_{\beta=1}^{N} \vec{h}_{\alpha\beta}^{1,0} \delta q_\beta + \sum_{\beta=1}^{N} \overleftrightarrow{k}_{\alpha\beta}^{1,1} \cdot \delta\mathbf{p}_\beta = \vec{s}_\alpha, \quad \alpha, = 1, 2, ..., N,$$

Dipole moment & hence the polarizability from atomic charges & dipoles

$$\delta\mathbf{p}_{mol} = \sum_{\alpha=1}^{N} (\mathbf{R}_\alpha \delta q_\alpha + \delta\mathbf{p}_\alpha)$$

Charges for CH$_4$ molecule

Atom	Charge[a]	Charge [b]
C	-0.484	-0.497
H	0.121	0.124
H	0.121	0.124
H	0.121	0.124
H	0.121	0.124

Charges for C$_2$H$_6$ molecule

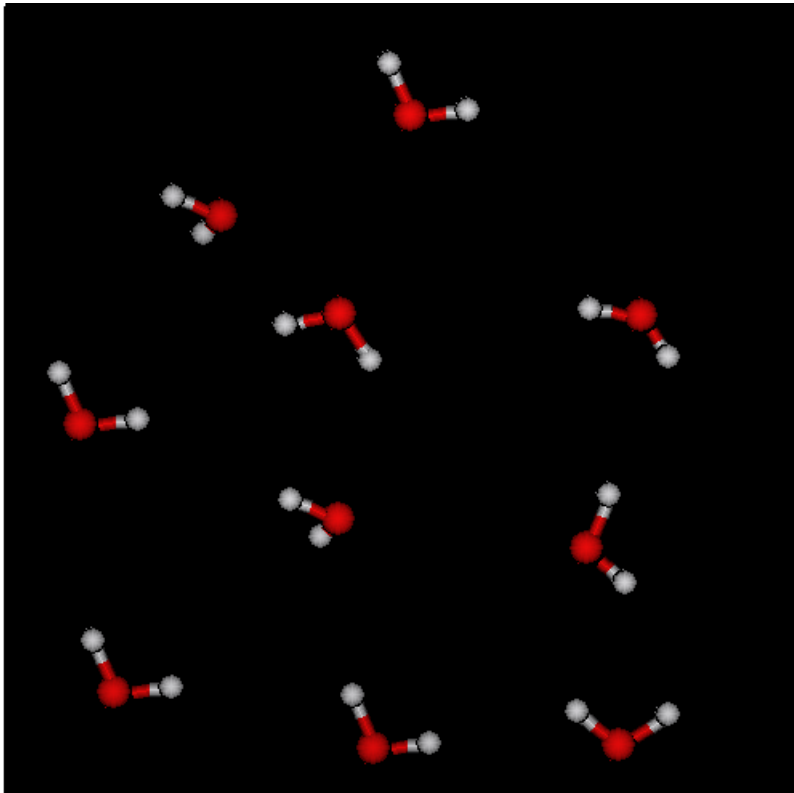| Atom	Charge[a]	Charge [b]
C	-0.339	-0.356
H	0.113	0.119
H	0.113	0.124
C	-0.339	-0.360
H	0.113	0.119
H	0.113	0.119
H	0.113	0.119
H	0.113	0.119

[a]-calculated from chemical potential equilization
[b]- calculated from ab initio based DFT

Table 2. Polarizability α (in a.u.) of simple molecular systems.

Molecule	Calculated α	Experimental α
HCl	17·11[a] 17·12[b]	17·76
CO	12·92 13·21	13·17
H_2O	9·72 8·54	9·79
CO_2	16·65 17·42	19·66
C_2H_2	21·99 22·25	22·49
HCHO	15·02 15·20	18·92
CH_4	20·70 20·82	17·52
CCl_4	79·03 79·29	70·93
CH_3Cl	34·38 34·51	31·2
$CHCl_3$	63·56 63·77	64·17

[a]

- Calculation of polarizability of molecules and molecular assemblies in terms of atomic ones
- A self consistent calculation of intermolecular interaction Potential
- Useful in Simulation: Polarizable point charge-point dipole model for water

Problem:
- Large polarization for long molecules
- Undesired charge transfer

Solution
- New atom-atom charge transfer model

Car Parrinello type ab-initio simulation using atomic charge & dipoles as dynamical variables
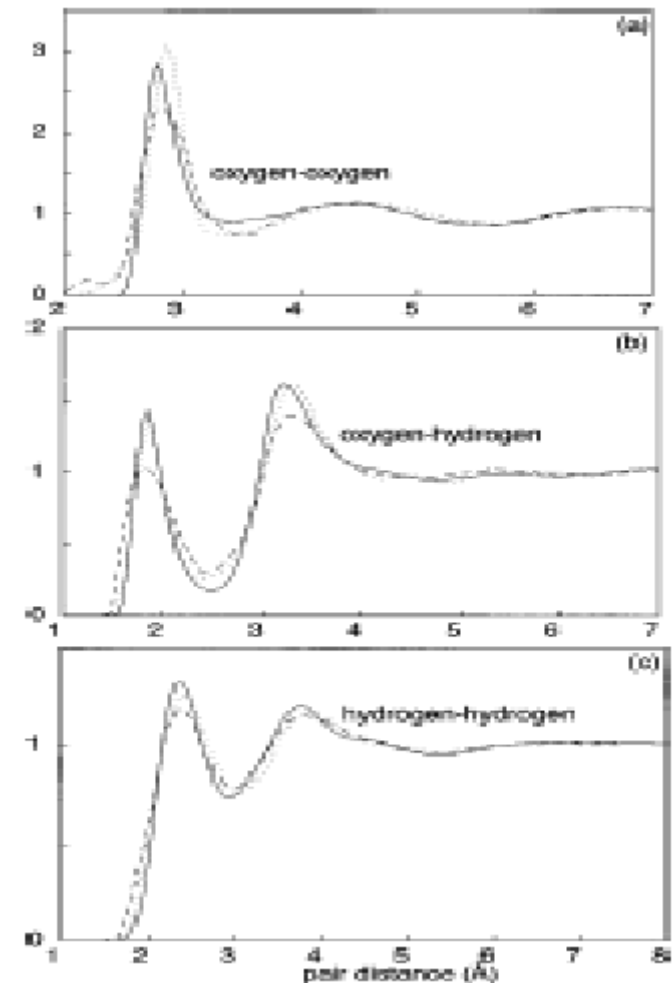
Effective Lagrangian:

$$L = \Sigma_i^{mol} \Sigma_\alpha^{atom} [(1/2)m_\alpha \dot{\mathbf{R}}_{i\alpha}{}^2 + (1/2)m_q \dot{q}_{i\alpha}{}^2 + (1/2)m_p \dot{\mathbf{p}}_{i\alpha}{}^2]$$

$$- U(\{q_{i\alpha}\}, \{\mathbf{p}_{i\alpha}\}, \{\mathbf{R}_{i\alpha}\})$$

$$- \lambda \Sigma_i \Sigma_\alpha q_{i\alpha} + \text{(geometry constraints)}$$

Action principle:

$$m_\alpha \ddot{\mathbf{R}}_{i\alpha} = - (\partial U / \partial \mathbf{R}_{i\alpha}) + \text{(geometry constraints terms)}$$

$$m_q \ddot{q}_{i\alpha} = - (\partial U / \partial q_{i\alpha}) - \lambda$$

$$m_p \ddot{\mathbf{p}}_{i\alpha} = - (\partial U / \partial \mathbf{p}_{i\alpha})$$

Effective Lagrangian:

$$L = \Sigma_i^{\,mol} \Sigma_\alpha^{\,atom} \, [(1/2)m_\alpha \dot{\mathbf{R}}_{i\alpha}^2 + ($$

$$+(1/2)m_p \dot{\mathbf{p}}_{i\alpha}^2 \,]$$

$$- U(\{\, q_{i\alpha}\,\},\{\mathbf{p}_{i\alpha}\,\},\{\mathbf{R}_{i\alpha}\,\})$$

$$- \lambda \, \Sigma_i \Sigma_\alpha \, q_{i\alpha} + (\text{geometry}$$

Action principle:

$$m_\alpha \ddot{\mathbf{R}}_{i\alpha} = - (\partial U/\partial \mathbf{R}_{i\alpha}) + (\text{geomet}$$

$$m_q \ddot{q}_{i\alpha} = - (\partial U/\partial q_{i\alpha}) - \lambda$$

$$m_p \ddot{\mathbf{p}}_{i\alpha} = - (\partial U/\partial \mathbf{p}_{i\alpha})$$

From CLUSTERS to CLUSTER ASSEMBLIES

Carbon clusters

Metal clusters & their assemblies

Electric Response Properties of Alkali Metal Clusters

Objective: To investigate the effect of electron correlation on the polarizability of Lithium and Sodium metal clusters
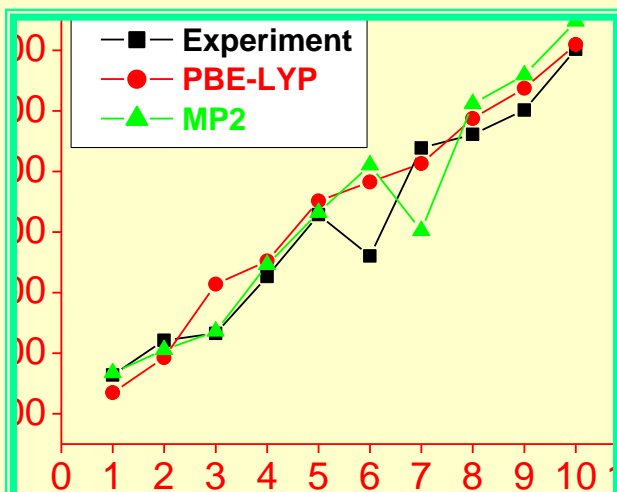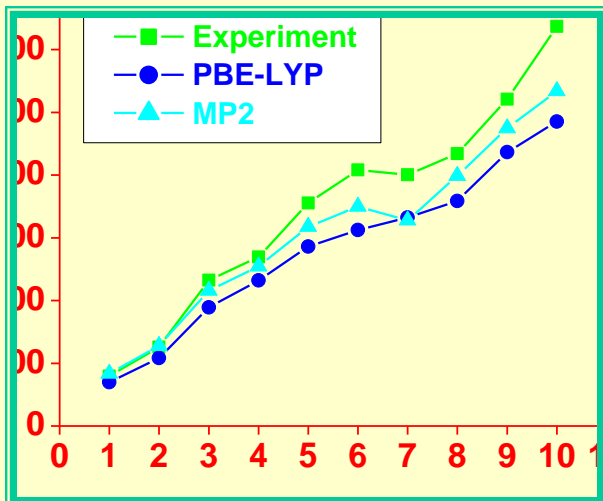
❖ **Electron correlation is found not to play any major role in the evaluation of polarizability of the Li clusters**

❖ **The polarizability calculated at zero Kelvin temperature is found to be higher than the experimental results measured at higher temperature**

❖ **The size evolution of the polarizability is very unusual for Li clusters**

❖ **In spite of same number of valence electrons and similar geometry, there is a difference in the polarizability evolution of Na and Li clusters**

Cluster Assembled Materials

Objective: Design of New/Novel Materials with Desired Properties through Assembly of Clusters (Artificial atoms)

Basic Requirements:

•Building blocks (clusters) must be very stable so that their individual identity is preserved in the new material.

•Intercluster interaction must be very weak to prevent them from collapse for a successful assembly

•**Metal/Semiconductor Magic Clusters**
•**Size-dependent Cluster Properties (Finite Size Effect)**
•**Tunable properties**

Cluster-assembled-Materials: Magic Clusters with intercluster interaction very Weak to prevent from collapse

Au$_4$ (planar) → Ti/Zr doping → Ti/ZrAu$_4$ (tetrahedral)

Au
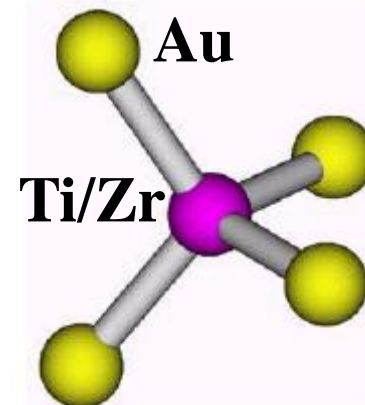
Ti/Zr

8 e$^-$ (4e$^-$ Ti/Zr + 4e$^-$ Au) Electronic shell closing

Tetrahedral structure Geometric shell closing

Magic Cluster with Directional bonding

BE/atom ~ 2.5 eV

Cluster (MAu$_4$)	R$_{M-Au}$		IP (eV)		EA (eV)		H-L (eV)
	DFT	MP2	DFT	MP2	DFT	MP2	DFT
TiAu$_4$	2.430	2.396	9.73	9.97	0.63	0.14	3.24
ZrAu$_4$	2.610	2.612	10.04	9.88	0.70	0.20	3.64

Calculated cluster-cluster interaction energies (DFT/MP2 method)

Systems	Interaction Energy (eV)
$(TiAu_4)_2$	7.04
$(ZrAu4)_2$	5.58

$(Mg_4)_2$	0.80
$(Na_8)_2$	0.36
$(TiH_4)_2$	1.60
$(TiX_4)_2$ (X=F, Cl, Br, I)	0.22-0.46
$(AlH_3)_2$	1.54

Unusually high Interaction Energy
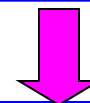
1. **Ti-Au-Ti Bridge bond (3c-2e Bonding)**
2. **Au-Au Aurophillic attraction**

Titanium/Zirconium doped Gold Clusters:
 Identity of Monomers are still retained in the dimer, implying that $M(Au)_4$ might be suitable for Cluster-Assembled-Material
• Unusually high inter-cluster Interaction Energy in Ti/Zr doped Magic Gold Clusters
• First time observation of 3c-2e bonding in metal cluster dimer

(a)

(b)
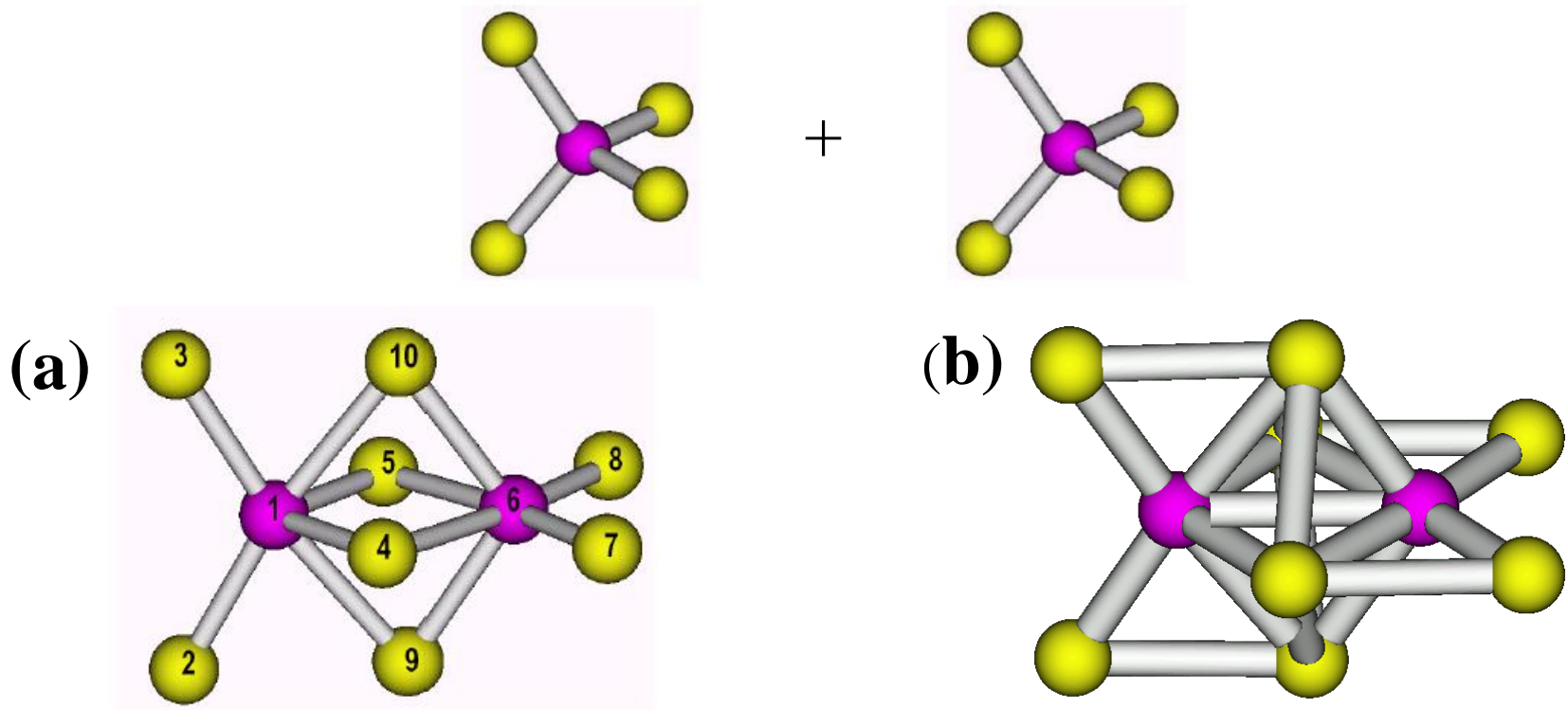
Optimized structures of MAu$_4$ dimer (M = Ti and Zr) (D$_{2d}$):
(a) Au-Au bonds are not shown to highlight the M-Au-M bridge bonds (b) both M-Au and Au-Au bonds are shown

proposed

1-D

3-D
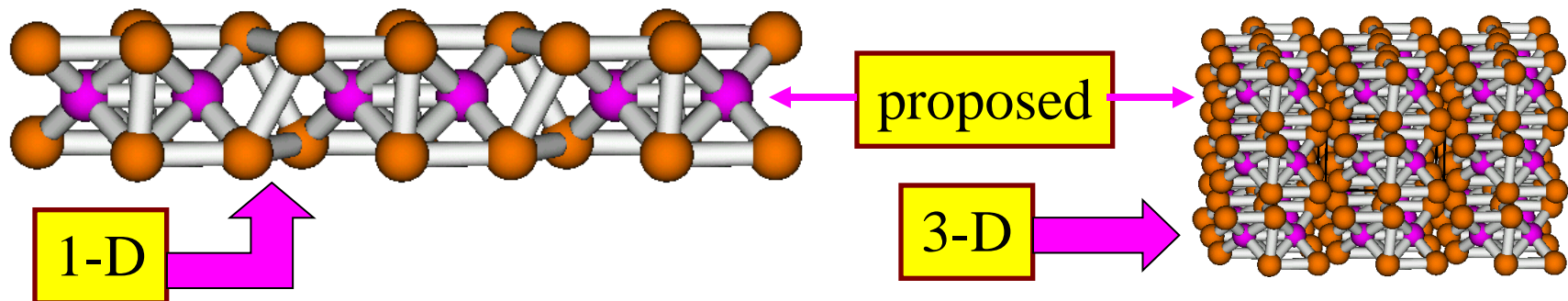
Assembly of jellium Metal Clusters

Metal Clusters within the jellium model
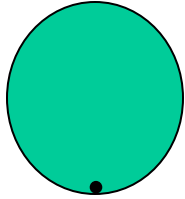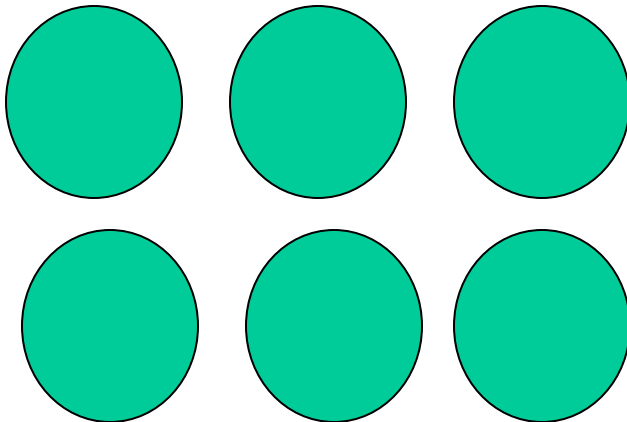
$$V(r) = (3Ze^2/R)-(2Ze^2/R^3)r^2, \text{ for } r < R$$
$$= -Ze^2/r, \text{ for } r > R$$

Reasonable success: Correct shell closing/ magic numbers

Occupancy according to oscillator
and not according to Coulomb potential

Assembly of jellium Metal Clusters

$n = 2k + l$
$l = 0, 2, ...n\text{-}2, n$ for even n
$l = 1, 3, ...n\text{-}2, n$ for odd n

Need for modified software

Optical Properties of Nanoparticles

Optical properties of bimetallic nanospheres: Effect of diffuse electron density profiles at the boundary surfaces

Malaya K. Nayak and Swapan K. Ghosh

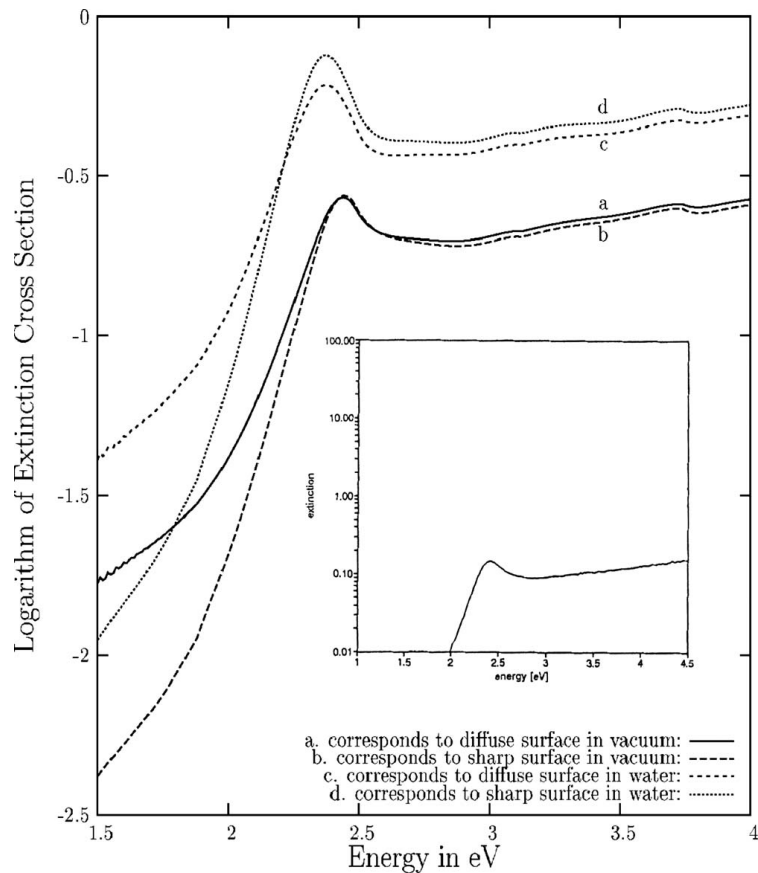*Theoretical Chemistry Section, Bhabha Atomic Research Centre, Mumbai 400 085, India*

FIG. 1. Plot of extinction cross section vs energy for a gold nanosphere of radius RAu=6.0 nm without Ag-shell. Plots a and b represent the extinction spectra with diffuse electron density and sharp electron density profile at the boundary surfaces, respectively, in vacuum m=1.0. Plots c and d represent the corresponding spectra in water medium m=1.77. The curve in the inset refers to corresponding experimental spectra measured in hydrosols.

The effect of diffuse electron density at the boundary surfaces of Au-core Ag-shell bimetallic nanospheres on their optical properties such as extinction spectra is investigated by considering a multiple shell model for both the interfaces consisting of exponentially decreasing electron density profiles corresponding to a minimized energy density functional. The dielectric constants for the shells of varying electron density have been obtained by proposing a new simple pproach. The diffuseness of the electron density at the boundary surfaces is found to give rise to peak broadening to some extent and also seems to favor the experimental spectra

From HARD MATTER to SOFT MATTER:

MICROSCOPIC ELECTRON DENSITY to MESOSCOPIC NUMBER DENSITY

Soft Matter of Hard Molecules

"Fragile Objects, Soft Matter, Hard Science, and
 the Thrill of Discovery",
by P.G. de Gennes & J. Badoz (Springer-Verlag, 1996)
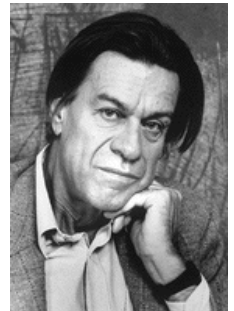
Soft Matter: Applications
- Nanoparticle synthesis using micelles as template
- Chemical reactions under confinement in micelles
- Spectroscopy & Dynamics in micellar environment
- Interface of chemistry, physics, biology, chemical engineering, materials science

Understanding Soft Matter:

Difficulty: 1) Interaction Potential unknown
2) Too many Particles

Remedy: 1) Assume Model interparticle potential (Hard sphere, Lennard-Jones etc) (Hard core interaction at short range but weakly interacting at a distance): Concept of "Hard Molecules"
2) Use single particle "Density" approach

Density based approach to Soft Condensed Matter

Various levels of complexity:

neutral liquid: Neutral hard sphere
                   Lennard-Jones interaction

Ionic fluid: Solute: charged hard spheres
                   Solvent: dielectric continuum
                              neutral hard sphere
                              dipolar hard sphere

Colloids: Screened Coulomb (DLVO)
Liquid Crystals: Hard rod anisotropic potential
Polymer: Hard sphere/harmonic chain

Interfaces: Confinement: Planar walls
                            Spherical cavity
                            Cylindrical pore

Potential: (Hard/L-J/ Coulombic potential)

Density based approach to Soft Condensed Matter

Various levels of complexity

neutral liquid: Neutral sphere

                                           interaction

Ionic fluid: hard spheres

                                           continuum

                                           sphere

                                           hard sphere

                                           Coulomb (DLVO)

                                           anisotropic potential

                                           sphere/harmonic chain

Interf   ment: Planar walls
                                            Spherical cavity
                                            Cylindrical pore

Potential: (Hard/L-J/ Coulombic potential)

Soft Matter of Hard Molecules

Soft Condensed Matter under Confinement:

NanoMaterials: one dimension in the range of 1 to 100 nm

Single Interface: Solid-Liquid Interface
Liquid-Liquid Interface
Liquid-Vapour Interface
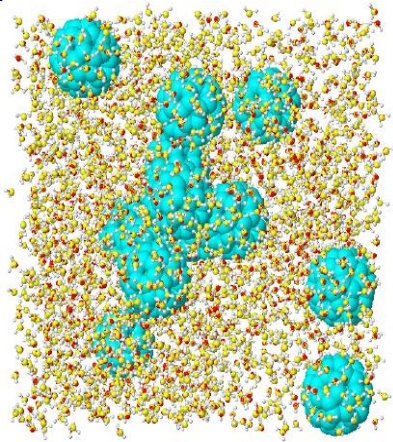
Solute-Solvent Interface
(spherical,   Cylindrical)
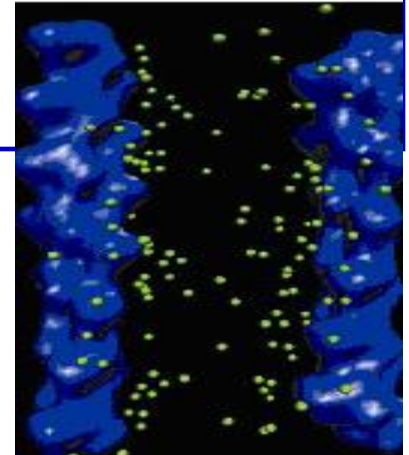
Two Interfaces: Liquid between two plates
Colloid interparticle interaction

Structure and Dynamics of Soft Matter
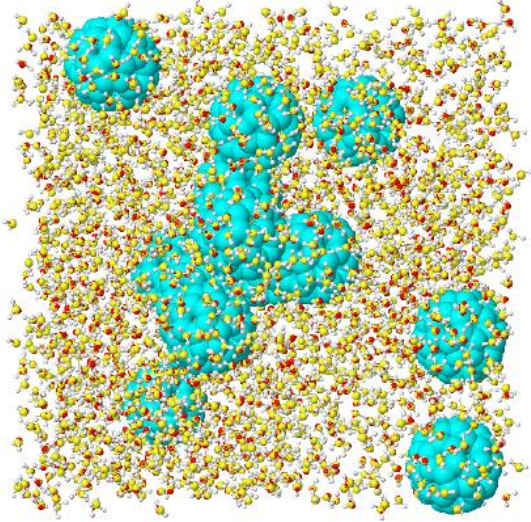
Large molecules in solvent
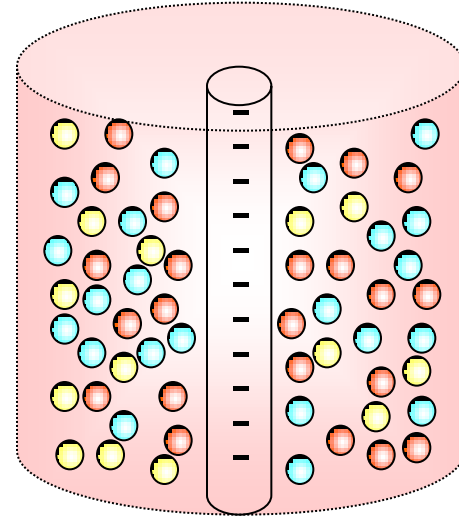
Cylindrical Double Layers
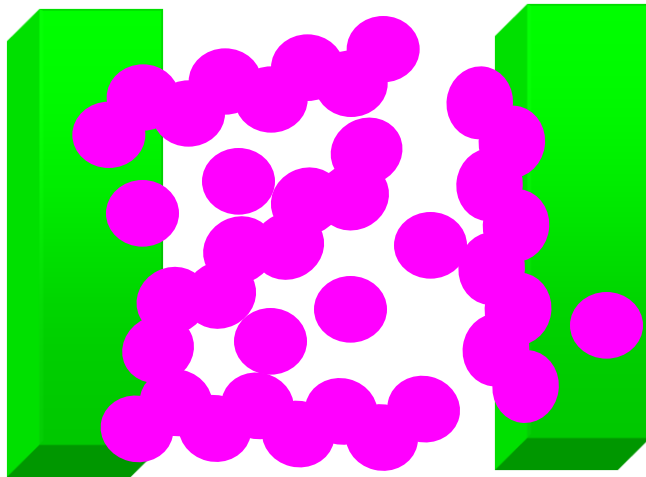
Polymers at Interfaces
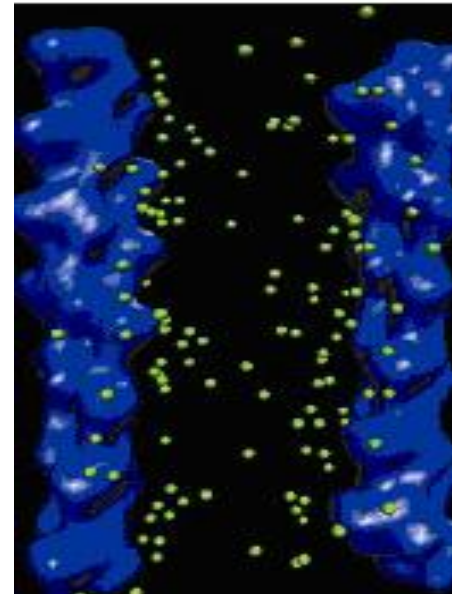
Electric Double Layer

Central Particle

Spherical Geometry

Negative ions

Ion Distribution around a micelle

Positive ions

Liquid Particles

Planar Geometry

Charged Walls

Electrode-Electrolyte Interface

Top-left panel: 1:1 Electrolyte, $c = 0.1M$, $\sigma^* = 0.30$. Curves labeled "Present Work" and "Simulation". Axes: $\rho_\alpha(z)/\rho_\alpha^0$ vs z/d.

Top-right panel: 1:1 Electrolyte, $c = 1M$, $\sigma^* = 0.70$. Curves labeled "Present Work" and "Simulation". Axes: $\rho_\alpha(z)/\rho_\alpha^0$ vs z/d.

Bottom-left panel: Curves labeled "Present Work" and "Simulation". Axes: $\psi^*(z)$ vs z/d.

Bottom-right panel: Axes: $\psi^*(z)$ vs z/d.
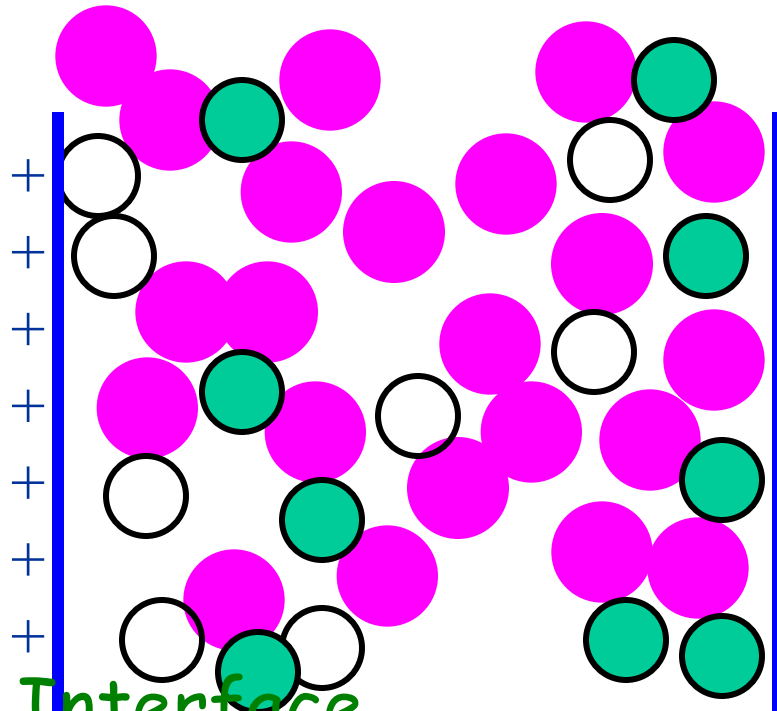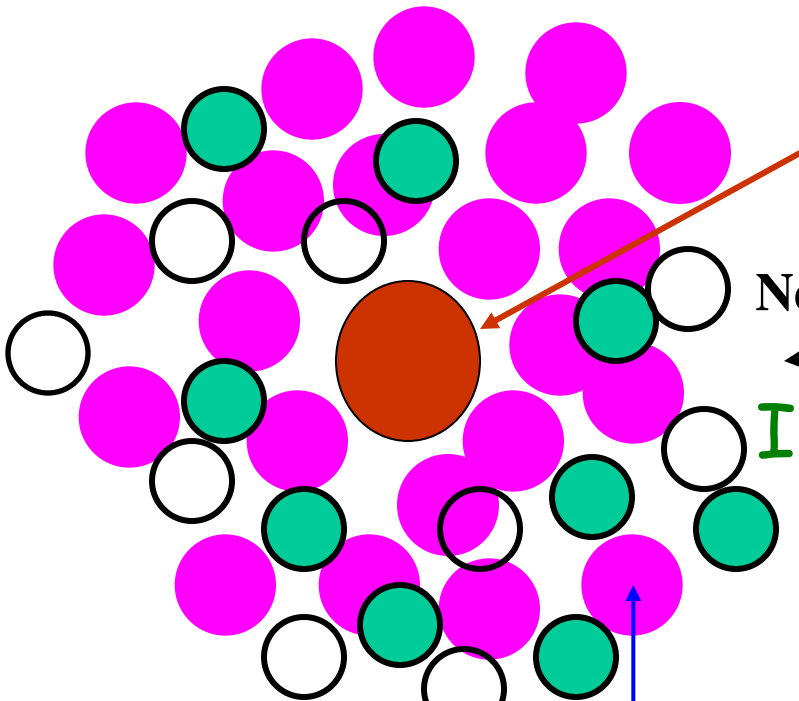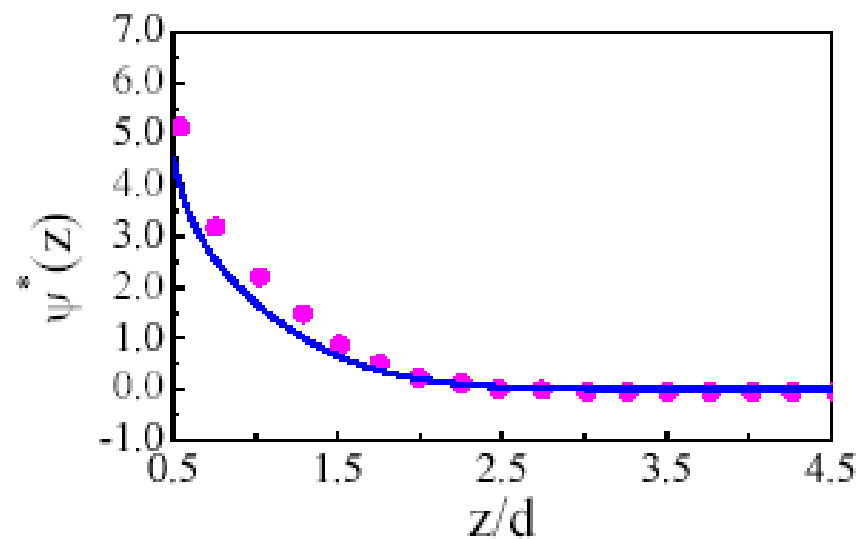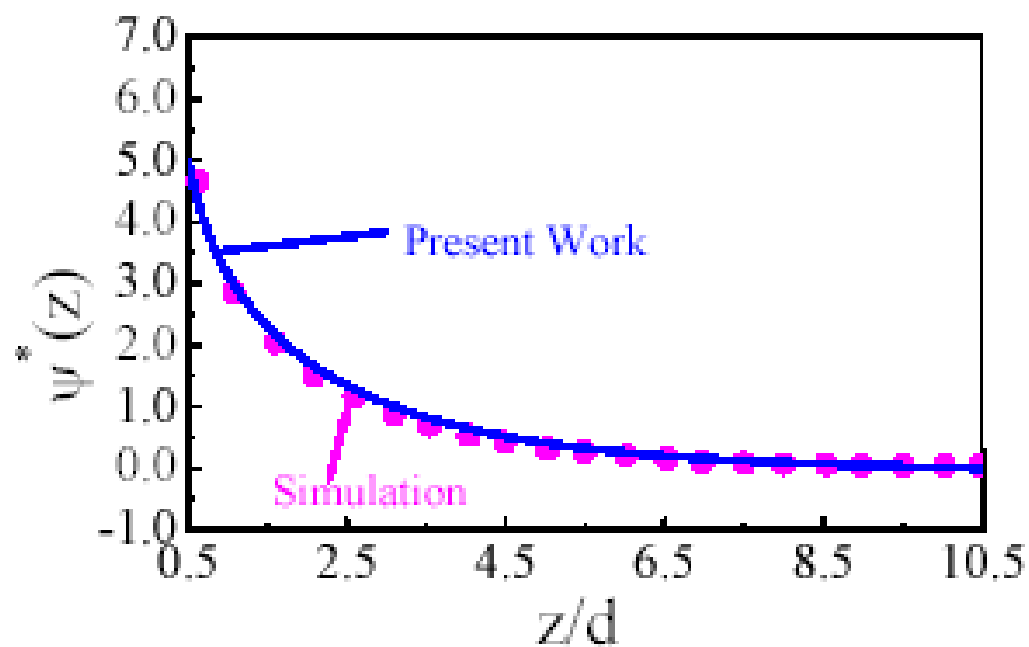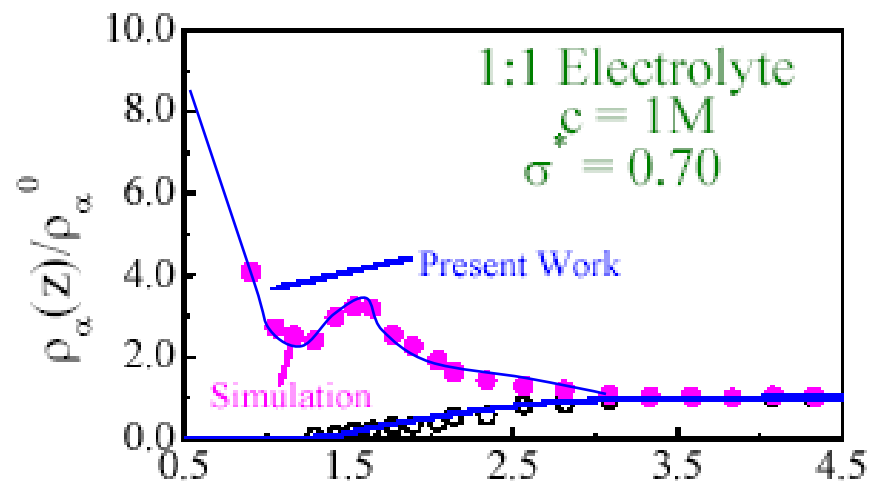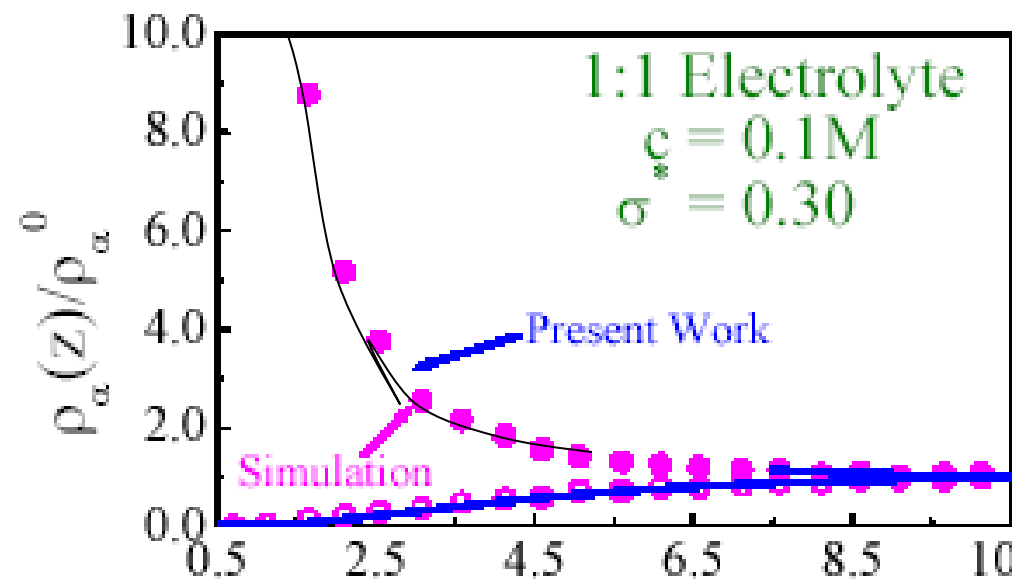
Restricted Primitive Model Charged hard sphere ions

Structure of cylindrical electric double layers: A systematic study by Monte Carlo simulations and density functional theory

Teena Goel, Chandra N. Patra,[a)] Swapan K. Ghosh, and Tulsi Mukherjee
Theoretical Chemistry Section, Chemistry Group, Bhabha Atomic Research Centre, Mumbai 400 085, India

concentration profiles for the 1:1 salt (NaCl) for 500 mM varying sizes of small ions. Symbols □, ○, △, open represent σ=2, 3, 4, 5, and 6 Å, respectively. The key is 1.

Cylindrical pore

Pos. Ion

Solvent

Neg. Ion
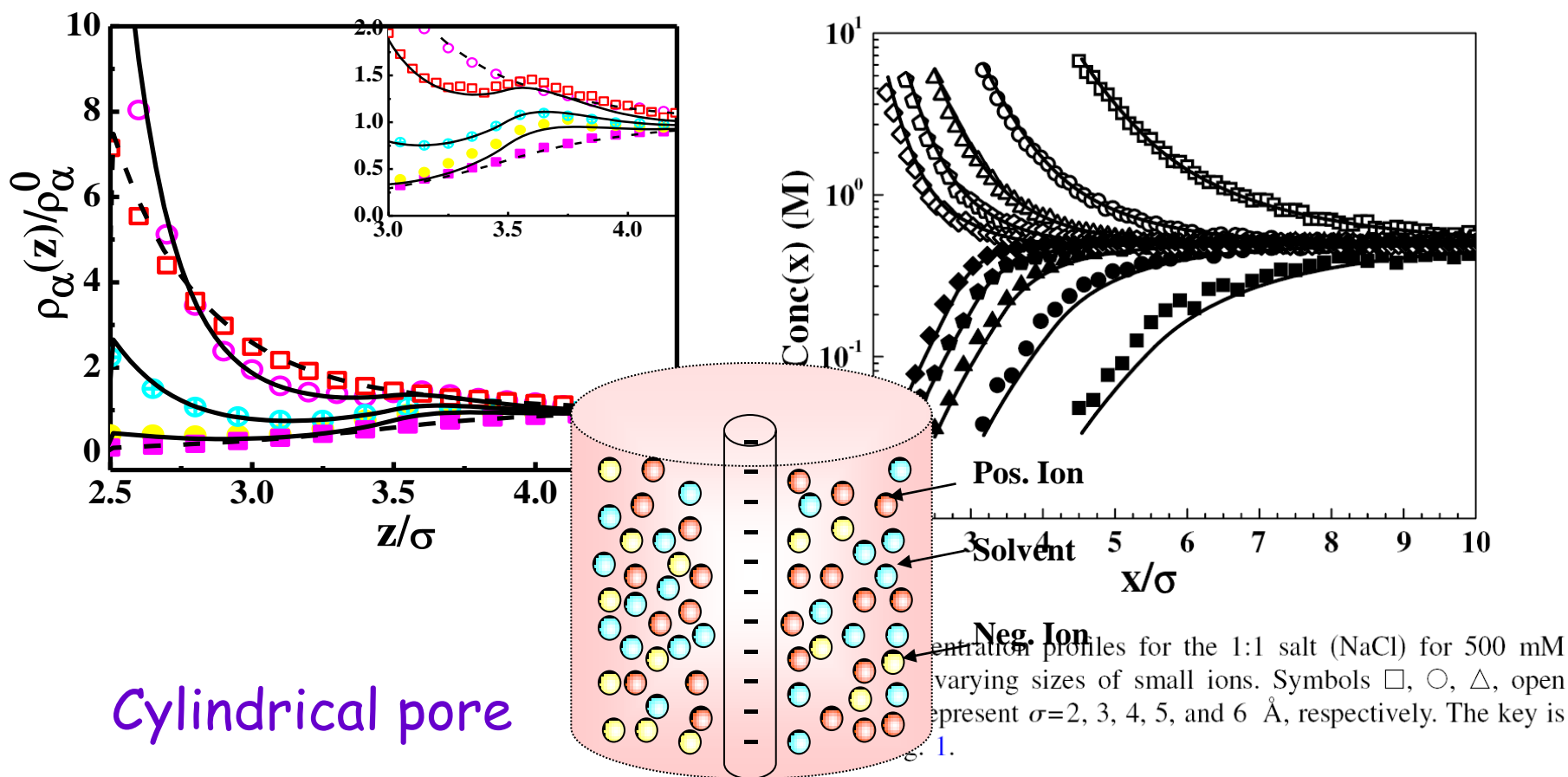
Structure of electric double layers:
A self-consistent weighted-density-functional approach

Chandra N. Patra and Swapan K. Ghosh[a]

Theoretical Chemistry Section, RC & CD Division, Chemistry Group, Bhabha Atomic Research Centre, Trombay, Mumbai 400 085, India

Earlier theories: Continuum theories

Spherical geometry: Debye-Huckel theory

Planar geometry: Guoy-Chapman theory

Fail to predict the nonmonotonic structure of ion distribution

Density Functional Theory includes effect of

Interparticle correlations (both short and long range)

$\rho_a(r) = \rho_a{}^0 \exp([-v_a(r) + v_{eff}(r)]/kT])$

- Effective potential due to interparticle correlation

$v_{eff}(r) = [C^{(1)}(r;\rho(r)) - C^{(1)}(\rho_0)] kT$ (WDA/Pert Theory)

Liquid-phase synthesis of nanomaterials

Nucleation and growth of particles: Role of supersaturation
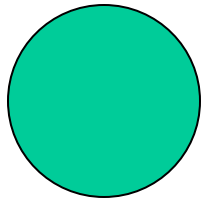
$$\Delta G = - \frac{4 \pi R^3}{3 \, v} \Delta\mu + 4 \pi R^2 \gamma$$

Critical radius for nucleation

$$R^* = \frac{2 \gamma v}{\Delta\mu}$$
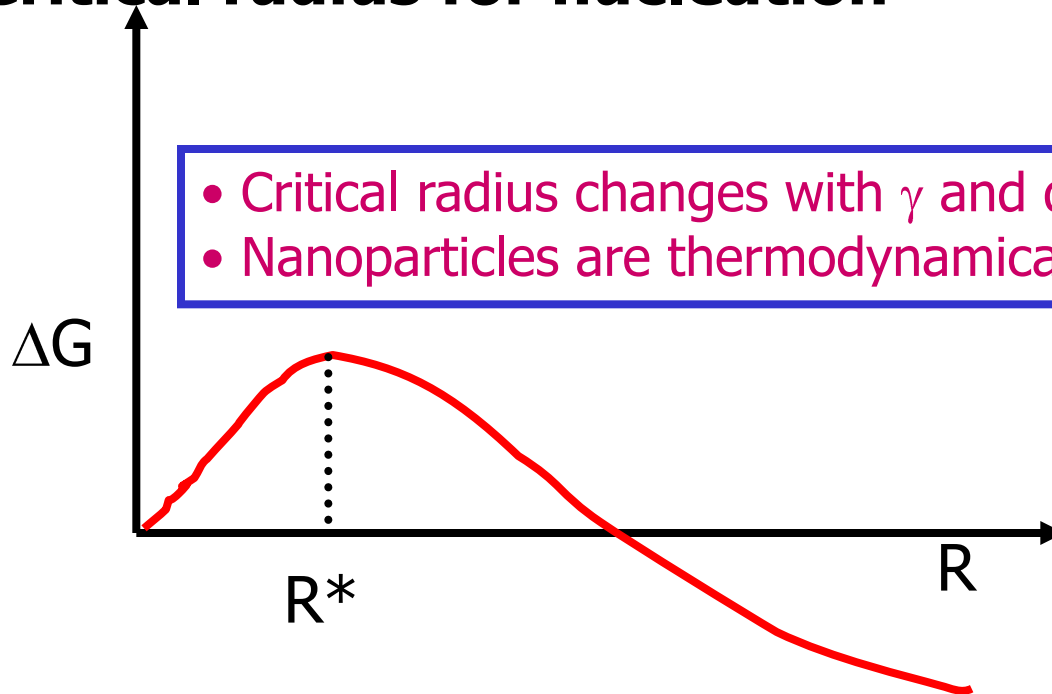
- Critical radius changes with γ and degree of supersaturation
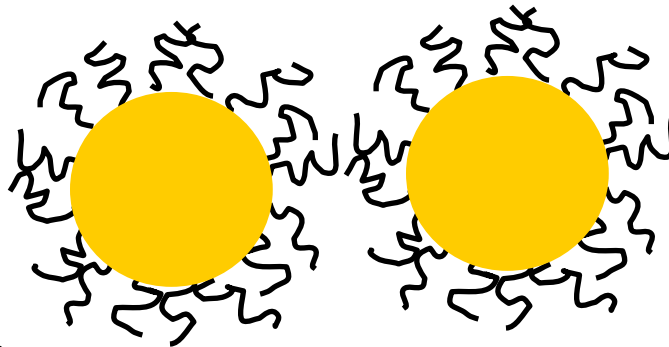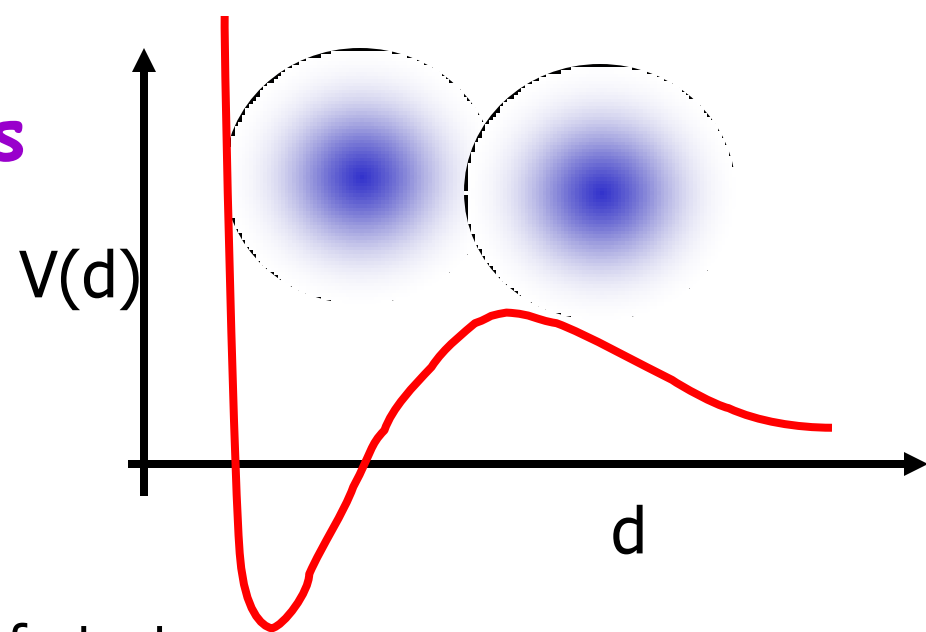- Nanoparticles are thermodynamically unstable

Stabilization of particles

1) Charge Stabilization

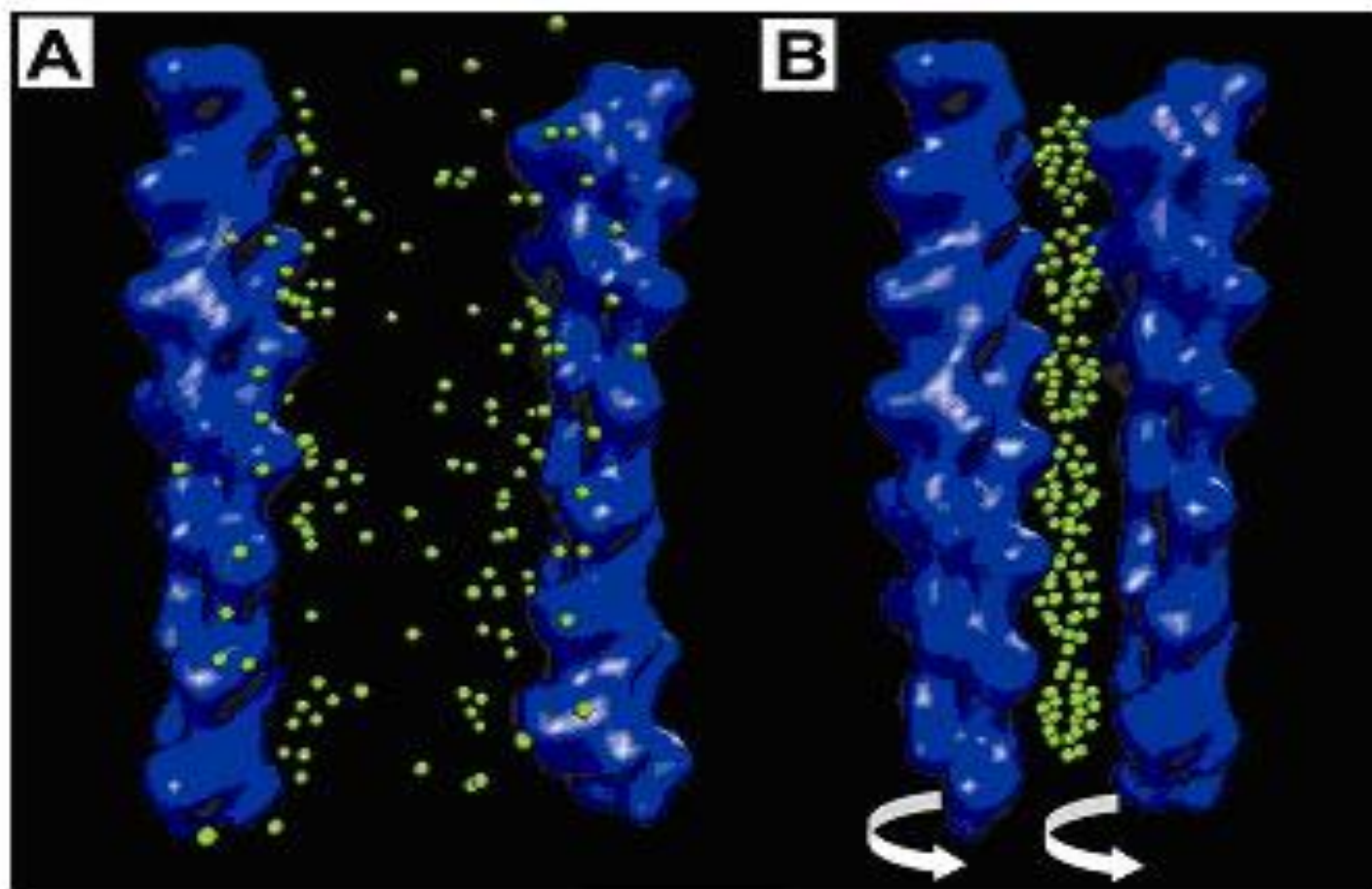2) Steric stabilization

Adsorption/ grafting of polymers or surfactants

3) Kinetic stabilization

Diffusion controlled growth

$V(d)$

d

Size Distribution of Nanoparticles:
- Use of Templates: Micelles, Microemulsion, etc
- Understanding the mechanism:

Schematic representations of uncondensed and condensed F-actin. (A) At low multivalent ion concentrations, two F-actin filaments maintain their native 13/6 symmetry and are unbound. (B) At high multivalent ion concentrations, the ions collectively form a CDW and bundle F-actin filaments.

Density functional approach to solvent-induced interactions in neutral liquids: Comparison with experimental results
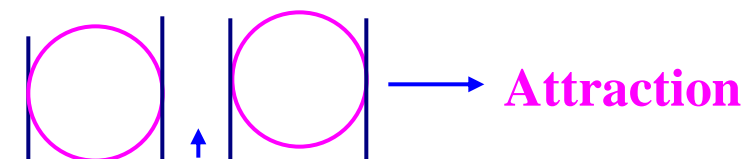
Chandra N. Patra and Swapan K. Ghosh

$\rho_0 = 0.956 \text{ gm / ml}$

$d = 8.5 \text{ Å}$
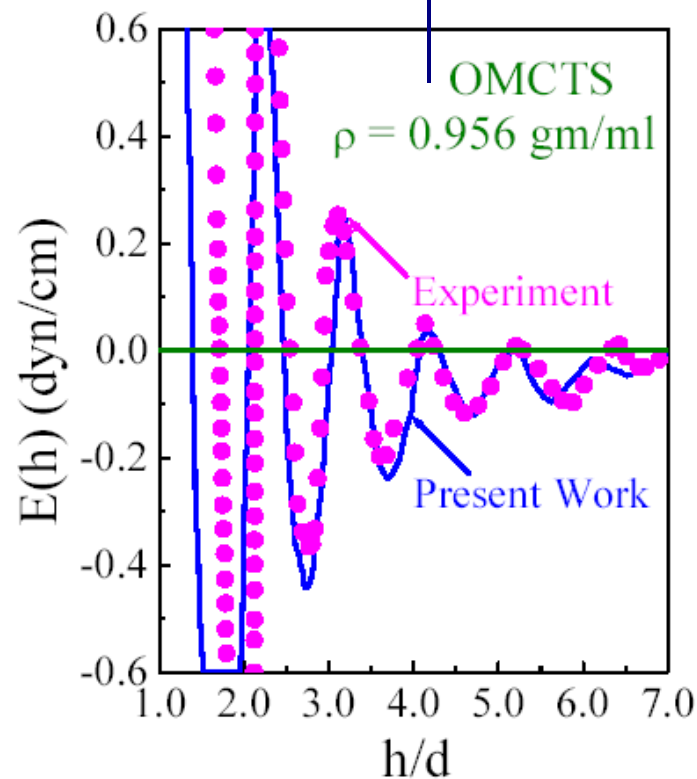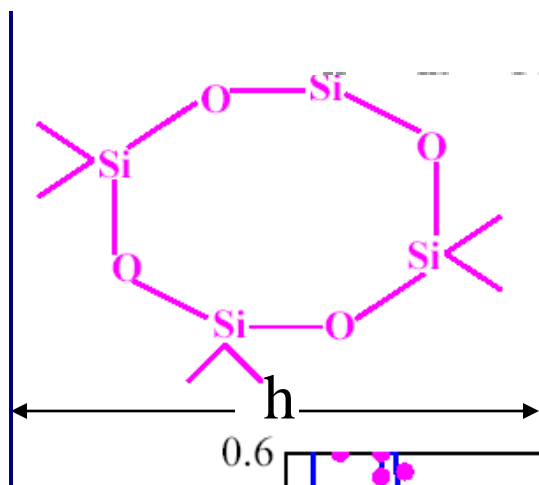
Weighted-density-functional theory of solvation forces in liquids

Chandra N. Patra and Swapan K. Ghosh

Heavy Water Division, Bhabha Atomic Research Centre, Bombay 400085, India

(Received 30 August 1993)
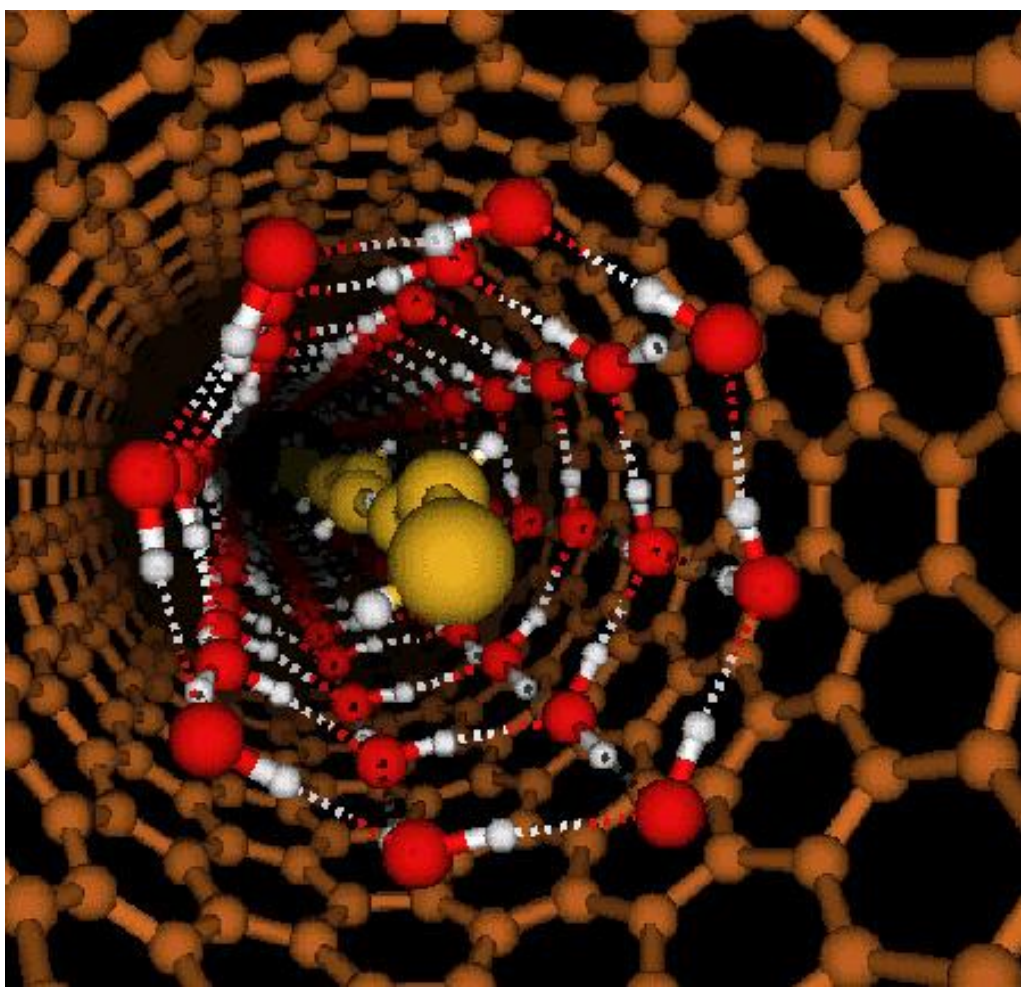
Oscillating nature of the force
Between two mica sheets
Confining a liquid

$$p(h) = -\frac{\partial \Omega}{\partial h}\bigg|_{T,\mu}$$

$$k_B T \rho(d/2; h)$$

$$f(h) = p(h) - p(\infty)$$
$$= k_B T\ \rho(d/2; h) - \rho(d/2; \infty)$$

$$E(h) = \int_h^\infty dh'\, f(h')$$

Confined liquid layers between two plates: Lubrication phenomena

**Nanotube Water**

The water molecules into a carbon nanotube exist in the form of a "wire", surrounded by another water structure, a cylindrical sheath of water. Neutron scattering along with computer Simulations. Fluid-like behavior was observed at temperatures far below the freezing point of normal water.

The water chain allows a freer movement of protons along the chain.

This anomalous behavior might help to explain other phenomena featuring nm-scale confined water such as water migration from soil to plants via xylem vessels and the proton translocation in transmembrane proteins.

Fluids inside planar Nanopores
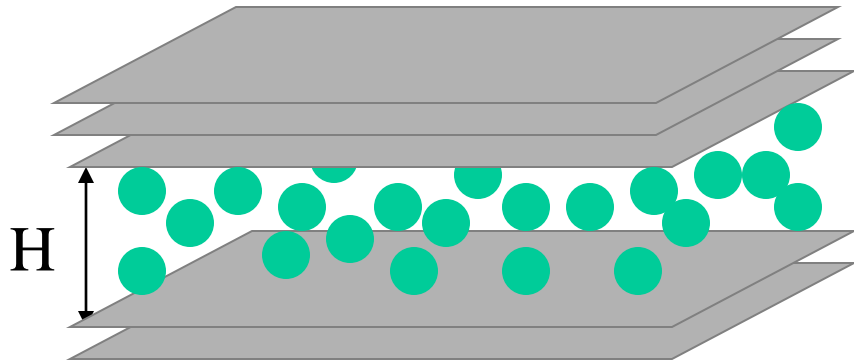
Slit shaped "micropores
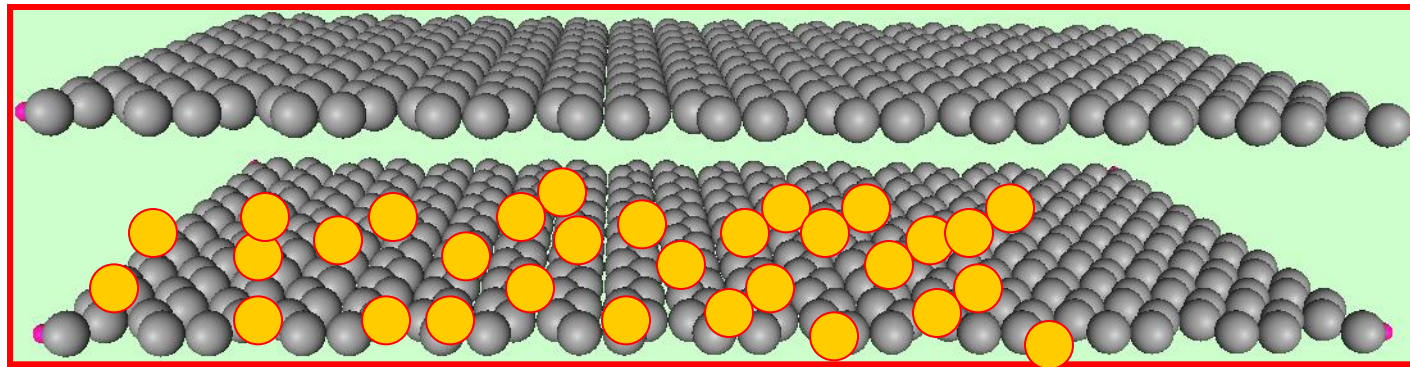
Adsorption in Nanopores

Adsorption of Lennard-Jones fluid mixture in a planar slit: A perturbative density functional approach

Niharendu Choudhury and Swapan K. Ghosh

Theoretical Chemistry Section, RC and CD Division, Chemistry Group, Bhabha Atomic Research Centre, Mumbai 400 085, India
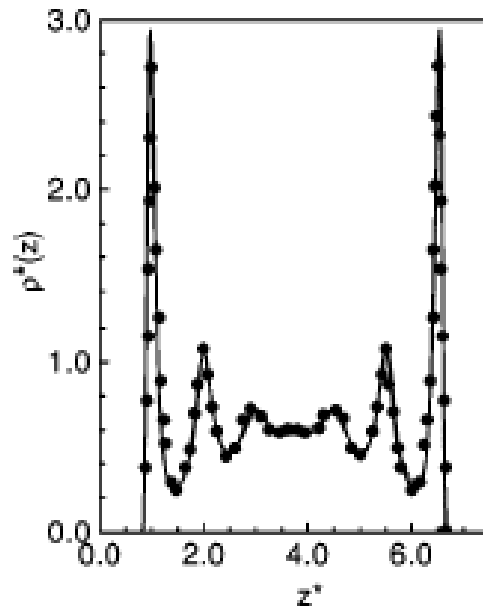

FIG. 4. Plot of density profiles $\rho^*(z)$ vs z^* for a pure Lennard-Jones fluid of bulk density $\rho_0^* = 0.5925$ in a planar slit of of width $H^* = 7.5$ at $T^* = 1.20$. The key is the same as in Fig. 2. Simulation results are taken from Ref. [44].
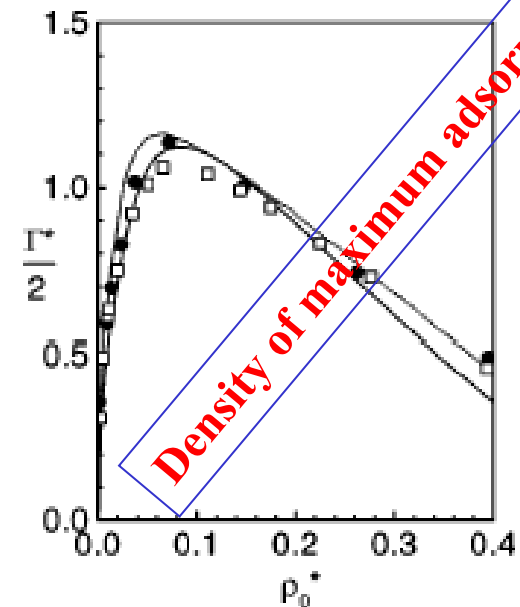

FIG. 6. Plot of excess adsorption isotherm per unit area Γ^* vs ρ_0^* of ethylene in carbon slit pore of width $H^* = 5$ at $T^* = 1.35$. The key is the same as in Fig. 2. Simulation results that are shown as circles are taken from Ref. [35(a)] (also reproduced in Ref. [39(a)]) and those shown as open squares are taken from Ref. [41].

Weighted-density-functional approach to the structure of nonuniform fluids

Chandra N. Patra and Swapan K. Ghosh[a]

*Theoretical Chemistry Section, RC & CD Division, Chemistry Group, Bhabha Atomic Research Centre,
Bombay 400 085, India*

The structure of simple nonuniform fluids is studied using a new weighted-density-functional approach based on the concept of universality of the free energy density functional and an assumption of a local dependence of its functional derivative on the weighted density. The theory uses as input the second-order direct correlation function and the radial distribution function of the corresponding uniform fluid which are obtained here from the integral equation theory with an accurate closure relation. The calculated numerical results on the density profiles of several confined inhomogeneous fluids are shown to compare quite well with the available simulation data. © 2003 American Institute of Physics. [DOI: 10.1063/1.1565326]
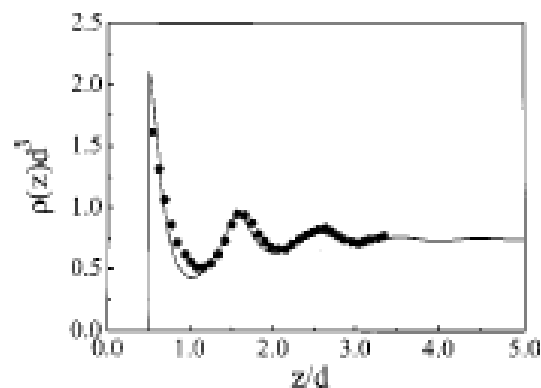

FIG. 3. Density profile of a Lennard-Jones fluid ($\rho_0^* = 0.75, k_B T/\epsilon = 1.304$) confined between two hard walls at separation $H = 13$. The solid curve refers to the results of the present work. Simulation results are shown as circles (Ref. 33).
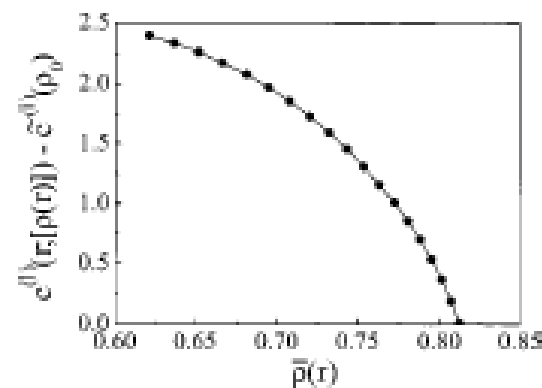

FIG. 5. Plot of the difference between the one particle correlation function of the inhomogeneous fluid $c^{(1)}(r;[\rho(r)])$ and its homogeneous fluid counterpart $\bar{c}^{(1)}(\rho_0)$ as a function of the weighted density $\bar{\rho}(r) = \int d\mathbf{r}' w(|\mathbf{r}-\mathbf{r}'|;\rho_0)$ for a hard sphere fluid at $\rho_0^* = 0.813$.

Structure of an inhomogeneous fluid mixture: A new weighted density-functional theory within a perturbative approach

Niharendu Choudhury and Swapan K. Ghosh[a)]

Theoretical Chemistry Section, RC & CD Division, Chemistry Group, Bhabha Atomic Research Centre, Mumbai 400 085, India
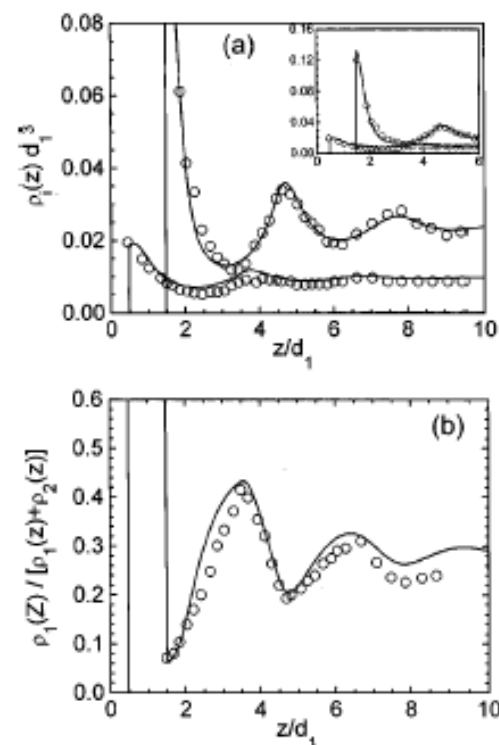
FIG. 1. (a) Plot of the density profiles $\rho_i(z)d_1^3$ vs z/d_1 for a hard-sphere mixture near a hard wall with $\eta=0.3435$, $\alpha=1/3$, and $x=0.7144$. Bottom curves: $\rho_1(z)$; Upper curves: $\rho_2(z)$. Solid lines represent results from the present approach and the symbols correspond to the simulation results (Ref. 15). (b) Plot of the concentration profiles $\rho_1(z)/(\rho_1(z)+\rho_2(z))$ vs z/d_1 for a hard-sphere mixture near a hard wall. The parameters and the key are same as in (a).
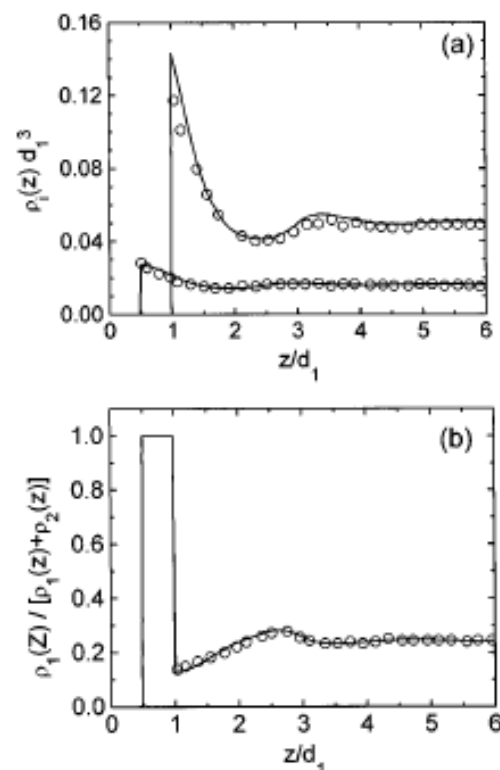
FIG. 2. (a) Plot of the density profiles $\rho_i(z)d_1^3$ vs z/d_1 for a hard-sphere mixture near a hard wall with $\eta=0.2204$, $\alpha=1/2$, and $x=0.7563$. The key is same as in Fig. 1(a). (b) Plot of the concentration profiles $\rho_1(z)/(\rho_1(z)+\rho_2(z))$ vs z/d_1 for a hard-sphere mixture near a hard wall. The parameters and the key are same as in (a).

Structure of nonuniform three-component fluid mixtures: A density-functional approach

Chandra N. Patra and Swapan K. Ghosh[a)]

Theoretical Chemistry Section, RC & CD Division, Chemistry Group, Bhabha Atomic Research Centre, Bombay 400 085, India
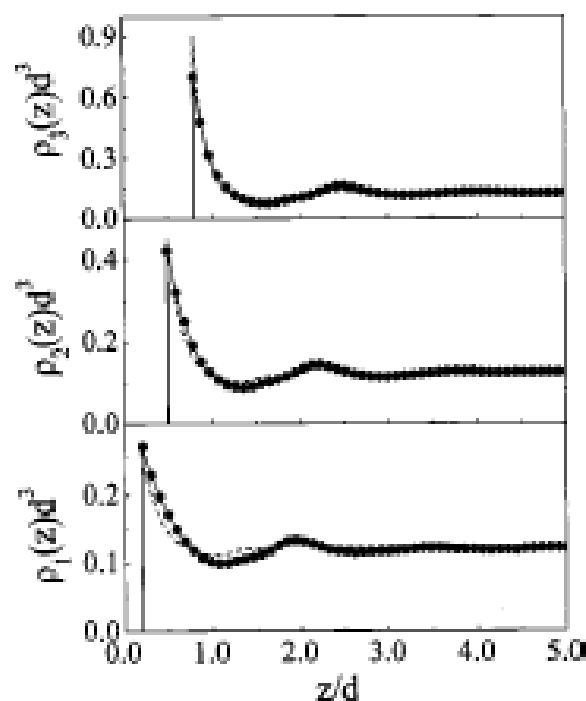
FIG. 1. Density profiles $\rho_i(z)d^3$ of a ternary hard sphere mixture near a hard wall. The system parameters are: diameters $d_1=0.4d$, $d_2=d$, $d_3=1.6d$, concentrations $x_1=x_2=x_3=1/3$, and bulk packing fraction $\eta=0.337$. The solid and dashed curves refer to the results obtained from SCDFA and SWDA, respectively. Simulation results are shown as circles.
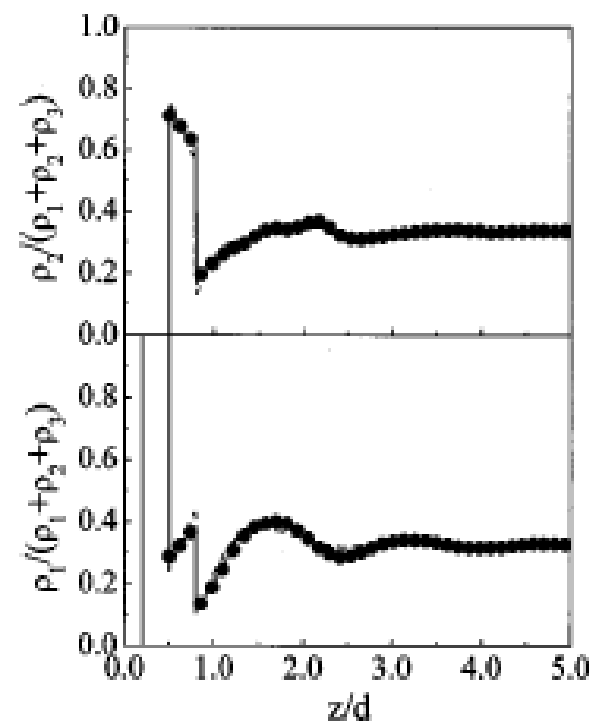
FIG. 2. Concentration profiles of the smaller- and the medium-sized spheres for a ternary hard sphere mixture near a hard wall. The key is the same as in Fig. 1.

Integral equation theory of penetrable sphere fluids:
A modified Verlet bridge function approach

Niharendu Choudhury and Swapan K. Ghosh[a)]

Theoretical Chemistry Section, RC & CD Division, Chemistry Group, Bhabha Atomic Research Centre, Mumbai 400 085, India
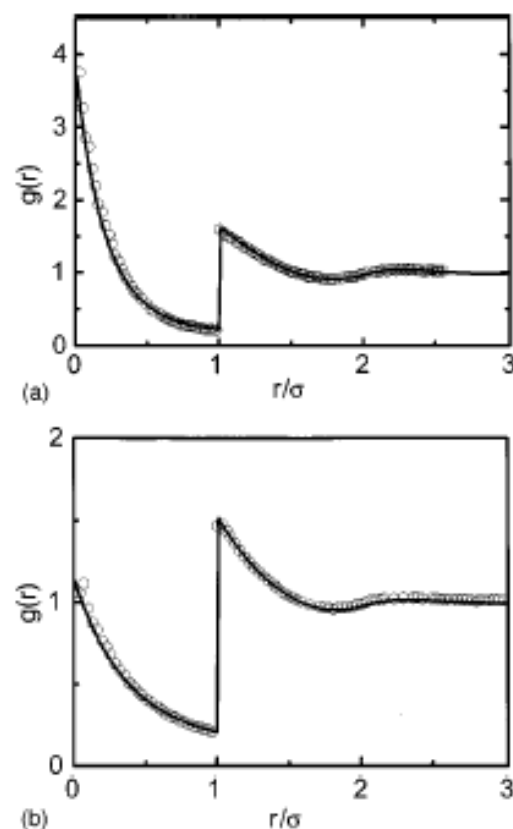
FIG. 4. Plot of the radial distribution function $g(r)$ vs r/σ for the penetrable sphere fluid at $T^* = 0.5$ and at packing fractions of (a) $\eta = 0.5$, (b) $\eta = 0.3$. The keys are the same as in Fig. 2.
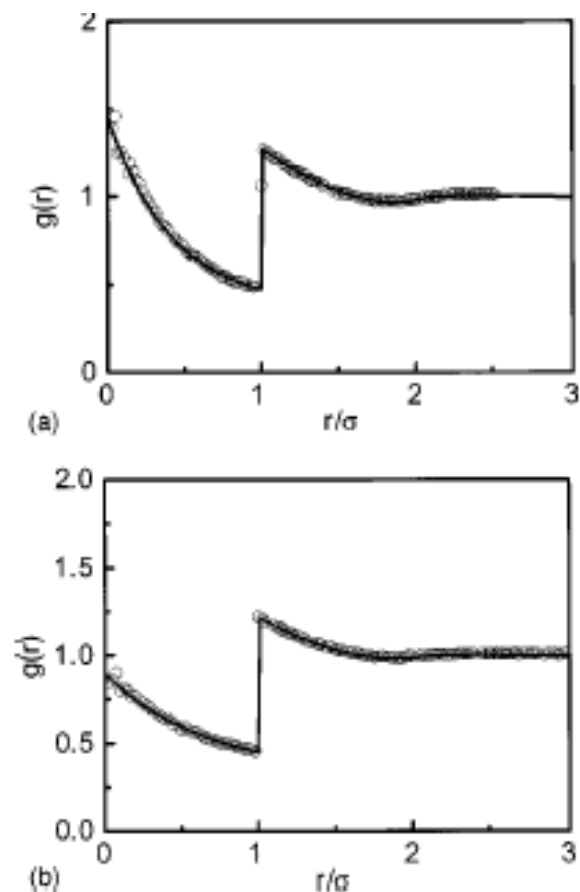

FIG. 5. Plot of the radial distribution function $g(r)$ vs r/σ for the penetrable sphere fluid at $T^* = 1.0$ and at the packing fractions of (a) $\eta = 0.5$, (b) $\eta = 0.3$. The keys are the same as in Fig. 2.

Bridge function and other structural properties of core-softened model fluids from molecular dynamics simulations

Niharendu Choudhury and Swapan K. Ghosh[*]

Theoretical Chemistry Section, RC & CD Division, Chemistry Group, Bhabha Atomic Research Centre, Mumbai 400 085, India
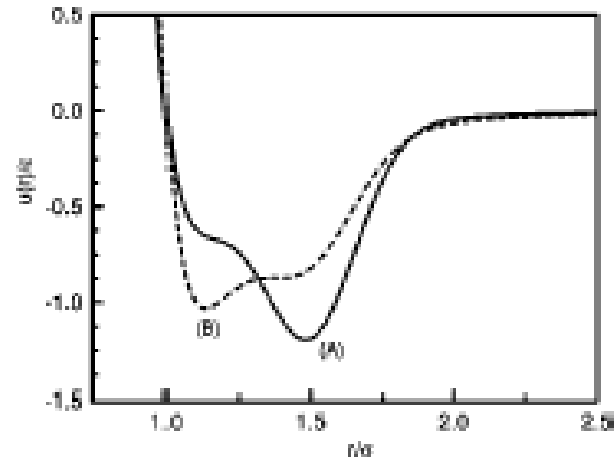
FIG. 1. Plot of core-softened potential $u(r)$ as a function of r/σ. The solid line represents $u(r)$ for system A and the dashed line represents that of system B.

$$u(r) = 4\epsilon\lambda_1\left[\left(\frac{\sigma}{r}\right)^{12} - \left(\frac{\sigma}{r}\right)^{6}\right] - \epsilon\lambda_2\exp\left[-\alpha\left(\frac{r}{\sigma} - \frac{r_0}{\sigma}\right)^2\right] \quad (1)$$
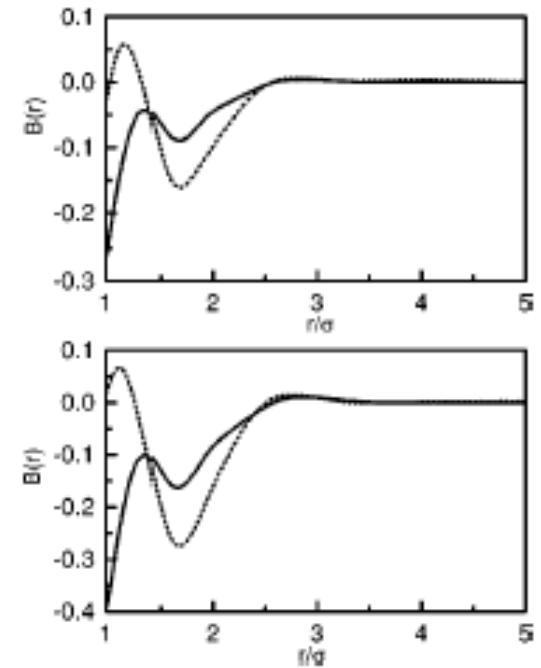

FIG. 5. Plot of the bridge function $B(r)$ vs r/σ for system A at $T^* = 1.5$ (upper panel) and at $T^* = 1.0$ (lower panel). The dotted line represents results for $\rho^* = 0.8$ while the solid line corresponds to the same for $\rho^* = 0.6$.

Simple weighted density functional approach to the structure of polymers at interfaces

Chandra N. Patra and Swapan K. Ghosh*

Theoretical Chemistry Section, RC&CD Division, Chemistry Group, Bhabha Atomic Research Centre, Mumbai 400 085, India
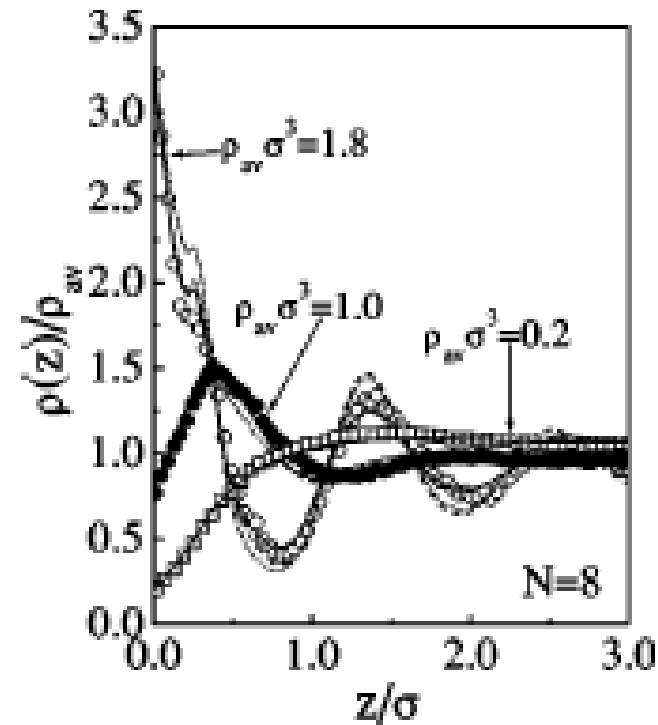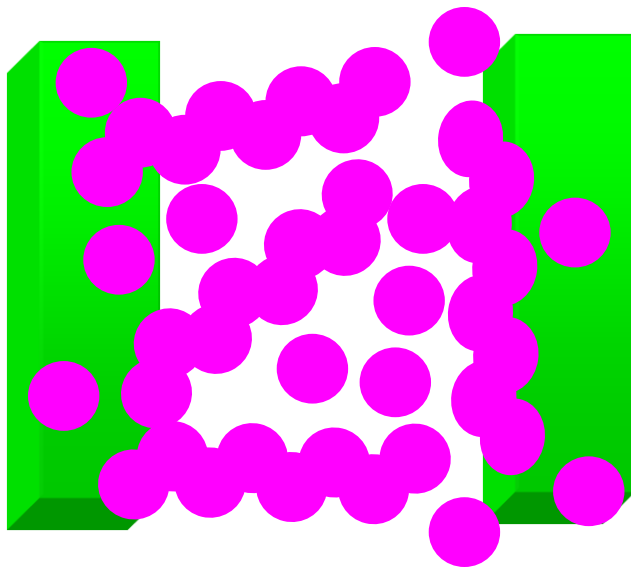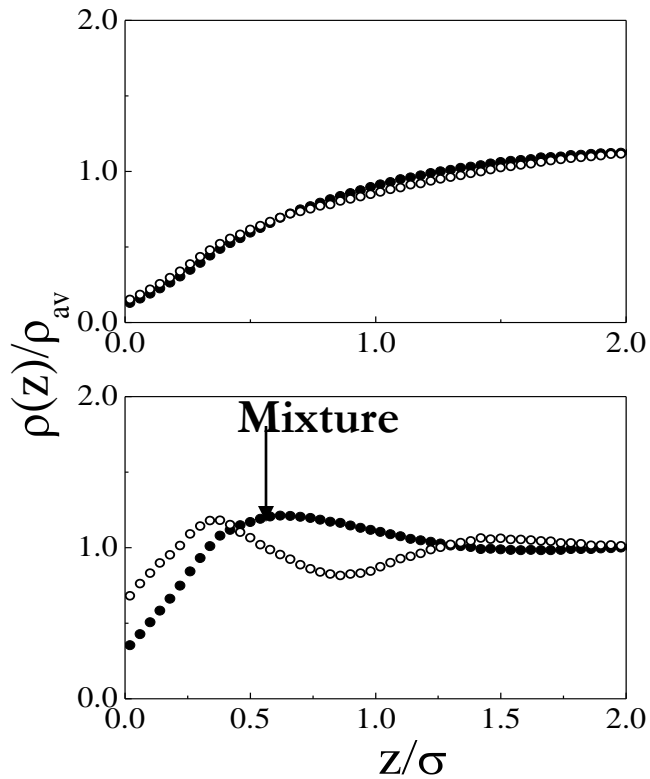
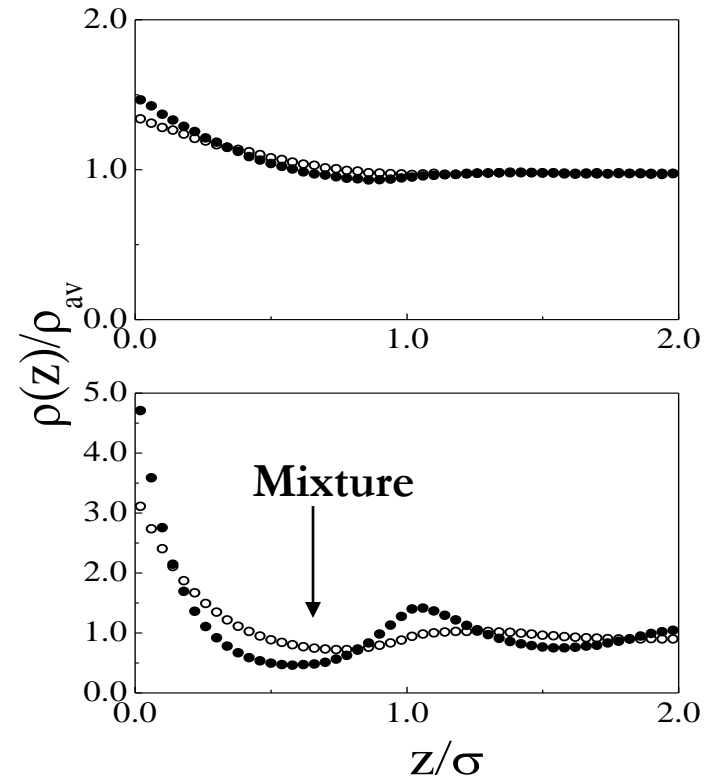FIG. 1. Density profiles of 8-mers at $\rho_{av}\sigma^3 = 0.2$, 1.0, and 1.8. Present work (——); YW theory [9] (······); Yethiraj [10] (— — —). Circles represent Monte Carlo simulations.

Results

Polymer Site Density

Solvent Density

✹ Contrary to usual expectations, the density profiles of chains in the mixture is more than that in pure components. The opposite is true for the solvent.

Colloids: A system of biological interest
Tunable interaction potential
DFT of inhomogeneous colloidal suspension
$$u(r_{12}) = A \exp[-\kappa(r_{12} - d)]/r_{12}$$
$$\kappa^2 = (4\pi\beta/\varepsilon)[\rho_0 Z e^2 + \Sigma \, \rho_\alpha Z_\alpha^2 e^2]$$
Tunable two-body interaction by changing ρ_0 and ρ_α

Colloidal dispersion in a planar slit/cylindrical pore
implication in blood flow through veins
flow through porous membranes
Phase ordering in charged colloids

Colloidal dispersion confined in a planar slit: A density functional approach

Niharendu Choudhury and Swapan K. Ghosh
Heavy Water Division, Bhabha Atomic Research Centre, Bombay 400085, India

We present a simple density functional approach for the prediction of the local density profile of a colloidal suspension confined in a charged planar slit. Both the interparticle and wall–particle interactions are modeled to be of screened Coulomb type. The short range part of the interparticle correlation is treated through a nonperturbative weighted density approach, while the long range contribution is treated perturbatively in terms of the density inhomogeneity. The input correlation functions for the bulk fluid are obtained through the rescaled mean spherical approximation. The calculated density profiles are shown on an average to compare well with results from computer simulation. © *1996 American Institute of Physics.* [S0021-9606(96)51222-5]
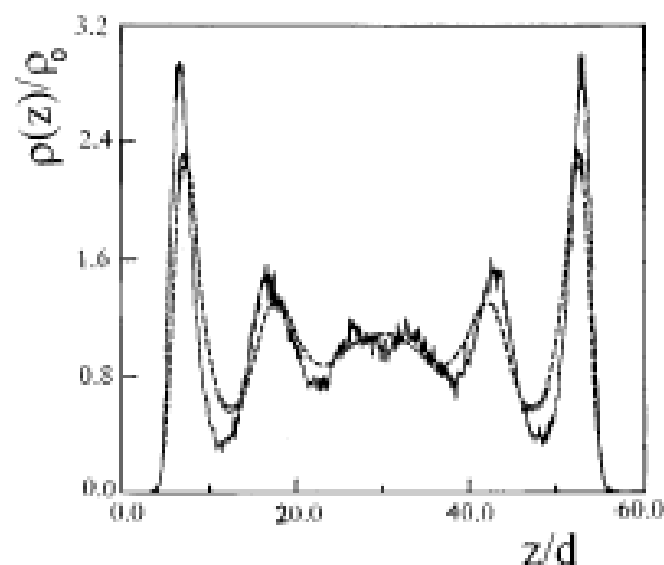
FIG. 3. Plot of the density profile $\rho(z)/\rho_0$ vs z/d for a model colloidal suspension for wall separation of $60d$. The parameters and the key are same as in Fig. 1.
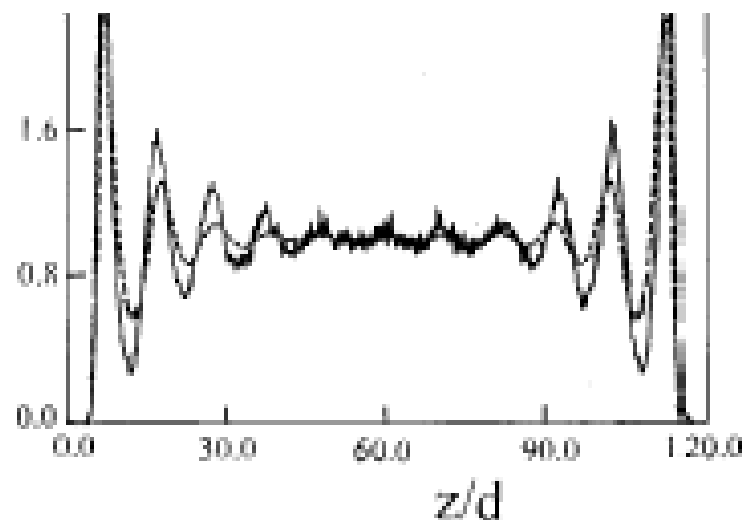

FIG. 4. Plot of the density profile $\rho(z)/\rho_0$ vs z/d for a model colloidal suspension for wall separation of $120d$. The parameters and the key are same as in Fig. 1.

Colloidal suspensions in charged cylindrical pores: A perturbative density functional approach

Niharendu Choudhury and Swapan K. Ghosh

Theoretical Chemistry Section, RC & CD Division, Chemistry Group, Bhabha Atomic Research Centre, Bombay 400 085, India
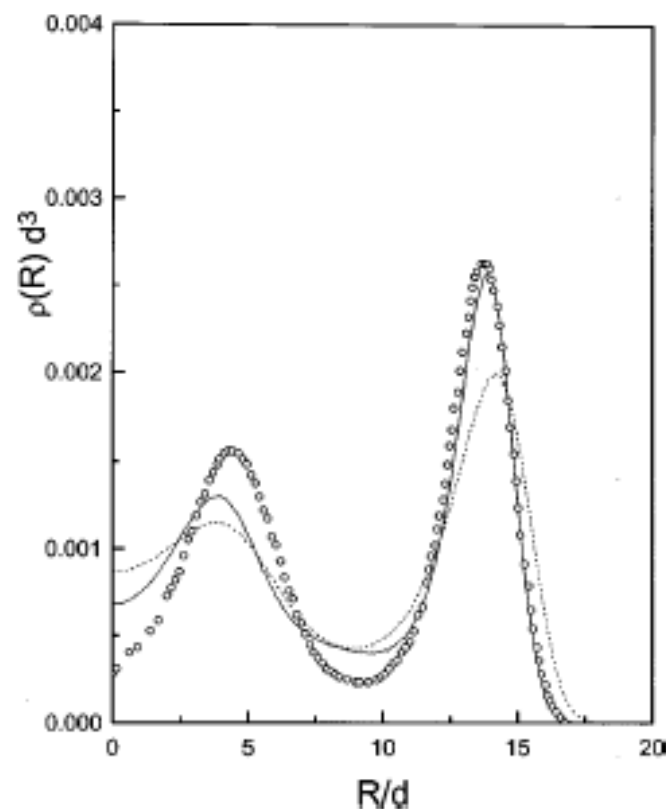
FIG. 1. Plot of density profile $\rho(R)d^3$ vs R/d for a model colloidal suspension with the bulk parameters $\rho_0 d^3 = 0.00084$, $k = 0.15$, and $\gamma = 464.73$ confined in a cylindrical pore with $R_0' = 30d$ and $K_w = 500$. Solid line, present third order perturbative scheme; dashed line, second order perturbative or HNC result; open circles, simulation result.
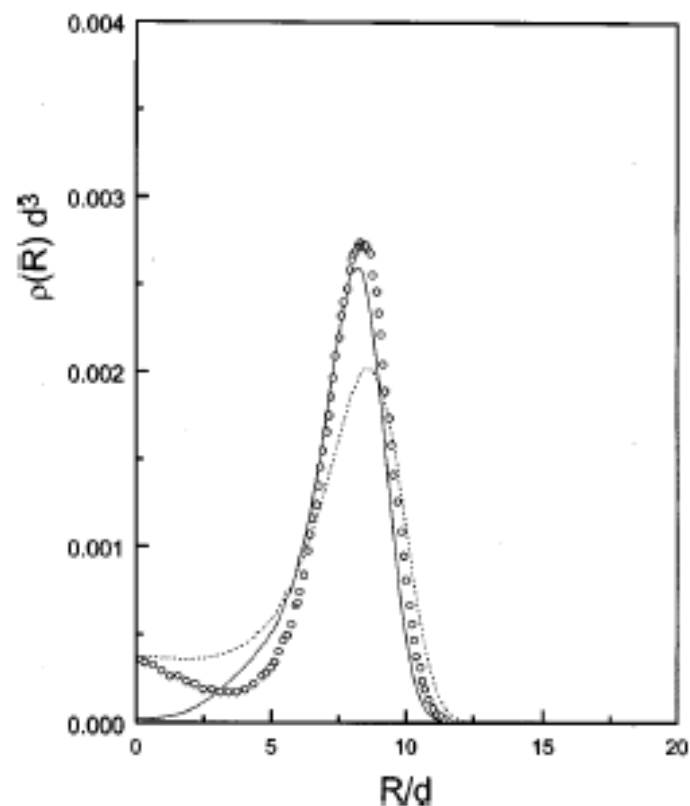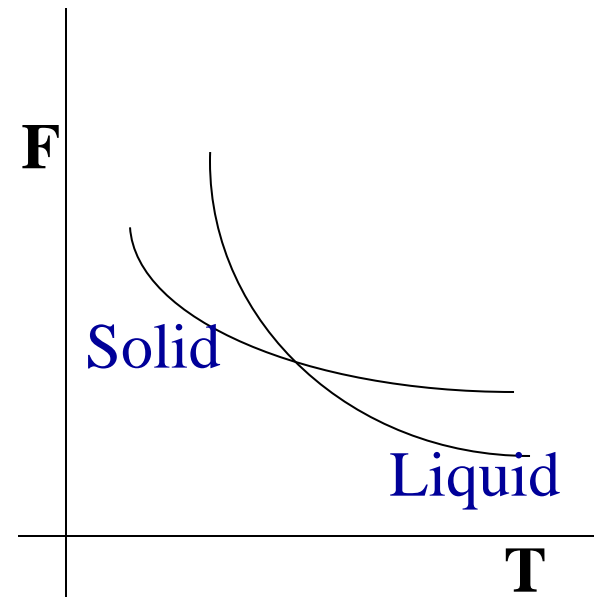
FIG. 2. Plot of density profile $\rho(R)d^3$ vs R/d for a model colloidal suspension confined in a cylindrical pore with $R_0' = 30d$ and $K_w = 1000$. The key and the bulk parameters are same as in Fig. 1.

Density Functional Theory of Freezing

- **Usual examples of inhomogeneous density caused by the field of external potential**

- **Spontaneous appearance of inhomogeneous density as a function of control parameter**

- **Examples of freezing as a function of temperature or density**

- **Free energy of the homo-geneous liquid phase and the inhomogeneous solid phase obtained as density functionals**

- **The point of crossing indicates phase transition**

$$V(r) = (Z^2 e^2 / \varepsilon)(1 + \kappa d / 2)^{-2} \exp[-\kappa(r - d)]/r$$

$$\kappa^2 = (4\pi\beta/\varepsilon)\left[\rho_0 Z e^2 + \sum_\alpha n_\alpha Z_\alpha^2 e^2\right]$$

$$\rho(\mathbf{r}) = \sum_i (\alpha/\pi)^{3/2} \exp[-\alpha(\mathbf{r} - \mathbf{R}_i)^2] \ ,$$

which can also be written as a sum in the reciprocal space, viz.,

$$\rho(\mathbf{r}) = \sum_G \rho(\mathbf{G}) \exp(i\mathbf{G}\cdot\mathbf{r}),$$

$$\rho(\mathbf{G}) = \rho_0 \exp[-G^2/4\alpha] \ ,$$

$$\beta\Delta F[\rho]/N = [\ln(\alpha/\pi)^{3/2} - \ln(\rho_0) - \tfrac{3}{2}]$$
$$- \tfrac{1}{2}\sum_G{}' \rho(\mathbf{G})^2 c^{(2)}(\mathbf{G}) + \Delta F_{\text{ex}}^{(3)}[\rho]/N \ , \qquad (14)$$

with the effective higher-order correlation contribution $\Delta F_{\text{ex}}^{(3)}$ defined as

$$\Delta F_{\text{ex}}^{(3)} = (\Delta F_{\text{HS}}^{\text{ex}})_{\text{MWDA}}[\rho] - (\Delta F_{\text{HS}}^{\text{ex}})_{\text{pert}}[\rho] \ , \qquad (15a)$$

with

$$(\Delta F_{\text{HS}}^{\text{ex}})_{\text{pert}}[\rho] = -\tfrac{1}{2}N\sum_G{}' \rho(\mathbf{G})^2 c_{\text{HS}}^{(2)}(\mathbf{G}) \ . \qquad (15b)$$

Density functional theory of ordering in charge-stabilized colloidal dispersions

Niharendu Choudhury and Swapan K. Ghosh
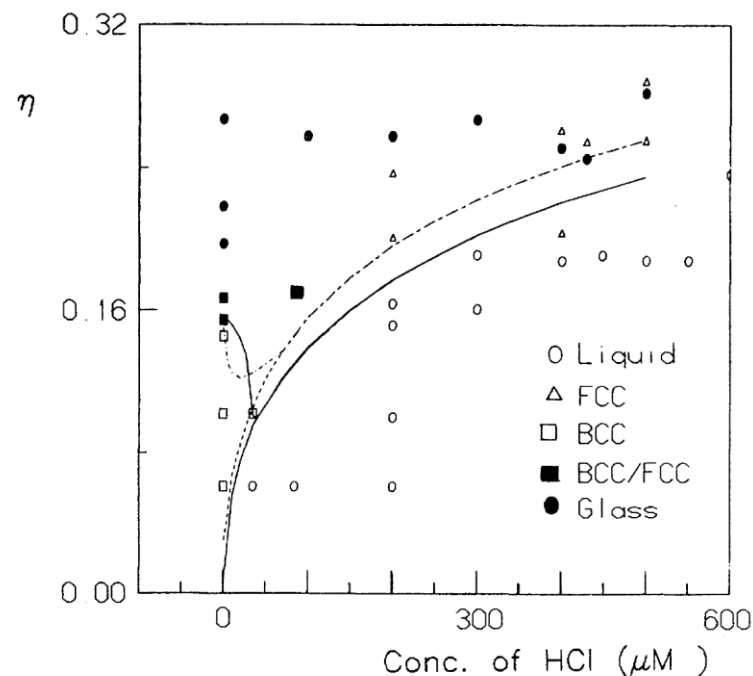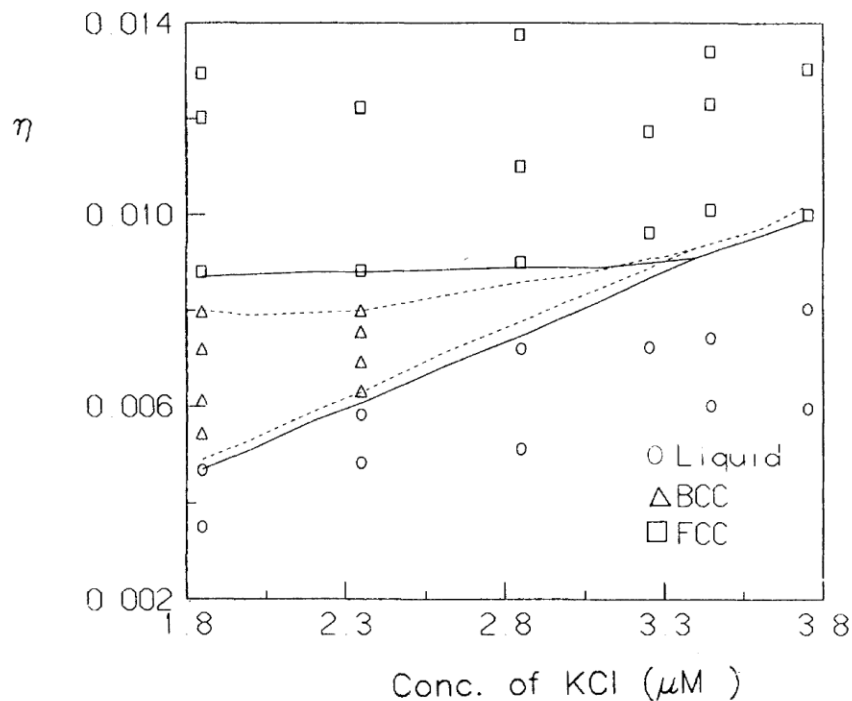*Heavy Water Division, Bhabha Atomic Research Centre, Bombay 400085, India*

FIG. 1. Phase diagram of charge-stabilized colloidal dispersion of a polystyrene sphere in water (system I): $- - -$, calculated results using scheme A; ——, calculated results using scheme B. The circles, triangles, and squares denote the experimental points of Monovoukas and Gast.

FIG. 2. Phase diagram of charge-stabilized colloidal dispersion of a polystyrene sphere in methanol (system II): $-\cdot-\cdot-$, calculated results using scheme A; ——— calculated results using scheme B. The squares, circles, and triangles denote the experimental points of Sirota *et al.*

Modified weighted density-functional approach to the crystal-melt interface

Niharendu Choudhury and Swapan K. Ghosh

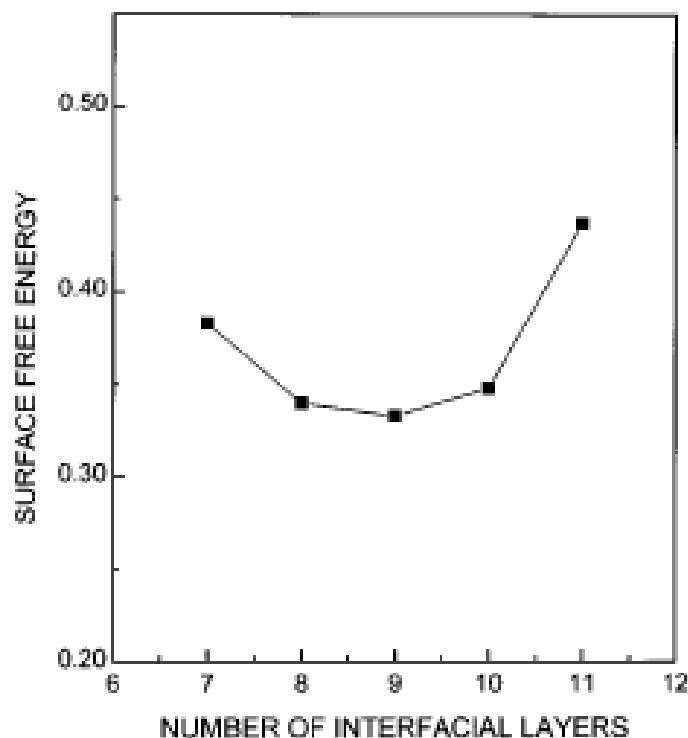*Heavy Water Division, Bhabha Atomic Research Centre, Bombay 400085, India*

FIG. 1. Plot of calculated surface free energy vs number of interfacial layers for fcc liquid (111) interface of hard sphere fluid.
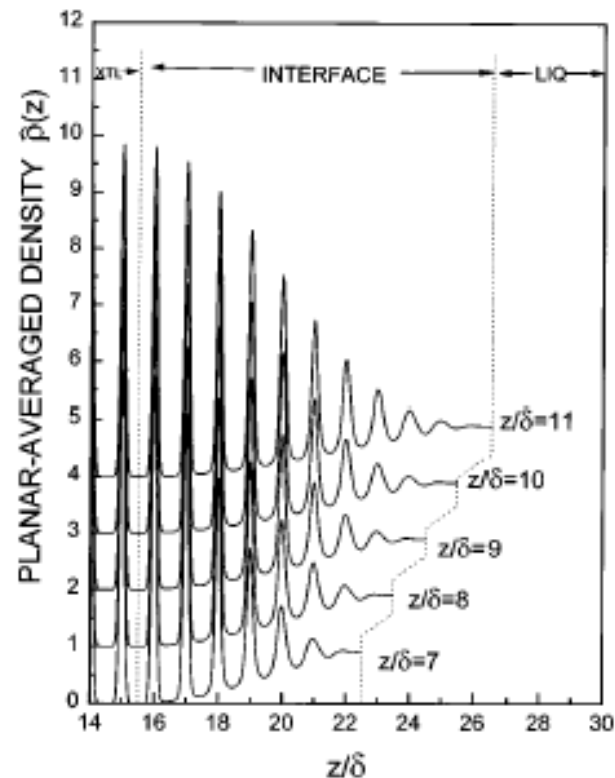

FIG. 2. Plot of planar averaged interfacial density profile $\bar{\rho}(z)$ for the (111) fcc liquid interface of hard sphere fluid for several values of interfacial width.

DYNAMICAL PHENOMENA

- *Diffusion Phenomena in Complex Fluid Mixtures*

- *Flow through Nanopores*

- *Diffusion Assisted End-to-End Relaxation Dynamics of Polymer Chain*

- *Trapping of Diffusion Assisted System in External Periodic Field: Coherent Stochastic Resonance*

- *One-Dimensional Unified Description of Multi-Dimensional Dynamical Processes in Condensed Phase*

Diffusion in Fluid Mixtures

• Diffusion is an important dynamical phenomenon for chemical reactions & other processes in condensed phase

• Difficulty in theoretical evaluation due to lack of knowledge of various dynamical correlation Functions

• Relationship between the transport coefficients and structural properties has remained as one of the most challenging and non-trivial tasks in the field of condensed phase dynamics.

New Universal Scaling Laws of Diffusion and Kolmogorov-Sinai Entropy in Simple Liquids

Alok Samanta,[1] Sk. Musharaf Ali,[2] and Swapan K. Ghosh[1,*]

[1]Theoretical Chemistry Section, RC &CD Division, Bhabha Atomic Research Centre, Mumbai 400 085, India
[2]Chemical Engineering Division, Bhabha Atomic Research Centre, Mumbai 400 085, India
(Received 11 September 2003; published 9 April 2004)

A new universal scaling law relating the self-diffusivities of the components of a binary fluid mixture to their excess entropies is derived using mode coupling theory. These scaling laws yield numerical results, for a hard sphere as well as Lennard-Jones fluid mixtures, in excellent agreement with simulation results even at a low density region, where the empirical scaling laws of Dzugutov [Nature (London) **381**, 137 (1996)] and Hoyt, Asta, and Sadigh [Phys. Rev. Lett. **85**, 594 (2001)] fail completely. A new scaling law relating the Kolmogorov-Sinai entropy to the excess entropy is also obtained.

- Universal Scaling Laws of Diffusivity

- Scaled Diffusivity expressed in terms of excess entropy obtained from the Radial Distribution Function g(**r**), (essentially number density around a solute).

$g(r)$

Density

r
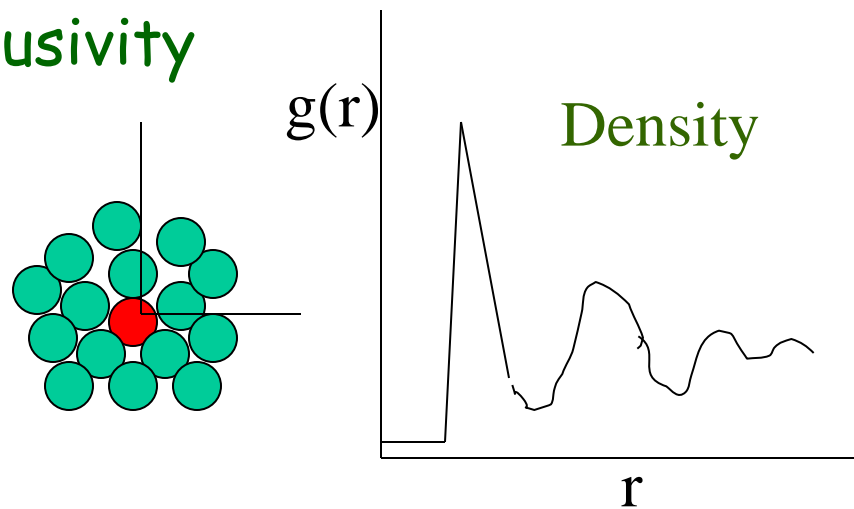
Universal Scaling Laws of Diffusivity derived for Fluid Mixtures by approximating the mode coupling theory expressions

Scaled Diffusivity: $D_\mu* = A \exp[-S_\mu]$

Excess entropy: $S_\mu = \sum_\nu \rho_\nu \int d\mathbf{r} \left[g_{\mu\nu}(\mathbf{r}) \ln g_{\mu\nu}(\mathbf{r}) - (g_{\mu\nu}(\mathbf{r}) - 1) \right]$
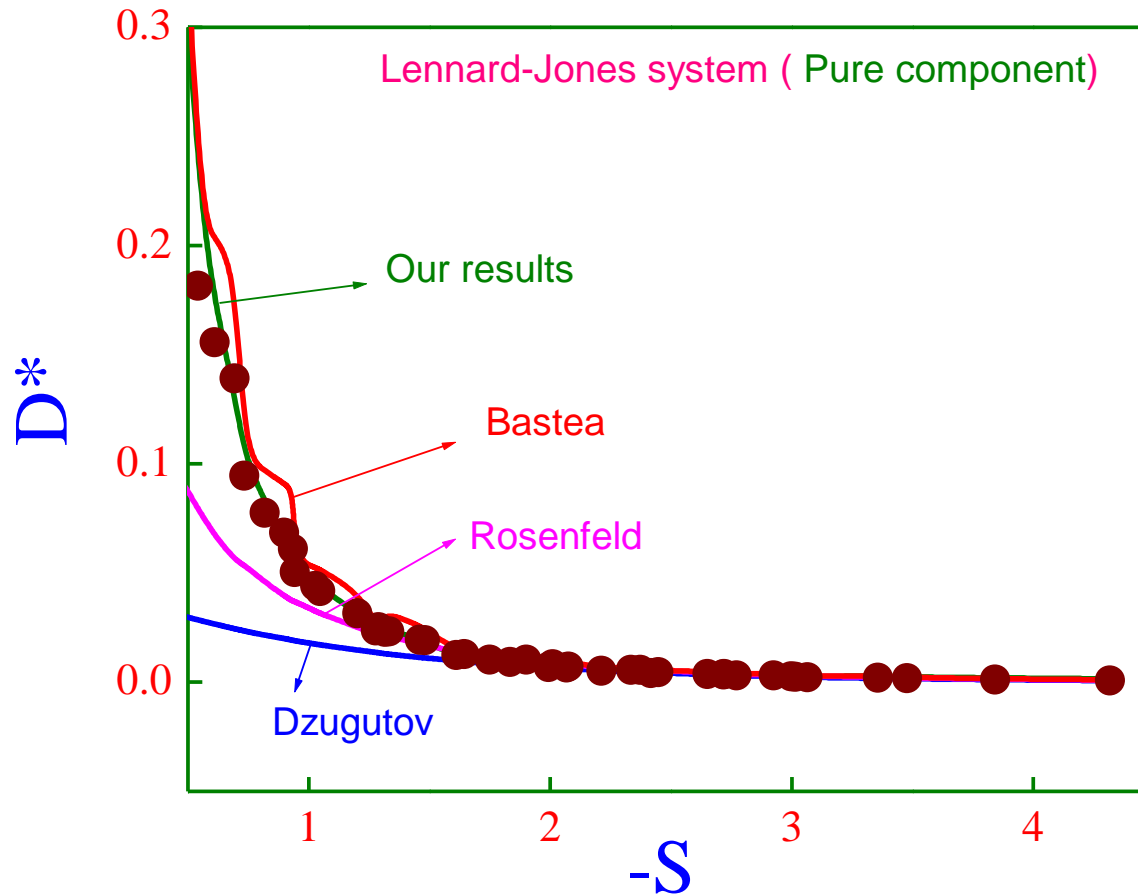
A. Samanta, Sk. M. Ali, and S. K. Ghosh, Phys. Rev. Lett. 87, 245901 (2001), ; 92, 145901 (2004).

Mode coupling theory of self and cross diffusivity in a binary fluid mixture: Application to Lennard-Jones systems

Sk. Musharaf Ali
Chemical Engineering Division, Bhabha Atomic Research Centre, Mumbai 400 085, India

Alok Samanta and Swapan K. Ghosh[a]
Theoretical Chemistry Section, RC & CD Division, Chemistry Group, Bhabha Atomic Research Centre, Mumbai 400 085, India

A microscopic approach has been developed for the self as well as cross diffusivity of a binary fluid mixture based on the concepts of mode coupling theory. Illustrative numerical results calculated for a Lennard-Jones fluid mixture are presented and are shown to be in good agreement with the available computer simulation results. The effects of mass, composition, interaction strength, and sizes of the components on the diffusivities are studied in order to obtain insight into the role of different modes in the diffusion process. The mass dependence of diffusivity is found to be weak with a power law behavior in contrast to the Enskog theory prediction of strong mass dependence. Also the mass and concentration of one component are found to have significant and interesting effects on the diffusivity of the other component. The new expressions derived here are shown to predict positive values for the cross diffusion constant over the various parameter ranges considered, which is consistent with the simulation results but unpredicted by other commonly used models. It is also found that the cross diffusion is significant in liquid Lorentz–Berthelot mixture for size ratio unity, strong interaction potential, and intermediate composition range. © *2001 American Institute*

Self-diffusivity of each component

$$D_\mu = \frac{k_B T}{\overline{\xi_\mu^0}(0)}$$

Friction coefficient:

$$\frac{1}{\overline{\xi_\mu^0}(s)} = \frac{1}{\overline{\xi_\mu^B}(s) + \overline{\xi_\mu^{\rho\rho}}(s)} + \frac{1}{\overline{\xi_\mu^T}(s)}$$

Binary short range contribution:

$$\overline{\xi_\mu^b}(0) = \frac{16\pi}{3}\left(\frac{k_B T}{2\pi}\right)^{1/2} \sum_\nu \left(\frac{m_\mu m_\nu}{(m_\mu + m_\nu)}\right)^{1/2} \rho_\nu \sigma_{\mu\nu}^2 g_{\mu\nu}(\sigma_{\mu\nu})$$

Density fluctuation contribution:

$$\xi_\mu^{\rho\rho}(t) = \left(\frac{k_B T \rho}{6\pi^2}\right) \sum_\nu \sum_{\nu'} \int_0^\infty dk\, k^4 G_\mu(k,t)\ c_{\nu\mu}(k) c_{\nu'\mu}(k) G_{\nu\nu'}(k,t),$$

Self dynamic structure factor

Transverse mode contribution:

$$\frac{1}{\xi_\mu^T(t)} = \frac{m_\alpha m_\beta}{3\pi^2 \rho m_\mu^2 (m_\beta x_\alpha + m_\alpha x_\beta)}\left(\frac{\Omega_\mu(0)}{\Omega_\mu^0(0)}\right)^2 \int_0^\infty dk\, k^2 |V_\mu(k)|^2 G_\mu(k,t) C_T(k,t).$$
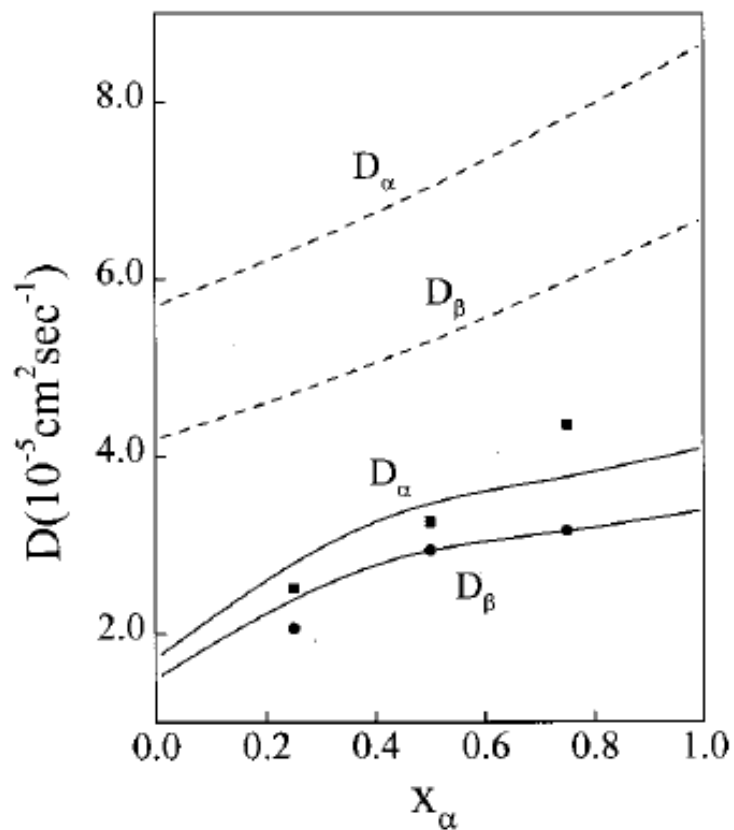
FIG. 4. Plot of self-diffusion constants vs concentration for the parameters: $\rho^* = 0.70$, $\epsilon_{\alpha\alpha}/k_B = 120.0$, $\epsilon_{\beta\beta}/k_B = 167.0$, $m_\beta/m_\alpha = 83.8/39.9$, $\sigma_{\beta\beta} = 3.633$ Å, $\sigma_{\alpha\alpha} = 3.405$ Å, and $T = 121.7$ K. The calculated mode coupling theory results are shown by solid lines, Enskog kinetic theory results by dashed lines and simulation results by symbols [D_α by (■) and D_β by (●)].
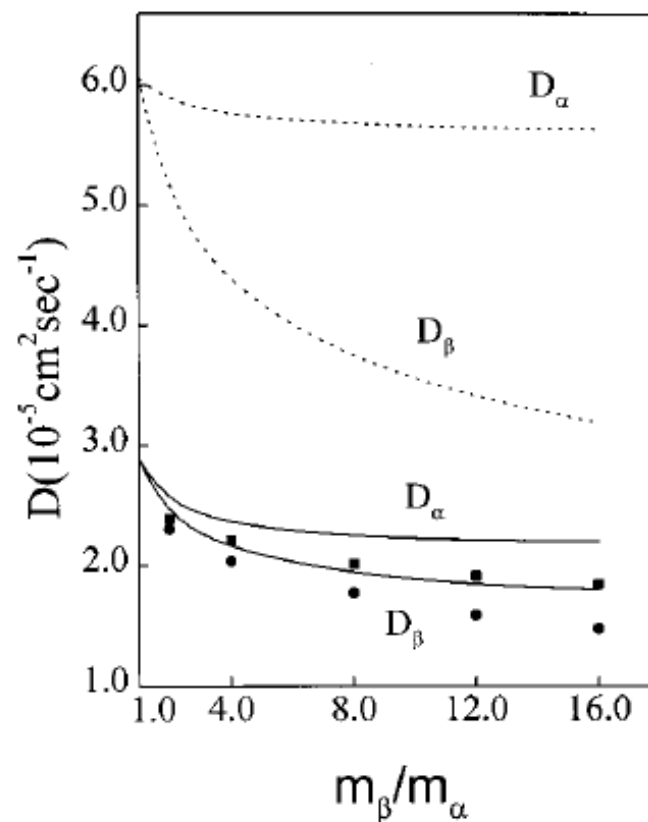
FIG. 2. Plot of the self-diffusion constants vs mass ratio at composition $x_\alpha = 0.8$ with other parameters same as in Fig. 1. Solid line (—) represents the present mode coupling theory results and dotted line (⋯) represents the Enskog theory results. Simulation results for D_α are shown by square (■) and D_β by circle (●).
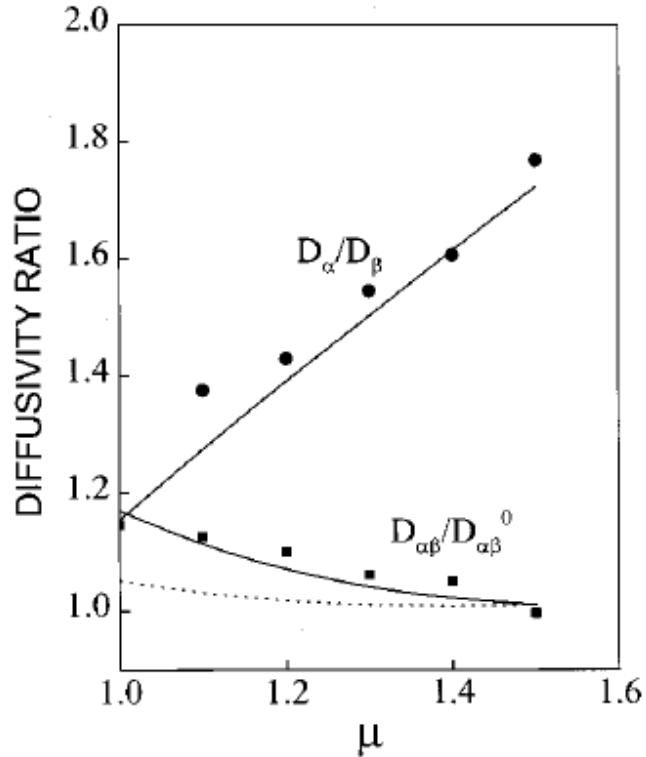
FIG. 6. Plot of the self (D_α/D_β) and mutual diffusivity ratio $(D_{\alpha\beta}/D^0_{\alpha\beta})$ as function of the size ratio $\mu(=\sigma_{\beta\beta}/\sigma_{\alpha\alpha})$ at $\nu=2.5$. Other parameters are same as in Fig. 5. The calculated mode coupling theory results are shown by solid lines (——) and simulation results by symbols [D_α/D_β by (●) and $D_{\alpha\beta}/D^0_{\alpha\beta}$ by (■)]. The Enskog theory results are shown by dashed lines (- - - -).

The MCT thus provides a route to the Diffusivity for a Fluid of uniform density.

For using MCT for Diffusion in Nanopores, where the density is inhomogeneous, a mapping to equivalent uniform fluid at each point in space through the concept of weighted density is to be done, using the so called Density Functional Theory for Classical Fluids
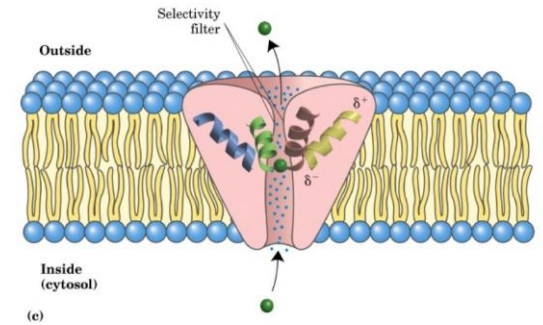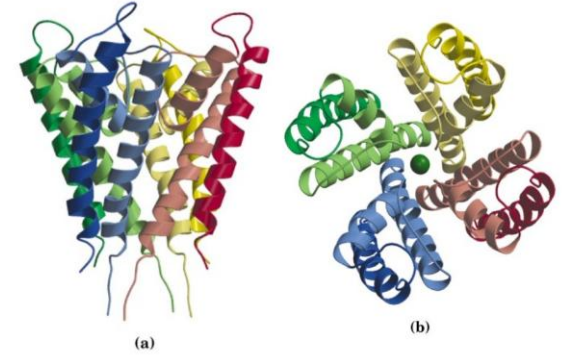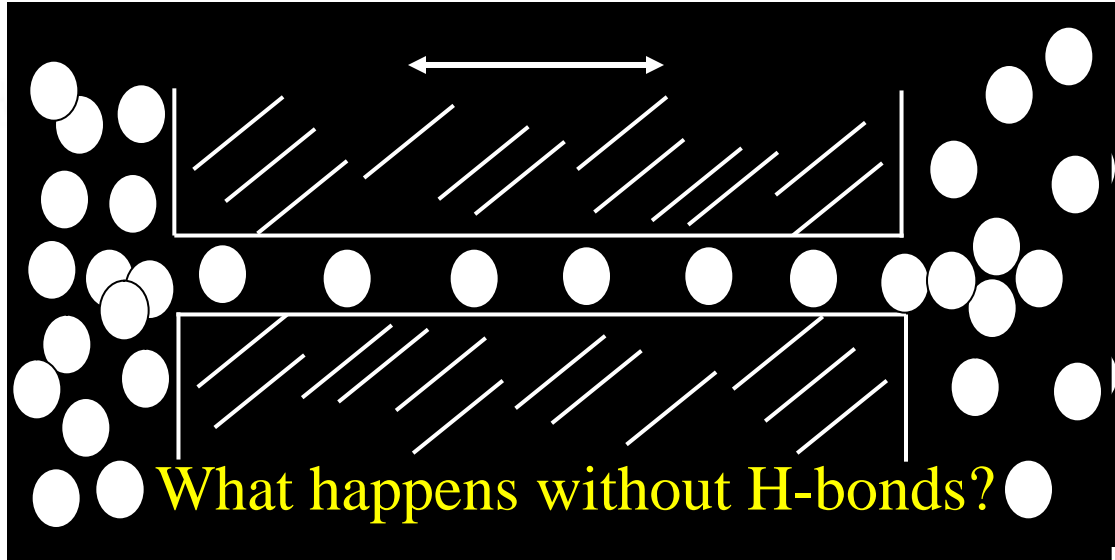
Diffusion in Nanopores
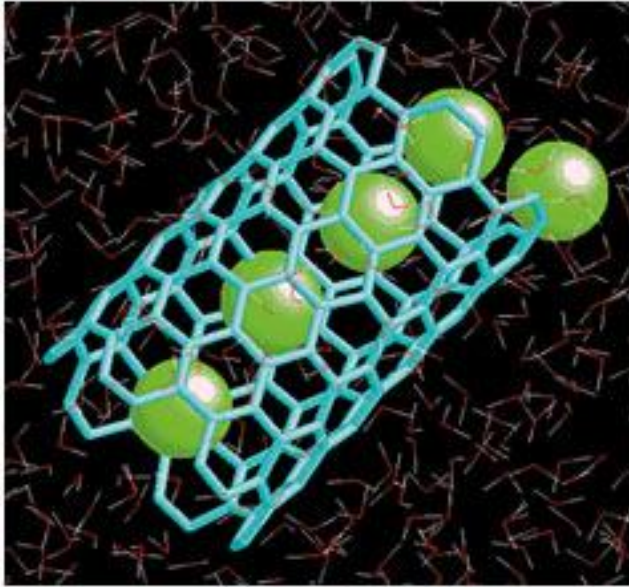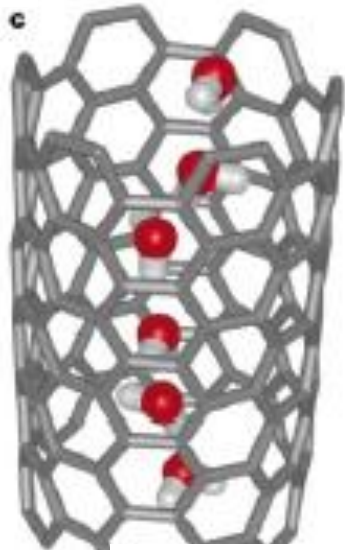
## Single-File Diffusion
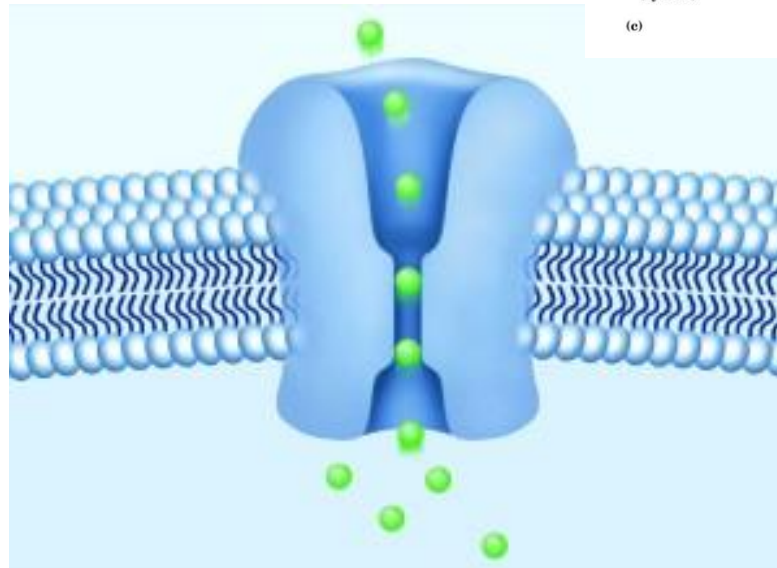
K+ ion Channel

Single-File conduction through smooth channel

Objective: To study the translocation dynamics of particles in a finite and smooth single-file channel connected with reservoirs at the ends: dependence on channel length and inter-particle interaction.

Water loses 2 of 4 H-bonds; yet it hydrates the C-nanotube

What happens without H-bonds?

Hummer G., Rasaiah J. C. and Nowortya J. P.,Nature, 414 (2001) 188.
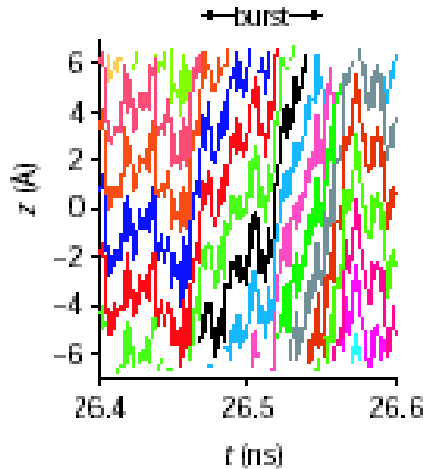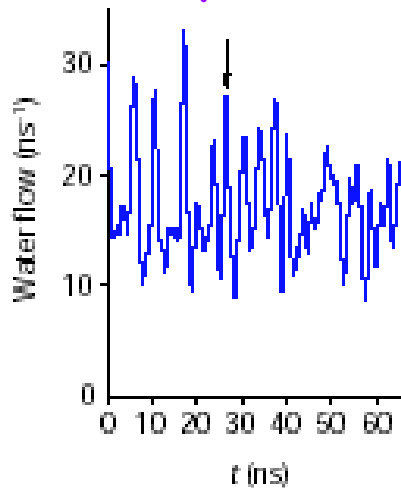
Rupturing the water chain involves energy cost - intermittent flow

Bursts in single-file motion mediated conduction

Shashwati Roy Majumder,[a)] Tusar Bandyopadhyay,[b)] and Swapan K. Ghosh[c)]
Theoretical Chemistry Section, Chemistry Group, Bhabha Atomic Research Centre, Trombay, Mumbai 400 085, India

Enhanced flow in smooth single-file channel

Shashwati Roy Majumder,[a)] Niharendu Choudhury,[b)] and Swapan K. Ghosh[c)]
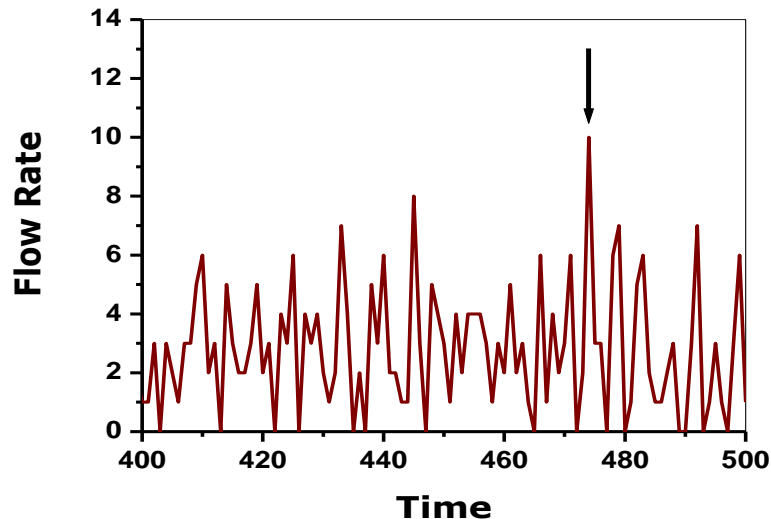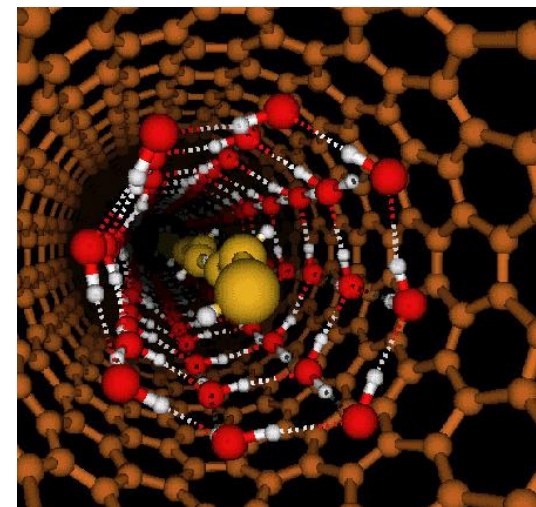*Theoretical Chemistry Section, Chemistry Group, Bhabha Atomic Research Centre, Trombay, Mumbai 400 085, India*

**Conduction Bursts- Universal Feature of Single File Motion**

•Single-File motion through narrow pores is beyond the realm of Fickian description

•No general appropriate analytical theory is available as yet

•What are the possible universal features of Single-File flow through a finite channel, connected to two reservoirs?

$$P_{tr}(t) \text{ (or, } P_r(t)) = \frac{\text{No. of translocated (or returned) particles within spent time } t}{\text{Total No. of translocated (or returned) particles within } 10^5 \text{ CA steps}}$$
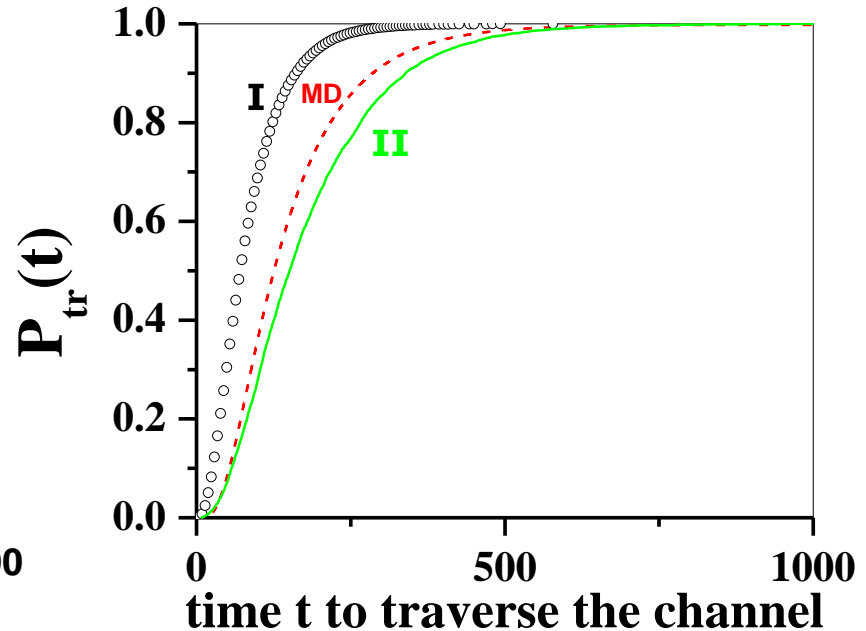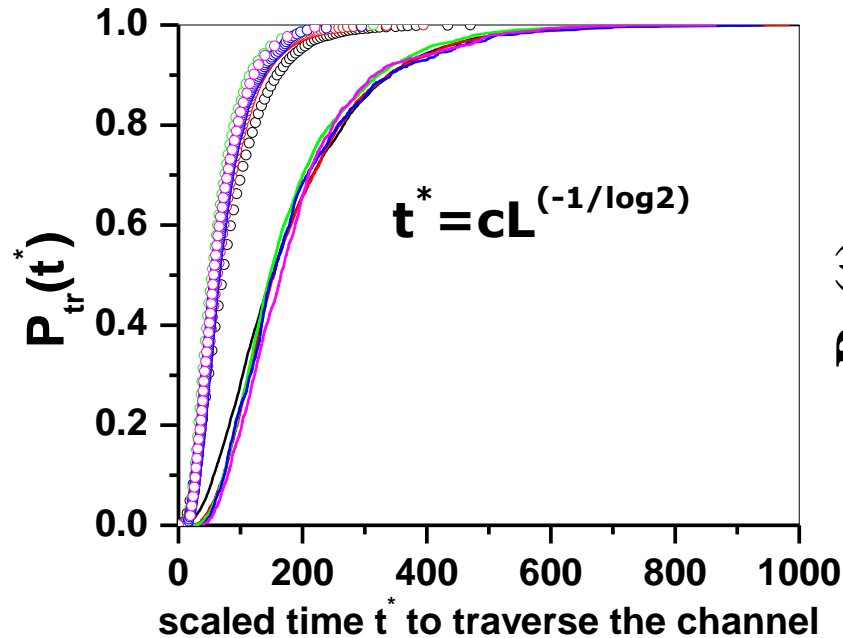
• Cumulative translocation probabilities for different channel lengths show universality as a function of scaled time t*.

• With proper scaling of time curves for different inter-particle interaction also shows universal behavior.

Remarks

- One hallmark of single-file diffusion is the conduction bursts, be it water or any other fluid.

- If the cumulative transport probabilities of particles through single-file channels of a given length is known, others can be obtained through proper scaling of time, without bothering about a further evaluation.

- Conduction of ions through ion-channels or blood flow through certain sized arteries / veins are single-file

- Separation of particles through cell membranes or O_2/food/drug release from blood to tissues occur intermittently rather than continuously !
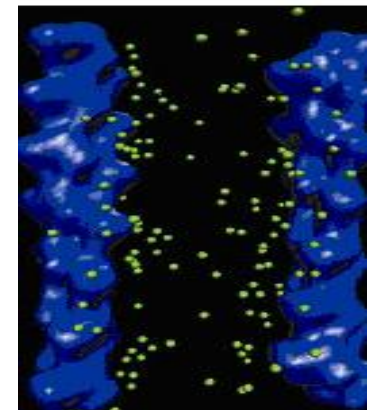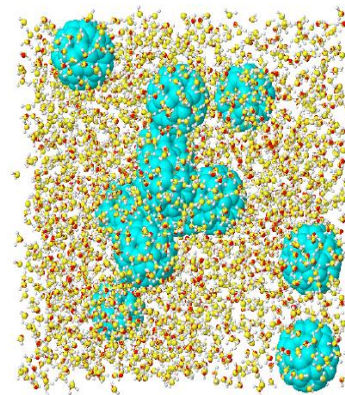
MCT for diffusion in Nanopores
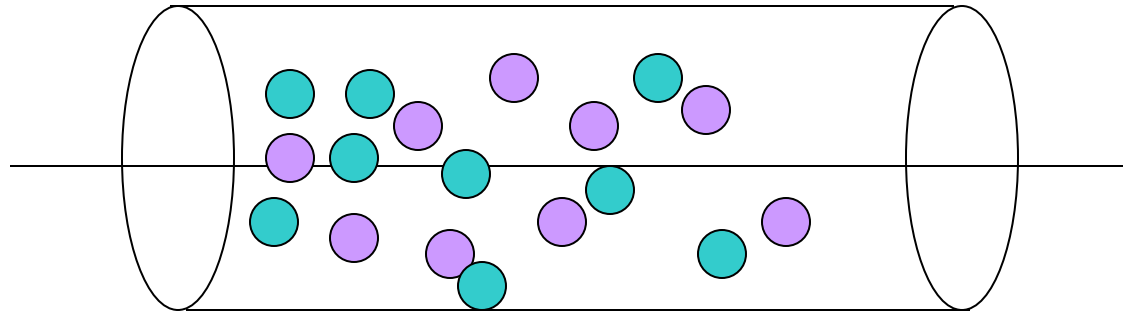
Inhomogeneous Density Distribution

Density functional Theory:
Versatile Tool for easy calculation of the inhomogeneous density distribution of Soft Condensed Matter under Confinement

Solid-Liquid Interface
Liquid-Liquid Interface
Liquid-Vapour Interface
Solute-Solvent Interface
(spherical, Planar, Cylindrical)

Diffusion assisted end–to–end relaxation of a flexible Rouse polymer chain: Fluorescence quenching through a model energy transfer

Tusar Bandyopadhyay[a] and Swapan K. Ghosh[b]

Theoretical Chemistry Section, Radiation Chemistry and Chemical Dynamics Division,
Bhabha Atomic Research Centre, Trombay, Mumbai 400 085, India
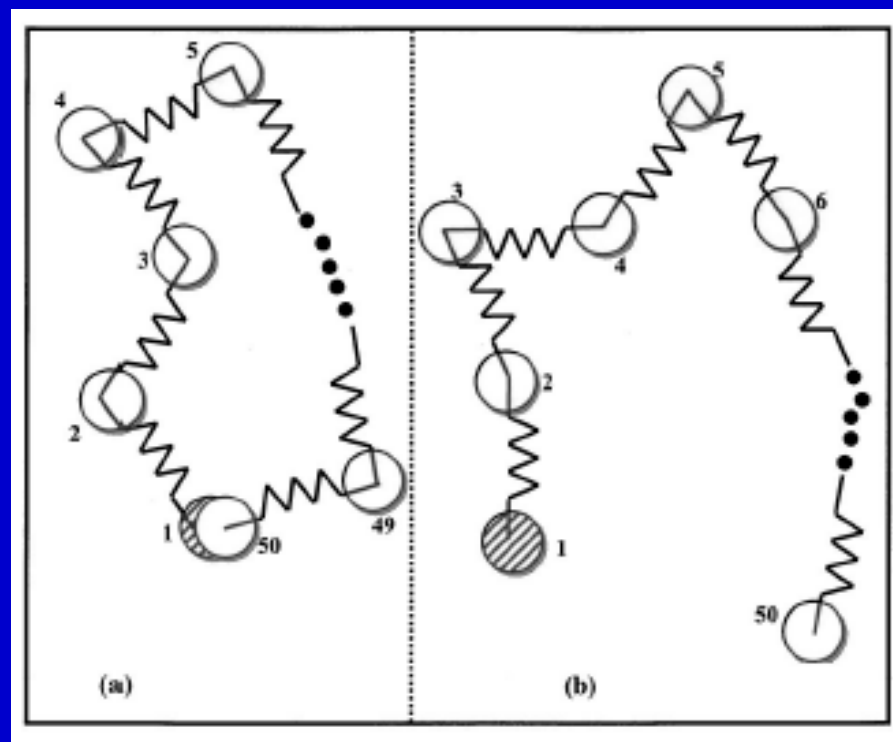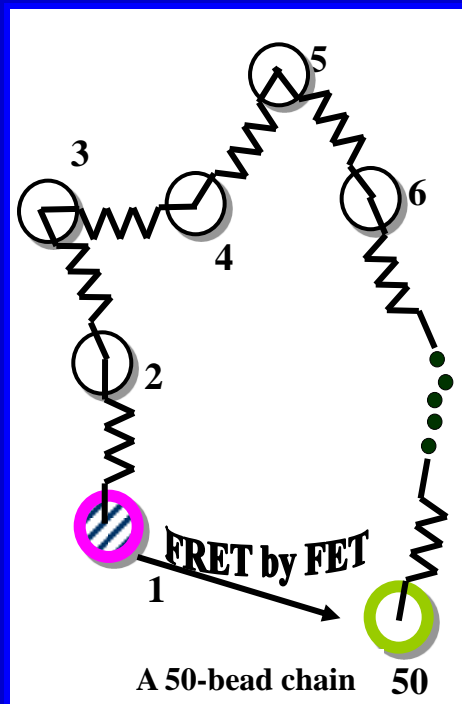
End-to-end relaxation of polymer (protein) chain

Chain Open

Chain Closure
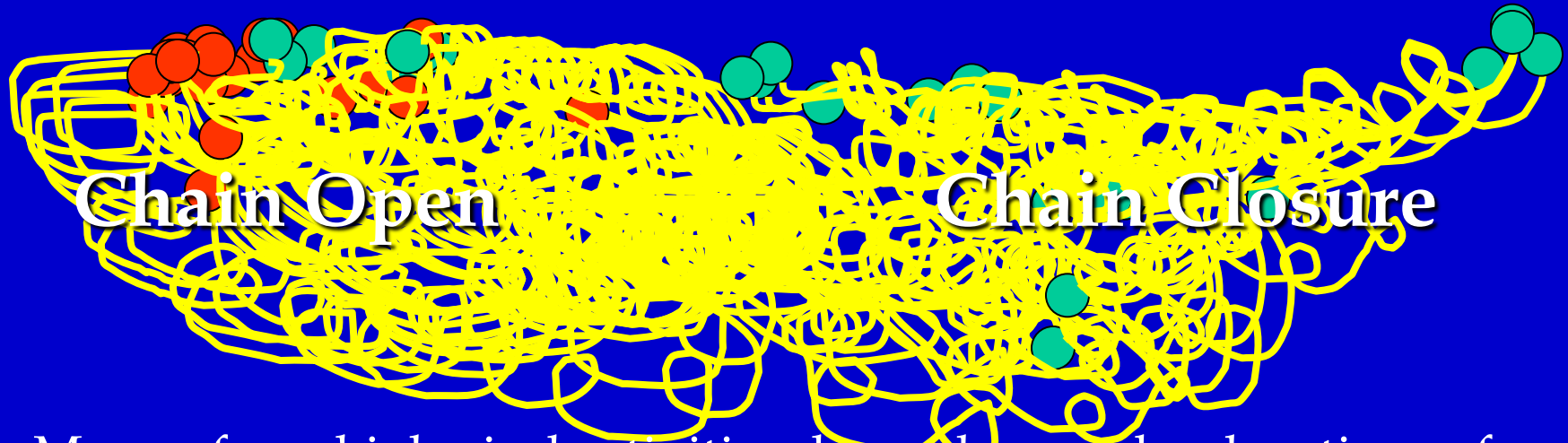
- Many of our biological activities depend on such relaxations of proteins and biopolymers

- **The problem :** How to distinguish between a closure and opening transitions, traditionally monitored by time-dependent fluorescence resonance energy transfer (FRET) signal

- **The Solution:** Theories have been developed utilizing Zwanzig's treatment of irreversible thermodynamics to address this issue. Criteria for a <u>definitive signature</u> of closure Transition have been formulated.

The result will have significant impact in the field of protein folding dynamics

Typical Results

Equilibrium Folded Chain

Without memory term

With memory term

BD Results

$S_p(\tau)$

Time(τ)

A Folding Transition

100 75 50 25 0

$\rho(r,t)$

α

Distance(r)

Coherent and incoherent trapping of a diffusion-assisted system in the presence of an external periodic field

Tusar Bandyopadhyay* and Swapan K. Ghosh[†]

Theoretical Chemistry Section, Radiation Chemistry and Chemical Dynamics Division, Bhabha Atomic Research Centre, Trombay, Mumbai 400 085, India
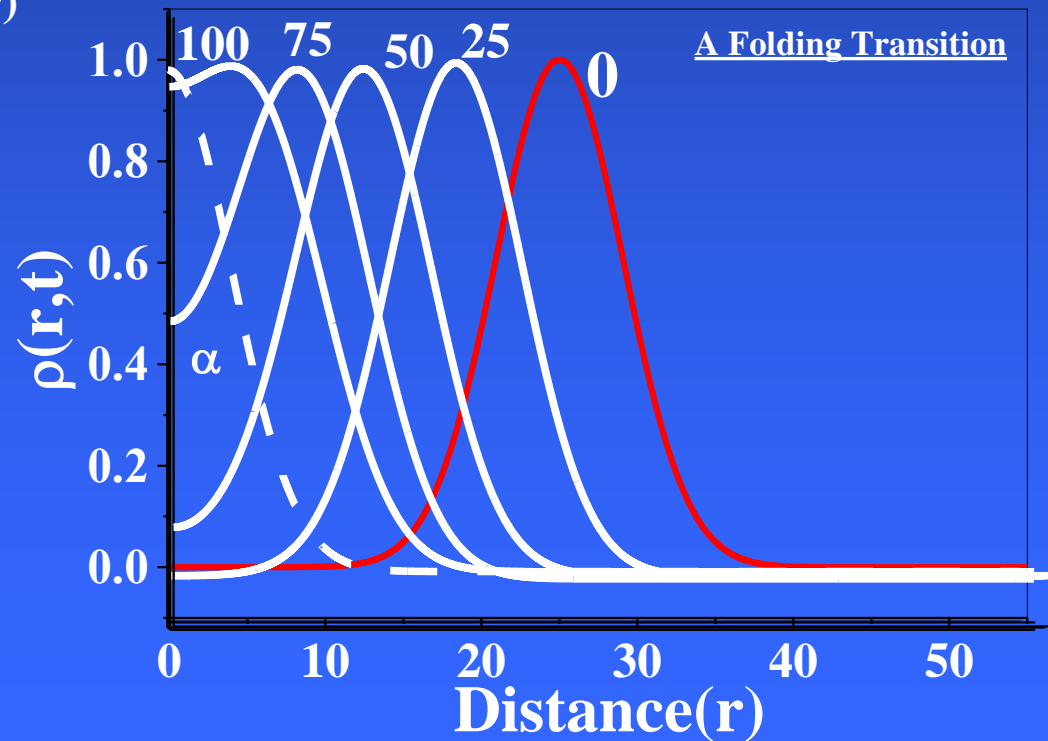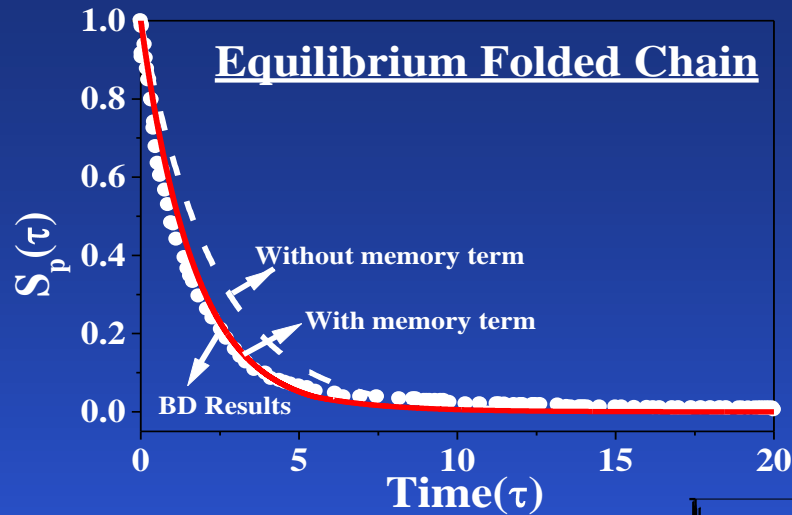
Field induced trapping on a line segment of a diffusion-driven system is studied with an aim to gain an insight into the occurrence of coherent stochastic resonance, which is thoroughly explored as synchronized (synchronization coherence) between the external bias, the noise in the system and to an optimum value by increasing the forcing frequency reveals a minimum in the nonmonotonic mean-free-passage time driven frequency, is also nonmonotonic when considered as a the mean and reveals a maximum exhibiting the least synchroniza-

Separation of ions by synchronization of External field, Noise in the system & Temporal trapping event
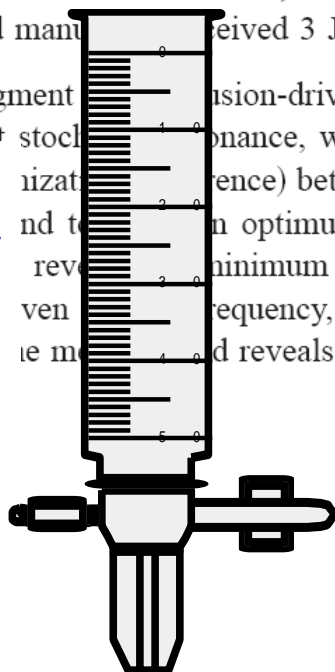
Electric Field

•**Coherent/Incoherent trapping at line boundaries is characterized & the counterintuitive constructive facet of noise behind the coherent trapping mechanism is explored**

Diffusion in 1-D in presence of Periodic Field

Coherent Stochastic Resonance: Interplay of Noise & Signal
Motivation

- Large molecular ions migrating through a gel medium in presence of external electric Field (**Forward Gel Electrophoresis)** separate mixtures of macromolecules

- A limitation: Size limit on the largest molecule that can be separated. Also, larger molecules exhibit size independent mobilities

- A simpler experiment (1986), replacing the continuous forward field with **alternating direction field**, led to success:
  - Biomolecules in desired size ranges resolved

  D. C. Schwartz and C. R. Cantor, Cell **37**, 67 (1984)
  G. F.Carle, M. Frank, and M. V. Olson, Science **232**, 65 (1986)

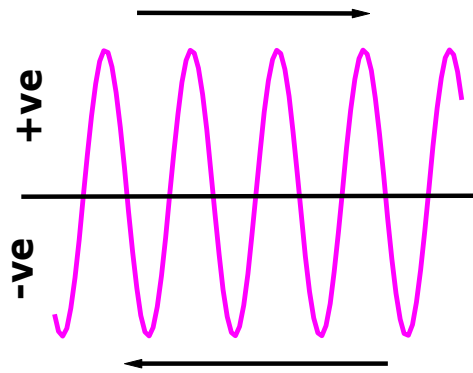- Fundamental aspects of the phenomena

Coherent and incoherent trapping of a diffusion-assisted system in the presence of an external periodic field

Tusar Bandyopadhyay* and Swapan K. Ghosh[†]

Theoretical Chemistry Section, Radiation Chemistry and Chemical Dynamics Division, Bhabha Atomic Research Centre, Trombay, Mumbai 400 085, India

Field induced trapping on a line segment of a diffusion-driven system is studied with an aim to gain an insight into the occurrence of coherent stochastic resonance, which is thoroughly explored as synchronized mean-free passages to the traps. Synchronization (coherence) between the external bias, the noise in the system and the temporal trapping events is found to attain an optimum value by increasing the forcing frequency towards the relevant resonant frequency, revealing a minimum in the nonmonotonic mean-free-passage time (MFPT) to trapping. The MFPT at a given forcing frequency, is also nonmonotonic when considered as a function of the diffusion coefficient of the medium, and reveals a maximum exhibiting the least synchroniza-tion effect (incoherent trapping).

Coherent Stochastic Resonance

Competitive dynamic interplay

+ve

-ve

Tim

Noise (diffusion) tend to equilibrate

Periodic bias tend to nonequilibrate
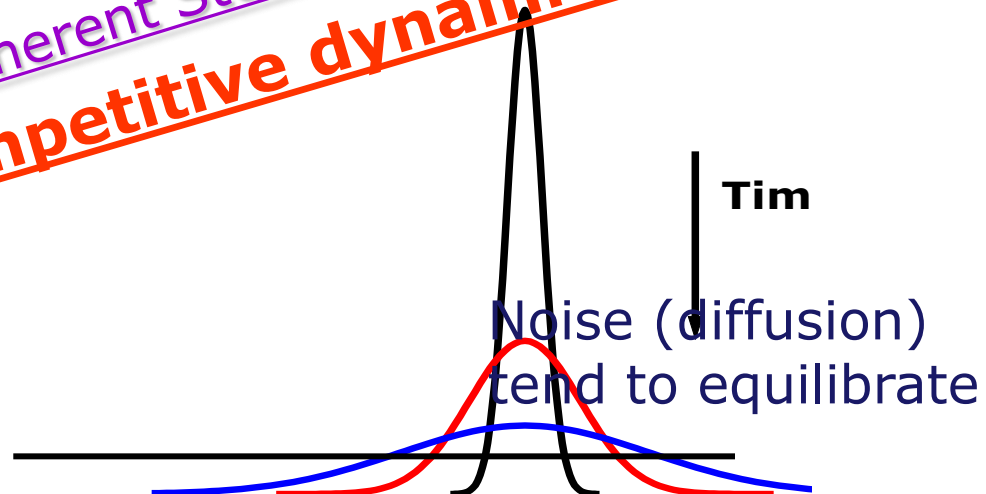
Mean First Passage Time Nonmonotonic with respect to frequency of periodic field & diffusivity
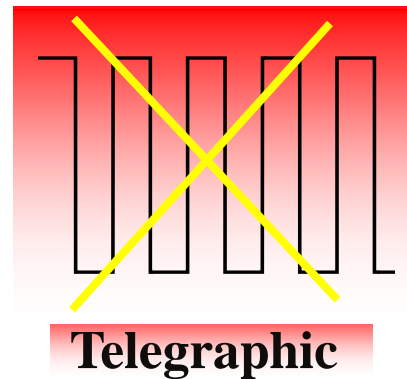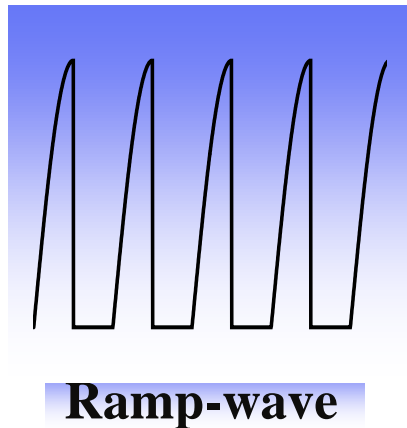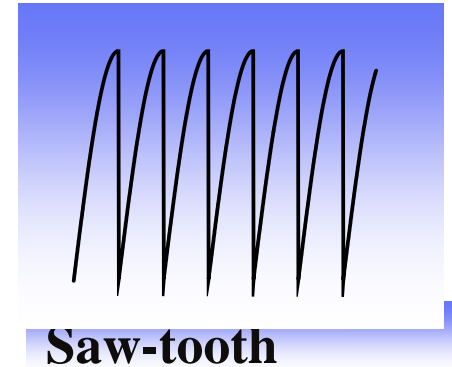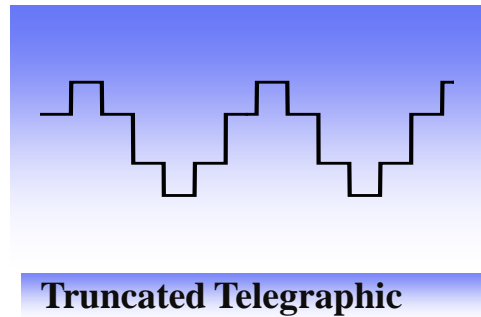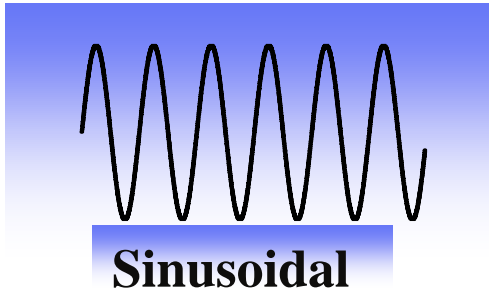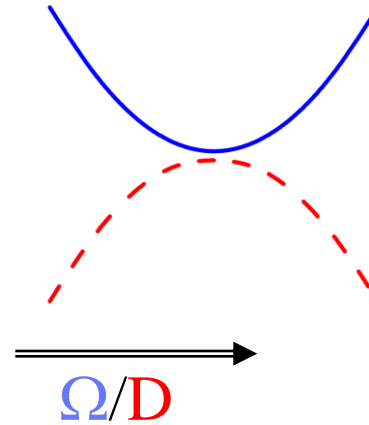
Ω/D

Sinusoidal

Truncated Telegraphic

Saw-tooth

Ramp-wave

Telegraphic

132

Coherent and incoherent trapping of a diffusion-assisted system in the presence of an external periodic field

Tusar Bandyopadhyay* and Swapan K. Ghosh†

Electric Field assisted trapping at line boundaries
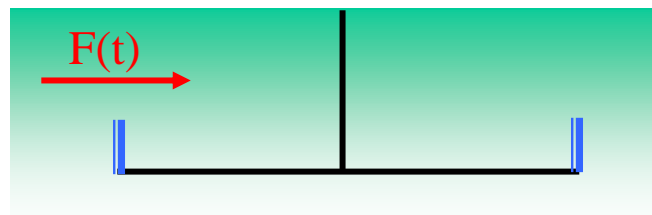
$$\frac{\partial \rho}{\partial t} = D \frac{\partial^2 \rho}{\partial x^2} - AF(\Omega t) \frac{\partial \rho}{\partial x}$$
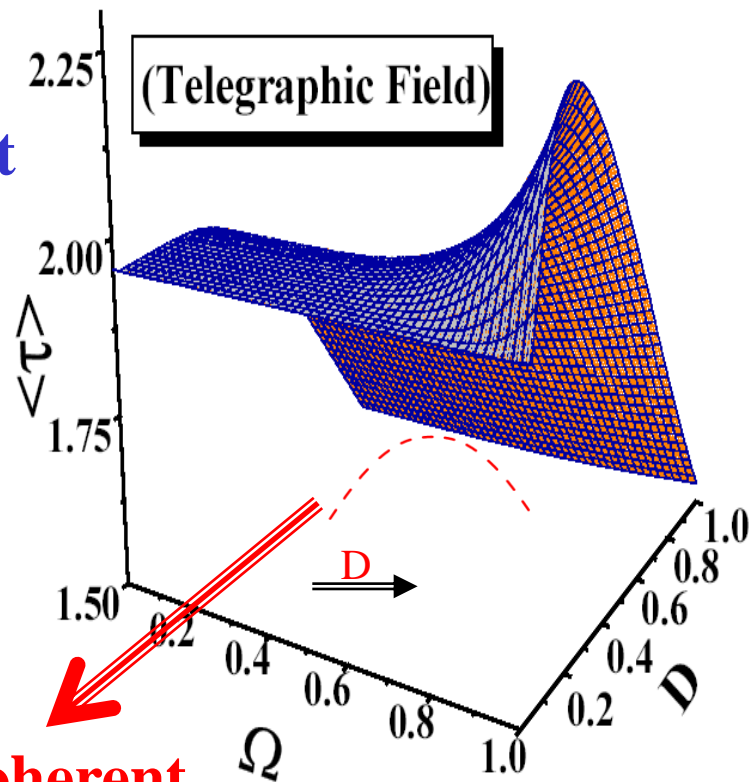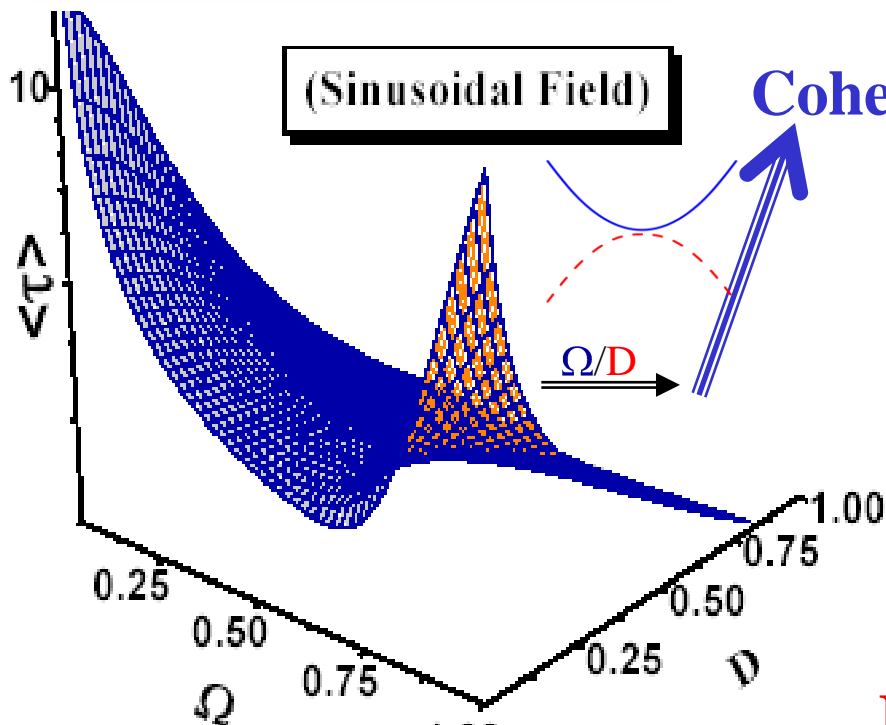
Minimum at suitable frequency for sinusoidal field

(a)

$\tau_F = 64.35$
$\langle\tau\rangle = 35.78$
$\tau_D = 40$

(c)

$\tau_F = \infty$
$\langle\tau\rangle = 38.68$
$\tau_D = 40$

(b)

$\tau_F = 28.31$
$\langle\tau\rangle = 27.24$
$\tau_D = 40$
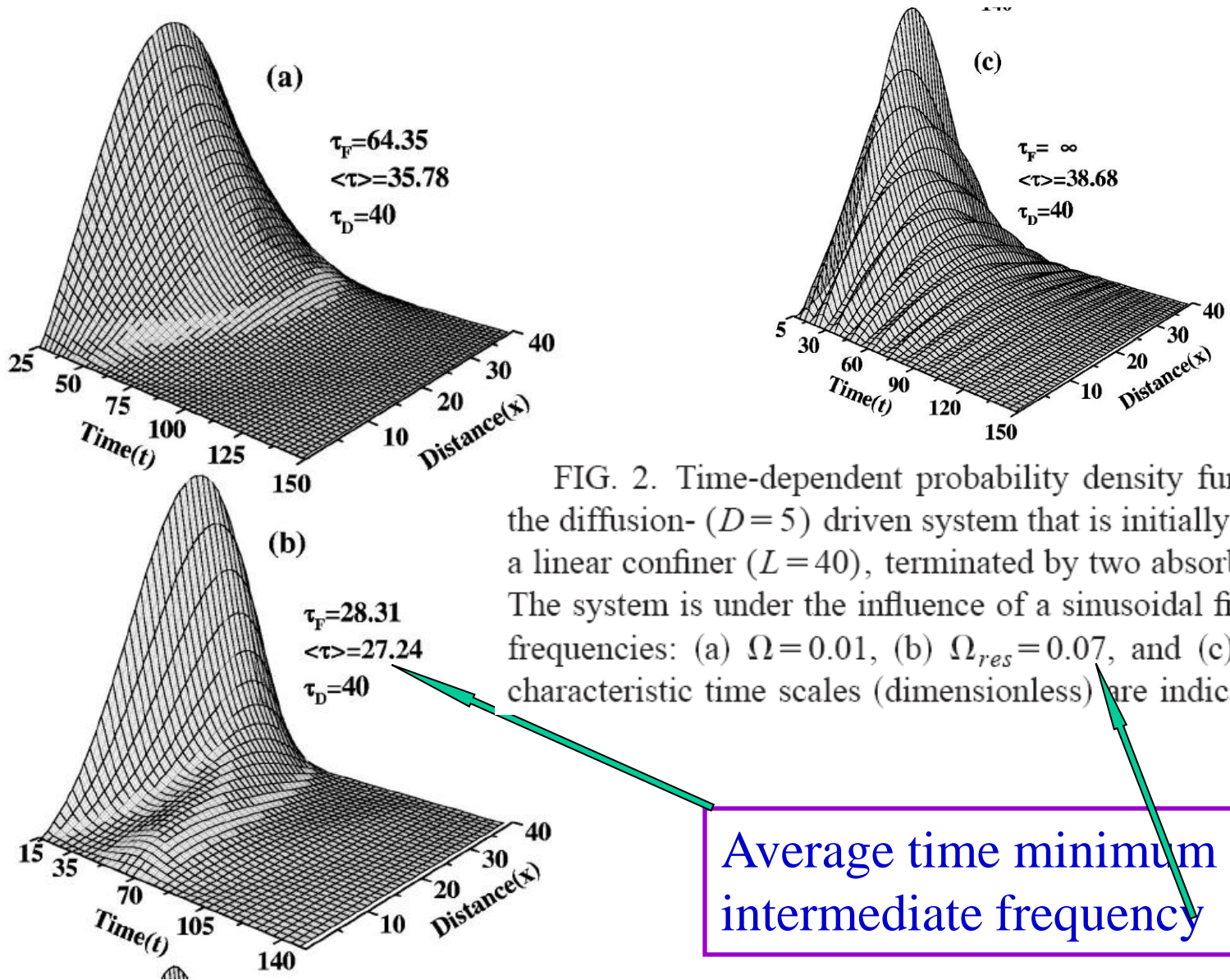
FIG. 2. Time-dependent probability density function $\rho(x,t)$ of the diffusion- $(D=5)$ driven system that is initially at the middle of a linear confiner $(L=40)$, terminated by two absorbing boundaries. The system is under the influence of a sinusoidal field with forcing frequencies: (a) $\Omega=0.01$, (b) $\Omega_{res}=0.07$, and (c) $\Omega=0.5$. Three characteristic time scales (dimensionless) are indicated.

Average time minimum at intermediate frequency

A One-Dimensional Energy Diffusion Approach to Multidimensional Dynamical Processes in the Condensed Phase

Alok Samanta and Swapan K. Ghosh*

Theoretical Chemistry Section, Bhabha Atomic Research Centre, Mumbai 400 085, India

We propose a generalized one-dimensional energy diffusion approach for describing the dynamics of multidimensional dynamical processes in the condensed phase. On the basis of a formalism originally due to Zwanzig, we obtain a one-dim**Energy Diffusion**perly selected relevant dynamical quantity and derive new analytical re   ultidimensional electron-transfer process,

Energy Diffusion

So far, the density has referred to electron density, particle number density, probability density for the end to end distance of polymer etc.

Now we consider the probability distribution $P(\gamma,t)$ denoting the probability of any microscopic phase-space variable A (in general multi-dimensional) constrained to have a value γ.

Thus, one can have a probability P(E,t) for a system to have energy E at time t and have an energy diffusion equation and consider the one-dimensional dynamics.

Theoretical Formalism

The basic approach is based on **an identification of a proper reaction coordinate (dynamical variable)**, obtaining a kinetic equation for the probability distribution of a microscopic phase-space variable **A (multi-dimensional)** constrained to have a value γ.

Distribution in γ space: $P(\gamma,t) = <\delta(A(t)-\gamma)>_{NE}$

One-dimensional generalised kinetic equation in γ-space

$$\partial P(\gamma,t)/\partial t = \partial/\partial\gamma\{\int_0^t d\tau\, D(\gamma,t-\tau)\, [\partial P(\gamma,t-\tau)/\partial\gamma +$$
$$\partial/\partial\gamma\{\beta V_{eff}(\gamma)\}\, P(\gamma,t-\tau)]\}$$

where time as well as γ-**dependent diffusivity** is defined as

$$D(\gamma,t)=<(dA(t)/dt)(dA/dt)|_{t=0}\, \delta(A(t)-\gamma)>/<\delta(A(t)-\gamma)>$$

and

effective Potential is: $\beta V_{eff}(\gamma) = -\ln<\delta(A-\gamma)>$

One-dimensinal description of the Two-dimensional Electron Transfer Reactions (ET)

Shown are the potential energy of the surface of the reactants on one side of the **transition state curve ABC**, and those of the product on the other side.

ET takes place when $V^P(Q,X) = V^R(Q,X)$.
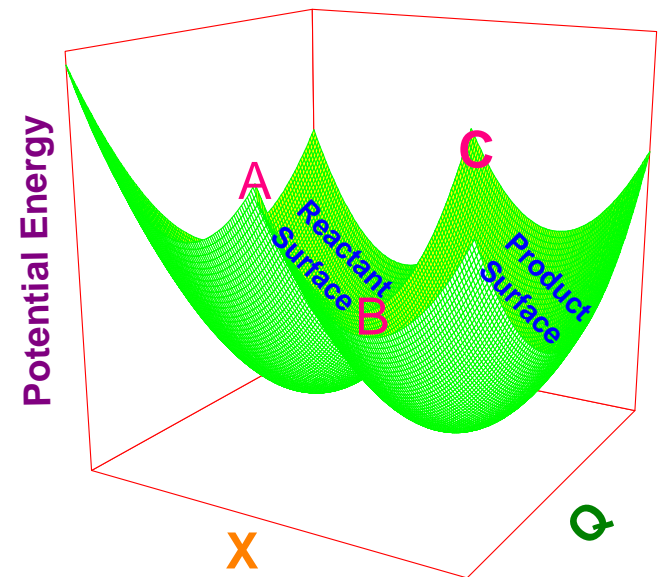
Fig.1

The relevant **microscopic operator** A for the ET reaction is taken as

$$A = V^P(Q,X) - V^R(Q,X) = \gamma$$

Potential energy

Reactant : $V^R(Q,X) = 1/2\ aQ^2 + 1/2\ X$

Product: $V^P(Q,X) = 1/2\ a(Q-Q_0)^2 + 1/2\ (X-X_0)^2 + \Delta G$

The relevant **microscopic operator A** for the ET reaction is taken as $A = V^P(Q,X) - V^R(Q,X)$.

Potential energy

Reactant : $V^R(Q,X) = 1/2\ aQ^2 + 1/2\ X^2$

Product : $V^P(Q,X) = 1/2\ a(Q-Q_0)^2 + 1/2\ (X-X_0)^2 + \Delta G$

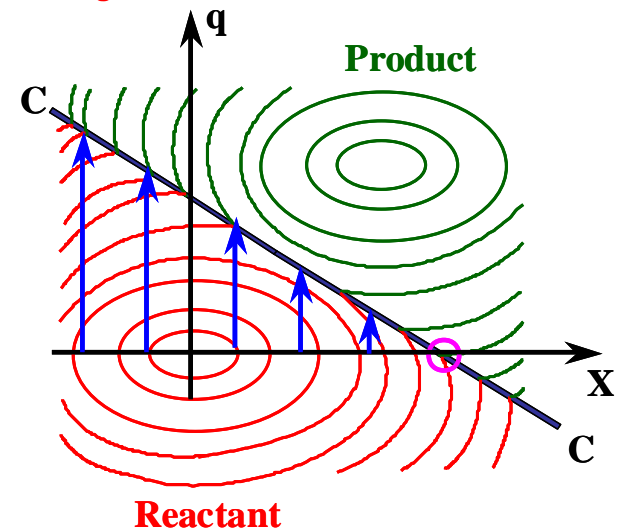## Kinetic Equation for the Reaction Coordinate of ET reactions

$$\partial P(\gamma,t)/\partial t = \int_0^t d\tau\ D_{eff}(\tau)\ \partial/\partial\gamma\ [\partial P(\gamma,\ t-\tau)/\partial\gamma + \beta/2\lambda_T[\gamma-(\lambda_T+\Delta G)]P(\gamma,t-\tau)] - k_0\delta(\gamma)P(\gamma,t)$$

where $D_{eff}(t) = D_{sol}(t) + D_{vib}(t)$; $D_{sol}(t) = X_0^2 < dX(t)/dt\ (dX/dt)|_{t=0} >$;

$D_{vib}(t) = (aQ_0)^2 < dQ(t)/dt\ (dQ/dt)|_{t=0} >$.

$\lambda_T = \lambda_{sol} + \lambda_{vib}$; $\lambda_{sol} = \frac{1}{2}\ X_0^2$; $\lambda_{sol} = \frac{1}{2}\ Q_0^2$.

ΔG represents the free energy of the ET reactions and ET reactions do occur with an intrinsic rate $k_0 = (2\pi)^2 J/h$ determined by the electron transfer integral J, corresponding to $\gamma=0$, i.e. when the reactant and product potential energies are equal.

It provides a one-dimensional energy diffusion equation of the reactive system and can be numerically solved much more easily than the two-dimensional Smoluchowski equation involving X and Q coordinates.

Rate   Constant for ET reactions

Probability of finding the system at time t in the reactant surface is defined as $P(t) = \int_{-\infty}^{\infty} d\gamma P(\gamma,t)$ and the average rate of electron transfer reaction k can be expressed as $k^{-1} = \int_0^{\infty} dt\, P(t) = k_{TST}^{-1} + k_d^{-1}$, where k_{TST} represents the transition state theory result expressed as

$$k_{TST} = k_0 (4\pi k_B T \lambda_T)^{-1/2}\, \exp[-(\Delta G + \lambda_T)^2 / 4k_B T \lambda_T]$$

whereas k_D^{-1} represents the rate constant for well dynamics and can be expressed in terms of the normalized non-equilibrium distribution in the absence of sink as $k_D^{-1} = \int_0^{\infty} dt [P_0(\gamma_0,t|\gamma_0,0) - P_0(\gamma_0,t|\gamma^*,0)]/P_0(\gamma_0)$, where γ^* and γ_0 correspond to the initial value of γ and position of the sink.

An analytical expression for k_D^{-1} can be obtained as

$$k_D^{-1} = (\pi k_B T \lambda_T)^{1/2}\, D_{eff}^{-1} \int_B^A dx\, \exp[x^2/4k_B T][1+erf(x/\sqrt{4k_B T \lambda_T})]$$

$$A = -(\lambda_T + \Delta G), \quad B = \gamma^* -(\lambda_T + \Delta G)$$
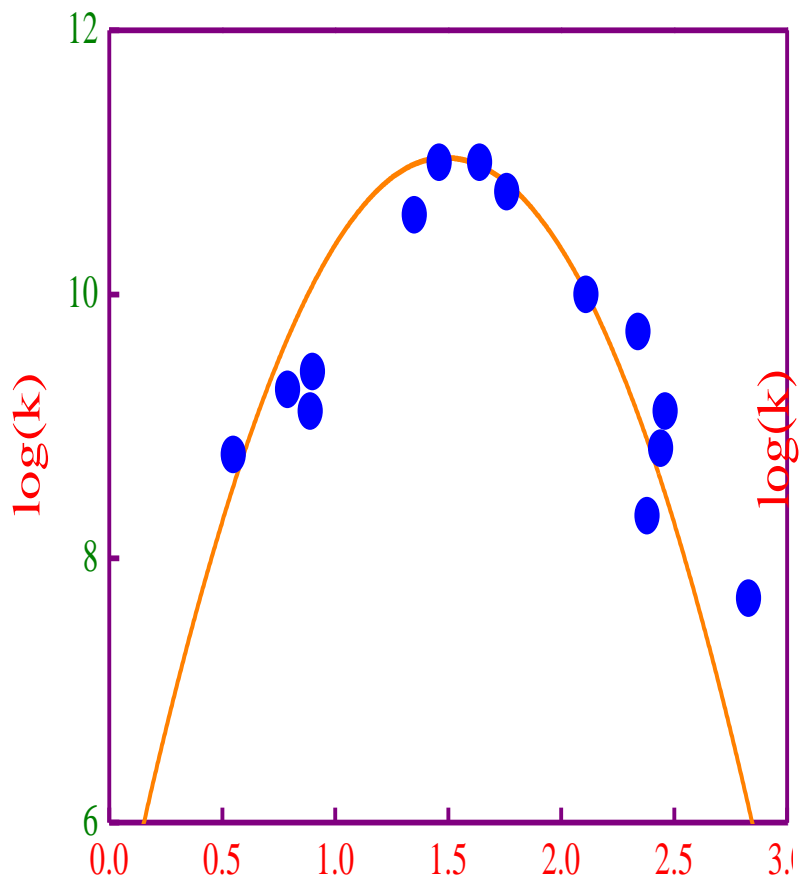
Charge recombination reactions in solvent separated ion pair
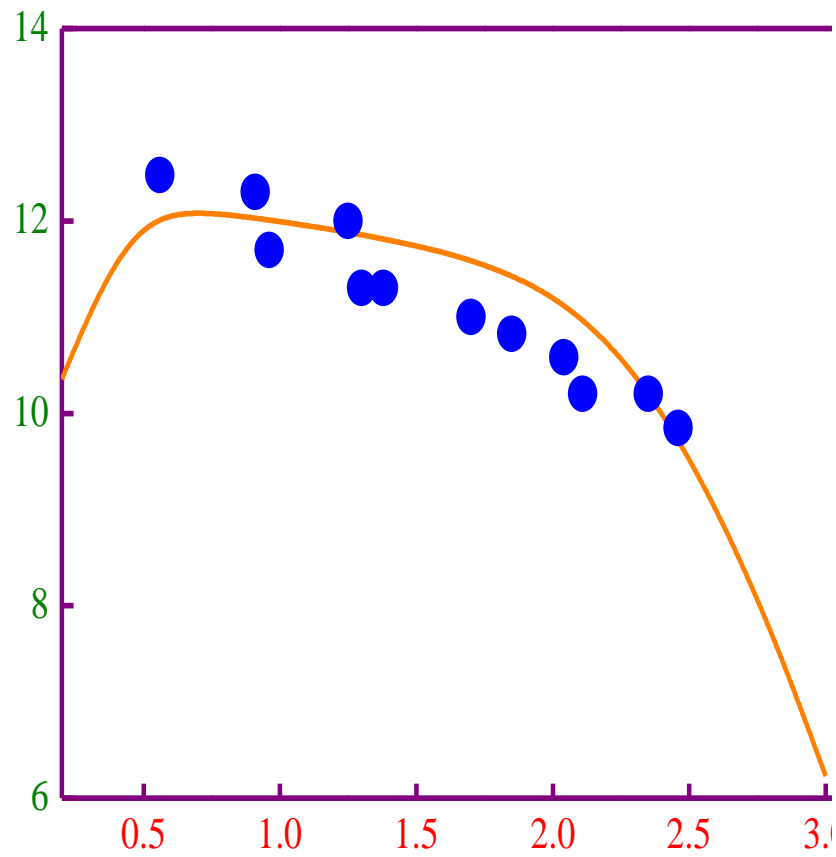
Charge recombination reactions in contact ion pairs

Nonequilibrium Solvation Dynamics

The most straightforward way to study the solvation dynamics is via **time dependent fluorescence Stokes shift.** In this experiment, a solute probe is optically excited, leading to a non-equilibrium state of the surrounding molecules which subsequently undergo rotational and translational relaxation to adjust to the new charge distribution, leading to energy lowering of the excited solute-solvent system and hence red shift in the fluorescence spectrum.

Excited State

Solvation

hν

Fluorescence
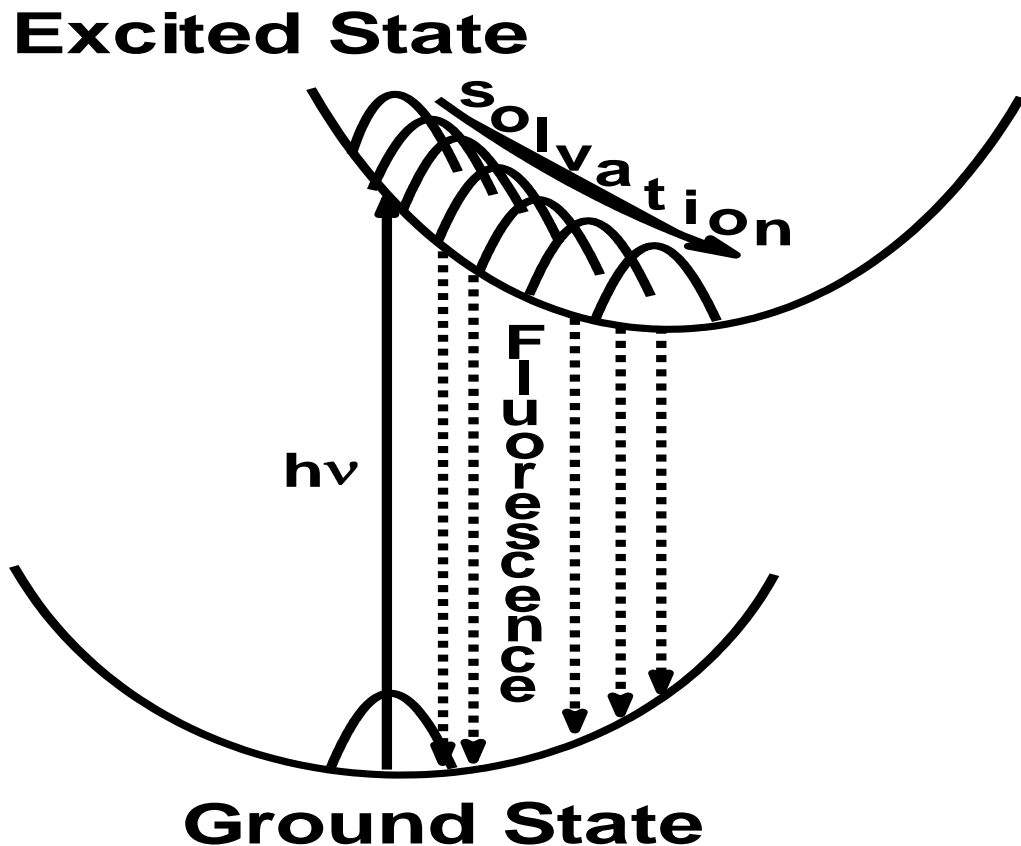
Ground State

Stokes shift function

$$S(t) = [\Delta E(t) - \Delta E(\infty)]/[\Delta E(0) - \Delta E(\infty)]$$

$\Delta E(t)$ is the energy gap between the ground and excited state.

Summary of density variables

- The **density** has reference to
      electron density in microscopic length scale,
  particle number density in mesoscopic scale,   &
  also probability density for the end to end
                distance of polymer etc.

- Also considered is the probability distribution $P(\gamma, t)$
      denoting the probability of any microscopic
  phase-space variable A (in general multi-dimensional)
  constrained to have a value γ.

- Thus, one can have a probability P(E,t) for a system to have energy E at time t and have an energy diffusion equation and consider the one-dimensional dynamics for an otherwise multi-dimensional dynamical process.

Summary & Conclusion

Density Concept plays an important role in providing a unified framework for Modelling at all length scales: *Electronic, Atomistic, Continuum Simulation*

Quantum DFT: Effective one-particle Schrodinger equation: Modelling with electron density

Application: Coarse-grained density in modeling Molecules, Materials & Intermolecular Interaction , Carbon nano Materials for H_2 adsorption, Cluster-assembled materials

Classical DFT: Effective Boltzmann type distribution with density-dependent effective potential: Modelling with particle number density

Examples: Structural and Dynamical Aspects of Soft Matter at interfaces .

Dynamical Phenomena: Density based approach useful

Versatility of DFT: Modeling Hard & Soft Materials at different length scales

THE TEAM

Dr Alok Samanta

Dr Tapan Ghanty

Dr Chandra Patra

Dr Niharendu Choudhury

Dr Tusar Bandyopadhyay

Dr Dilip Maity

Dr Shashwati Roy

Dr KRS Chandrakumar

K. Srinivasu

Dr Malaya Nayak

Brindaban Modak

Naresh K Jena

TEAM

Together
Everybody
Achieves
More

Dr Alok Samanta

Dr Tapan G

andra Patra

Dr Niharendu Choudhury

Dr Tusar Bandyopadhyay

Dr Dilip Maity

Dr Shashwati Roy

Dr KRS Chandrakumar

K. Srinivasu

Dr Malaya Nayak

Brindaban Modak

Naresh K Jena

Thank You

WISH YOU ALL HAPPY 2010